SCREENING OF AUTOSOMAL RECESSIVE CHARCOT-MARIE-TOOTH (ARCMT2), DISTAL HEREDITARY MOTOR NEUROPATHY (dHMN) AND HEREDITARY SPASTIC PARAPLEGIA (HSP) PATIENTS FOR MUTATIONS IN AXONAL NEUROPATHY GENES

by

H. Başak Şenergin

B.S., Molecular Biology and Genetics, Istanbul Technical University, 2004

Submitted to the Institute for Graduate Studies in
Science and Engineering in partial fulfillment of
the requirements for the degree of
Master of Science

Graduate Program in Molecular Biology and Genetics
Boğaziçi University

2006

ACKNOWLEDGEMENTS

First, I would like to thank my thesis supervisor Assoc. Prof. Esra Battaloğlu for her continuous support, guidance and valuable critisms throughout the study.

Besides my advisors, I also would like to thank to the rest of my thesis committee Prof. A. Nazlı Başak and Prof. Yeşim Gülşen Parman for evaluating this thesis.

I would like to thank to Prof. Yeşim Gülşen Parman and Dr. Erkingül Shugaiv for contacting patients and providing their blood samples and clinical data used in this study.

My special thanks goes to the old and new members of the CMT group: İbrahim, Birdal, Rezan, Öncü, Duygu, Ayaz and Çiğdem for their help and friendship.

Last, but not least, I thank my family for unconditional support and encouragement to pursue my interests, even when the interests went beyond boundaries of geography.

ABSTRACT

SCREENING OF AUTOSOMAL RECESSIVE CHARCOT-MARIE-TOOTH (ARCMT2), DISTAL HEREDITARY MOTOR NEUROPATHY (dHMN) AND HEREDITARY SPASTIC PARAPLEGIA (HSP) PATIENTS FOR MUTATIONS IN AXONAL NEUROPATHY GENES

Charcot-Marie-Tooth Disease (CMT), distal Hereditary Motor Neuropathy (HMN) and Hereditary Spastic Paraplegia (HSP) constitute the largest group of inherited diseases affecting the peripheral nervous system.

In the scope of this thesis, the genetic background of autosomal recessive CMT2 disease was investigated in a cohort of Turkish families and isolated cases. For this purpose, GDAP1 and LMNA genes were investigated by SSCP analyses, and linkage to 19q13.1 locus was tested by homozygosity mapping. The study was extended to screening of the small heat shock protein genes, HSPB1, and HSPB8, that have been recently shown to be responsible for autosomal dominant CMT2 and distal HMN. The involvement of another heat shock protein gene, HSP60, was screened for mutations in a small group of Hereditary Spastic Paraplegia patients.

Exclusion of all known loci responsible for ARCMT2 in a family demonstrated that there is at least one more locus responsible for the disease phenotype. Only one of the CMT4 patients was found to be mutated in *GDAP1*. Another causative mutation was identified in *HSPB1* in a CMT2 patient. Clinical diagnoses of the patients were found to be compatible with the genetical diagnoses. All other patients tested negative for mutations in the GDAP1, LMNA, HSPB1, HSPB8, and HSP60 genes although several novel or previously repoted polymorphisms were detected. Absence of mutations in these patients indicated that the contribution of these genes to the appropriate disease phenotypes is low in the Turkish population.

ÖZET

AKSONAL NÖROPATİ GENLERİNİN OTOZOMAL ÇEKİNİK CHARCOT-MARIE-TOOTH (ARCMT2), DİSTAL HEREDİTER MOTOR NÖROPATİ (dHMN) VE HEREDİTER SPASTİK PARAPLEJİ (HSP) HASTALARINDA TARANMASI

Charcot-Marie-Tooth (CMT), distal Kalıtsal Motor Nöropati (dHMN) ve Herediter Spastik Parapleji (HSP) en geniş kalıtsal periferik sinir sistemi hastalıkları grubunu oluştururlar.

Tez kapsamında, Türk ailelerinde ve izole olgularda otozomal çekinik CMT2 (ARCMT2) hastalığının genetik altyapısı araştırıldı. Bu amaçla bu hastalıktan sorumlu olduğu bilinen GDAP1 ve LMNA genleri SSCP yöntemi ve 19q13.1 kromozom bölgesi homozigotluk haritalaması kullanılarak incelendi. Çalışma, otozomal baskın CMT2 ve dHMN'den sorumlu oldukları henüz bulunan küçük ısı-şok proteinlerini kodlayan HSPB1 ve HSPB8 gen taramalarını da içine alacak şekilde genişletildi. Bir başka ısı-şok proteinini kodlayan HSP60 geni de daha küçük bir grup olan kalıtsal spastik paraplezi hastalarında mutasyonlar için tarandı.

ARCMT2'den sorumlu olan üç kromozom bölgesinin bir ailede tümüyle dışlanması ile hastalıktan sorumlu en az bir genin daha olduğu gösterildi. CMT4 hastalarından sadece birinde *GDAP1* gen mutasyonu belirlendi. Diğer bir hastalık mutasyonu ise bir CMT2 hastasında *HSPB1* geninde bulundu. Bu hastalarda genetik tanının klinik tanı ile örtüştüğü görüldü. Diğer hastaların GDAP1, LMNA, HSPB1, HSPB8, ve HSP60 genlerinde hastalıktan sorumlu mutasyonlar taşımadıkları belirlendi ancak bu hastalarda normal bireylerde de görülebilen çeşitli polimorfizmler tanımlandı. Bu bulgular, sözkonusu genlerin Türk toplumunda bu hastalıklar üzerindeki etkisinin yaygın olmadığını gösterdi.

TABLE OF CONTENTS

LIST OF FIGURES

LIST OF TABLES

LIST OF ABBREVIATIONS

A	Adenine
AD	Autosomal Dominant
APS	Ammonium Peroxodisulfate
AR	Autosomal Recessive
ARCMT2	Autosomal Recessive Charcot-Marie-Tooth Disease Type 2
ARMS	Amplification Refractory Mutation System
BSCL2	Bernardinelli-Seip congenital lipodystrophy 2 (seipin)
bp	Base pair
C	Cytosine
CD_3	$\alpha_{2,8}$-sialyltransferase
CHN	Congenital Hypomyelinating Neuropathy
CMT	Charcot-Marie-Tooth Disease
CNS	Central Nervous System
CNTN1	Contactin gene 1
Cx32	Connexin 32
DCTN1	Dynactin 1
dHMN	Distal Hereditary Motor Neuropathy
DNA	Deoxyribonucleic acid
DRM	Desmin-Related Neuropathy
DSP	Dual Specificity Phosphatase
DSS	Dejerine Sottas Syndrome
dNTP	Deoxyribonucleotidetriphosphate
EDTA	Ethylenediaminetetraacetic acid
EGFP	Enhanced Green Fluorescent Protein
EGR2	Early growth response-2 gene
EMP3	Epithelial membrane protein 3
EtBr	Ethidium Bromide
G	Guanine

GARS	glcyl-tRNA synthetase
GDAP1	Ganglioside-induced differentiation-associated protein 1
GFP	Green Fluorescent Protein
GJB1	Gap Junction Beta
GSH	Glutathione
GST	Glutathione S-Transferase
HMSN	Hereditary Motor and Sensory Neuropathy
HMSNL	Hereditary Motor and Sensory Neuropathy-Lom
HMSNR	Hereditary Motor and Sensory Neuropathy-Russe
HNPP	Hereditary Neuropathies with Liability to Pressure Palsies
HSP	Hereditary Spastic Paraplegia
HSP60	Heat Shock Protein 60
HSPB1	Heat-shock 27-kD protein-1
HSPB8	Heat-shock 22-kD protein-8
IGHMBP2	Immunoglobulin mu-binding protein 2
kb	Kilo base
KDa	Kilo Dalton
KIF5A	Kinesin family member 5A
LMNA	Lamin A/C
MAPKAPK-2	Mitogen-Activated Protein Kinase-Activated Protein Kinase2
Mb	Mega base
MFN1	Mitofusin 1
MFN2	Mitofusin 2
MPZ	Myelin Protein Zero
mRNA	Messenger ribonucleic acid
MTMR	Myotubularin Related
NCV	Nerve Conduction Velocity
NDRG1	N-myc downstream-regulated gene 1
NEFL	Neurofilament-light gene
OD_{260}	Optical density at 260 nm
OMIM	Online Mendelian Inheritance in Man
ORF	Open Reading Frame
PAGE	Polyacrylamide Gel Electrophoresis

PCR	Polymerase Chain Reaction
PMP22	Peripheral Myelin Protein
PNS	Peripheral Nervous System
PRPH	Peripherin gene
PRX	Periaxin gene
PTP	Protein Tyrosine Phosphatase
RBC	Red Blood Cell
REEP1	Receptor Expression-Enhancer Protein 1
rpm	revolution per minute
SBF2	SET Binding Factor 2
SDS	Sodiumdodecylsulphate
SET	Suvar3-9, Enhancer-of-zeste, Trithorax
SETX	Senataxin
SID	SET Interacting Domain
sHSP	Small heat shock protein
SNP	Single Nucleotide Polymorphism
SSCP	Single Strand Conformation Polymorphism
T	Thymine
TBE	Tris-EDTA- Boric acid
TE	Tris-EDTA
TEMED	N, N, N, N'-Tetramethylethylenediamine
U	Unit
UTR	Untranslated region
UV	Ultraviolet

1. INTRODUCTION

Peripheral neuropathies are a large group of inherited diseases that have their affects in motor, sensory and autonomic nervous systems (Irobi *et al*., 2004; Stojkovic, 2006). Conventionally, hereditary peripheral neuropathies are classified according to the clinical findings (Boerkoel *et al.*, 2003). However, identification of the causative genes led to development of a sub-classification system (Hanemann and Ludolph, 2002).

Charcot-Marie-Tooth Disease (CMT) and Hereditary Motor Neuropathy (HMN) constitute the largest group of inherited peripheral neuropathies. Hereditary Spastic Paraplegia (HSP) is also a common disease affecting the peripheral nervous system. The genetic basis of these diseases were analyzed in the scope of this thesis.

1.1. Charcot-Marie-Tooth (CMT) Disease

Charcot-Marie-Tooth disease affects both motor and sensory nerves and is the most common inherited peripheral neuropathy in humans (Charcot and Marie 1886; Tooth, 1886). Although most of the CMT families present autosomal dominant inheritance, all Mendelian inheritance patterns are observed in the disease (McKusick, 1992; Suter, 1994). The prevalence of CMT with all forms combined is one in every 2500 individuals (Skre, 1974). CMT is characterized by distal muscle weakness and atrophy mostly in the lower extremities, distal sensory loss, absent or diminished tendon reflexes and skeletal deformities like pes cavus and claw hands (Dyck and Lambert, 1968a, b; Charcot and Marie, 1886).

The conventional classification of the disease is based on nerve biopsy and electrophysiological findings. The first category is CMT Type 1 that is characterized by reduced median motor nerve conduction velocity (MNCV<38 m/s) and presence of onion bulbs due to repetitive de- and remyelination. An X-linked category with dominant features was also included in this group (Rozear *et al.,* 1987; Hahn *et al.*, 1990; Sevilla *et al.*, 2003). The second category, CMT2, is characterized by normal or near normal MNCV values (>38 m/s) and axonal degeneration (Dyck and Lambert, 1968a, b; Harding and

Thomas, 1980; Sevilla *et al.*, 2003). An intermediate group with MNCV values between 27-35 m/s was also suggested to be inherited in autosomal dominant or recessive pattern (Rouger *et al.,* 1997; Senderek *et al.*, 2003a). As the genetic studies improved the knowledge about Charcot-Marie-Tooth disease and unravelled the genetic heterogeneity (Figure 1.1), CMT1 and CMT2 were further divided into sub-classes according to the genes mutated or the loci involved. Autosomal recessive form of axonal CMT is named as ARCMT2 while demyelinating autosomal recessive form of CMT is called CMT4 (Sevilla *et al.*, 2003).

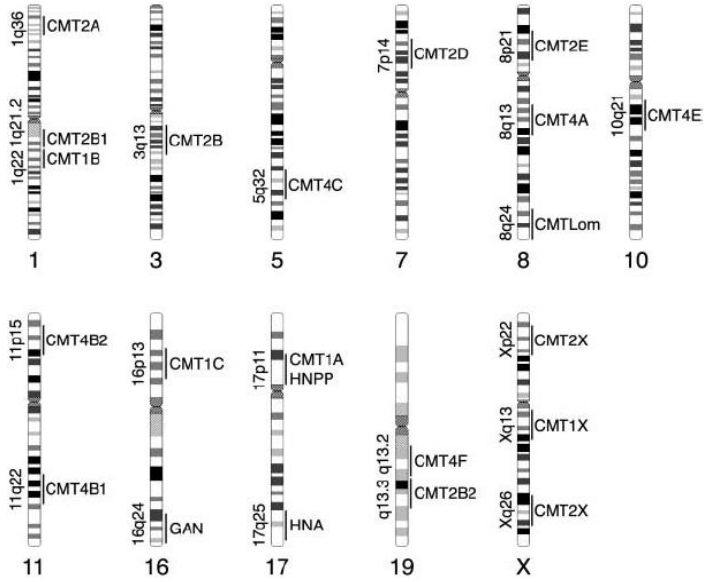

Figure 1.1. Genetic Heterogeneity of CMT (Berger *et al.*, 2002)

1.1.1. Charcot-Marie-Tooth Disease Type 4 (CMT4)

Charcot-Marie-Tooth Disease Type 4 (CMT4) is a complex group of early onset demyelinating neuropathy and inherited in autosomal recessive pattern. The disease is more severe in comparison with the dominant forms. The early age of onset and quick progression of distal limb weakness with atrophy help the characterization of the disease. However, as an indicator of genetic heterogeneity, the variations between the pathological and electrophysiological characteristics of the CMT4 patients are also quite recognizable (Othmane et. al, 1993). According to the affected loci or the genes, eight subtypes of CMT4 have been identified (A, B, C, D, E, F, G and H) (Table1.1) (www.molgen.ua.ac.be/ CMTMutations/).

Table 1.1. CMT Type 4 genes and loci (Azzedine *et al.*, 2003a; www.molgen.ua.ac.be/CMTMutations/)

Affected Gene	Loci	Feature	Nomenclature
GDAP1	8q13-q21	Demyelinating & Axonal	CMT4A, ARCMT
MTMR2	11q23	Demyelinating	CMT4B1
SBF2 / MTMR13	11p15	Demyelinating	CMT4B2
SH3/TPR	5q23-q33	Demyelinating	CMT4C
NDRG1	8q24.3	Demyelinating	CMT4D (HMSNL)
EGR2	10q21.1-q22.1	Demyelinating	CMT4E
PRX	19q13.1-13.3	Demyelinating	CMT4F
Unknown	10q22-q23	Demyelinating	CMT4G (HMSNR)
Unknown	12p11.21-q13.11	Demyelinating	CMT4H

1.1.1.1. CMT4A. The clinical definition of CMT4 type A is given by hypomyelination in nerve biopsy and slow motor nerve conduction velocity (NCV). The patients have delayed motor development and the onset is usually before two years of age. Physical changes like claw-hands and pes cavus appear by the end of the first decade as a result of the quick progression of the weakness and atrophy, which involve upper extremities after the distal muscles of the limbs. Patients may become wheel-chair dependent and also develop kyphosis. Deep tendon reflexes disappear and a moderate sensory loss in vibration senses and proprioception are observed (Ben Othmane et. al, 1993; Baxter *et. al,* 2002). Other common symptoms are skeletal deformities and scoliosis and there is no increase in the levels of the cerebrospinal fluid (CSF) protein (Ben Othmane et. al, 1993). In CMT4A, it is not easy to decide the first causative of the disease because of severe nerve damage affecting both the myelin and the axons (Pedrola *et al.,* 2005).

The linkage studies among Tunisian CMT4 families localized the causative gene for CMT4A to 8q13-21.1 region (Ben Othmane et. al, 1993; 1995; 1998). Ganglioside-induced differentiation-associated protein-1 (*GDAP1*) was one of the candidate genes in this locus. Consequently, the gene was reported to be mutated in the affected individuals both with demyelinating (Baxter *et al*, 2002) and axonal neuropathy (Cuesta *et al.*, 2002).

The gdap1 protein was first identified in Neuro2a cells, a mouse neuroblastoma cell line, upon transfection with GD3 synthase cDNA (α2,8 sialyltransferase). The transfection results in high expression of gdap1 and cell differentiation with neurite sprouting in adult mouse brain (Liu *et al.*, 1999). *GDAP1*, the human orthologue of the gene, is a 13,9 kb long sequence and contains an ORF of 1077 nucleotides with 6 exons (Cuesta *et al.*, 2002). The single transcript of the gene is 4.1 kb long and encodes 358 amino acids. The mouse and human homologs of the gene have 94 per cent homology at the amino acid level (Liu *et al.*, 1999).

According to the phylogenetic analyses based on the amino acid sequence, GDAP1 is a member of a newly discovered monophyletic group of glutathione S-transferases (GSTs) (Marco *et al.*, 2004). GST enzymes have roles in antioxidant pathways and in cellular detoxification of xenobiotic and endobiotic compounds (Salinas and Wong, 1999; Nelis *et al.*, 2002). The GST group involving *GDAP1* is referred as *GDAP1* group and has some distinctive features with respect to other GSTs. The sequences of the two GST domains of *GDAP1* are different from that of other GSTs. In addition, in the GDAP1 group of proteins, two GST domains are separated by a structure composed of additional amino acids that is defined as α4-α5 loop (Figure 1.2). Lastly, the two putative transmembrane domains located in the carboxyl-terminal sequence of GDAP1 between amino acid residues of 292-311 and 319-340 are not present in any putative relatives of GDAP1 as they are cytosolic proteins (Marco *et al.*, 2004).

GDAP1 was found to be predominantly expressed in the nervous system but the protein is also detected in skeletal muscle, heart, and liver in both mouse and human. On the other hand, *GDAP1* expression level is higher in central than in peripheral nerves and it is expressed not only in neurons but also in Schwann cells (Cuesta *et al.*, 2002). Although *GDAP1* is expressed in CNS, there is no central nervous system involvement in the patients with *GDAP1* mutations which suggests involvement of different signaling pathways in myelination processes in the peripheral and the central nervous systems (De Sandre-Giovannoli *et al.*, 2003). It is also possible that *GDAP1* has a different function or its loss can be compensated by other proteins in CNS (Nelis *et al.*, 2002).

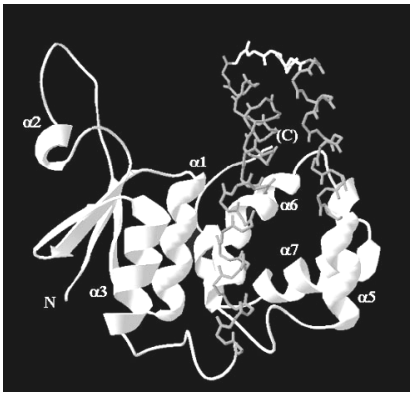

Figure1.2. Predicted three-dimensional structure for human GDAP1 (Marco *et al.*, 2004)

GDAP1 was found to be an integral membrane protein located in the outer membrane of mitochondria by colocalization experiments using the mitochondrial marker MitoTracker and *GDAP1* constructs fused with EGFP overexpressed in COS-7 and SH-SY5Y cells and western blotting of the mitochondrial fraction of SH-SY5Y cells. However, the exact positions of the transmembrane domains in the membrane are not known yet (Figure 1.3) (Niemann *et al.*, 2005).

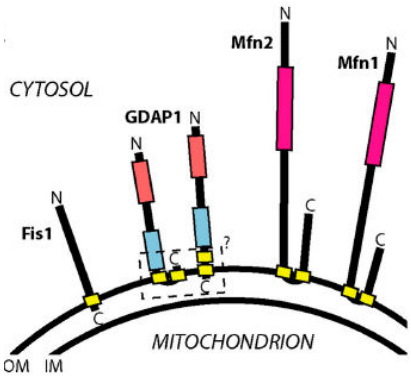

Figure 1.3. Hypothetical localization of GDAP1 on mitochondrial outer membrane (Niemann *et al.*, 2005)

Although many hypotheses were suggested for the function of GDAP1, its role in the cell is still not known completely. First, it was suggested that *GDAP1* mutations might be disrupting the interaction between axons and Schwann cells because of the involvement of *GDAP1* mutations in patients both with axonal and demyelinating features (Cuesta *et al.*, 2002; Shy *et al.,* 2002). Later on, because of the roles of GSTs in antioxidant pathways and

cellular detoxification, protection of myelin membranes against free radicals was suggested as the role of GDAP1 in the cell (Mattson, 2002). However, the discovery of the mitochondrial localization of the protein proposed new possibilities for its function. Niemann *et al.* speculated that despite the mitochondrial localization of the protein, GDAP1 may still have a GST function as there is a glutathione (GSH) dependence for mitochondrial morphology and low GSH concentrations causes the mitochondria to go into fusion and form a tubular network (2005). However, GST activity of the full length protein was not tested as it could not be kept in soluble form because of the transmembrane domains and the truncated *GDAP1* constructs lacking the two transmembrane domains did not show GST activity (Pedrola *et al.*, 2005; Shield *et al.*, 2006).

Because of disrupted morphologies of mitochondria in the presence of mutated *GDAP1*, its role in mitochondrial structure was investigated. RNAi knock-down of *GDAP1* in N1E-115 neuroblastoma cells caused tubular mitochondrial morphology in comparison with untransfected cells while the overexpression introduces fragmentation indicating a role for GDAP1 in the mitochondrial fission (Niemann *et al.*, 2005; Pedrola *et al.*, 2005). Mitofusion genes (*MFN1* and *MFN2*) are known to be involved in the mitochondrial fusion (Züchner *et al.*, 2004). Coexpression of *MFN1* or *MFN2* with *GDAP1* in COS-7 cells showed the same morphology with the untransfected and control transfected cells and this also indicates that two proteins compensates the effects of each other further supporting that GDAP1 is a mitochondrial fission protein. However, although GDAP1 is known to be involved in mitochondrial fission whether the CMT phenotype is due to the disrupted mitochondrial network directly or as a result of the mitochondrial transport remains to be elusive (Niemann *et al.*, 2005).

The heterogeneous locations of the 24 *GDAP1* mutations (Figure 1.4, www.molgen.ua.ac.be/CMTMutations/) identified in CMT patients indicate that the GST domains, C-terminal transmembrane domain and α4-α5 loop are all required for the normal functioning of the protein (Marco *et al.*, 2004). This idea was further supported by expression studies performed with different *GDAP1* mutant constructs in COS7 cells. The proteins truncated at their transmembrane domains lost the ability to localize to the mitochondria and to function properly, while the missense point mutations did not affect the mitochondrial localization of the protein (Niemann *et al.*, 2005; Pedrola *et al.*, 2005).

Although it was previously thought that the loss of normal GDAP1 function is the cause of CMT4A phenotype, the identification of mutations in dominant cases (Claramunt, *et al.*, 2005) also indicated a possible toxic gain of function of the protein (Pedrola *et al.*, 2005).

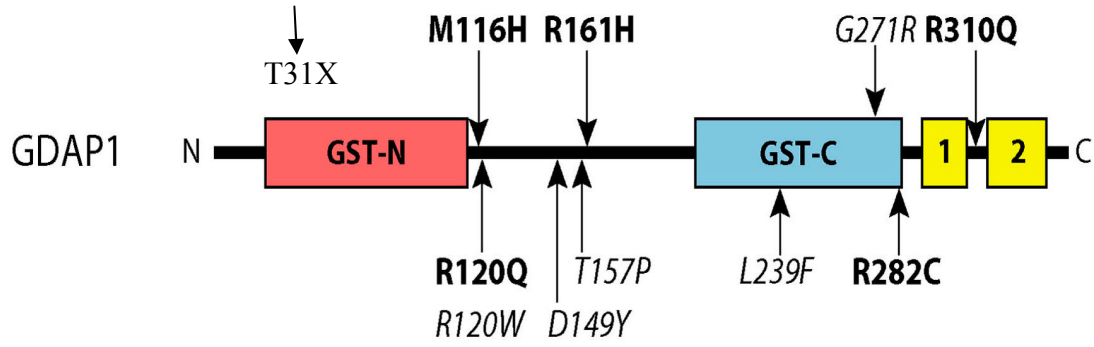

Figure 1.4. Schematic view for domains of *GDAP1* and location of some of the mutations (GST-N, amino terminal glutathione S-transferase domain; GST-C, carboxyl terminal glutathione S-transferase domain; 1 and 2 transmembrane domains) (modified from Niemann *et al.*, 2005)

The variable nature of the disease and mutations make genotype-phenotype correlations difficult depending on the small number of patients (Ammar *et al.*, 2003). For example, the same mutation can give rise to axonal or demyelinating symptoms (Nicholson and Ouvrier, 2002). Moreover, c.482G>A (p.R161H) mutation was found to cause a dissimilar severity in nerve biopsies of two siblings taken at the same age (Ammar *et al.*, 2003). Furthermore, it was suggested that, vocal cord paresis could be allelic to the CMT4A as it segregates with p.Q163X and p.S194X mutations of the GDAP1 gene (Nelis *et al.*, 2002; Cuesta *et al.*, 2002; Nicholson and Ouvrier, 2002). In addition, the presence of pyramidal signs only in some patients with p.M116R mutation but not in the others indicates the role of epigenetic factors as well as genetic factors in the disease (Biancheri *et al.*, 2006).

1.1.1.2. CMT4B. The first locus linked to CMT4B was on chromosome 11q23 in a Southern Italian family (Bolino *et al.*, 1996). On the other hand, Ben Othmane *et al.* found linkage in a Tunisian family to 11q15. Another Tunisian family which has no linkage to neither of the identified loci indicated further heterogeneity for the disease (1999).

In 2000, myotubularin-related protein-2 (*MTMR2*) gene which is a dual specificity phosphatase (DSP) was found to be mutated in the patients that were linked to the 11q23 region. The subtype was named as CMT4B1. Loss of function mutations identified in the study, except the premature termination, disrupts either PTP/DSP domain or SID domain. It was hypothesized that in the absence of *MTMR2,* a substrate, which is not identified yet, might be phosphorylated causing Schwann cells to proliferate and results in the myelin overgrowth of the peripheral nerve (Bolino *et al.,* 2000).

The gene mutated in CMT4B2 patients was identified in 2003 as SET (Suvar3-9, Enhancer-of-zeste, Trithorax) Binding Factor 2 (*SBF2*) in a Turkish inbred family. SBF2 is a member of pseudo-phosphatase branch of myotubularins and because of being highly homologous to *MTMR2* gene, it was a good candidate. The deletion of exons 11 and 12 in four affected individuals hypothetically causes the disruption of the N-terminal of the protein which is highly conserved in *SBF2* in different species (Senderek *et al.*, 2003b). Azzedine *et al.* also declared that they have identified two nonsense mutations in a newly discovered gene and they named it as *MTMR13* (2003), which was the SBF2 gene previously reported by Senderek *et al.* (2003b).

1.1.1.3. CMT4C. CMT4C is an autosomal recessive sensory-motor neuropathy characterized by scoliosis which starts in childhood or adolescence (Leguern et al, 1996).

The disease was localized to the 5q23-q33 region in an Algerian family (Leguern, *et al.*, 1996) and refined to a 1.7 Mb region. *KIAA1985*, a transcript in this region, was found to be mutated in the affected individuals. Its hypothetical translation gives rise to a protein from a new protein family which codes for multiple SH3 and TPR domains. These domains are speculated to be involved in protein complex formations; thus, the protein is suggested to act as an adapter or docking molecule. Because of its neural expression, it is a good candidate gene. Eight truncation mutations were identified in affected families (Senderek *et al.,* 2003c).

1.1.1.4. CMT4D (HMSNL). CMT4D is also known as hereditary motor and sensory neuropathy–Lom (HMSNL) named after the geographic region where the disease was first described. It is an autosomal recessive form of CMT disease (Kalaydjieva *et al.*, 1996).

The disease, linked to the 8q24.3 region in the genome, is an early onset neuropathy and patients develop deafness between 20-40 years of age. After the refinement of the linked region, *N-myc downstream-regulated gene 1* (*NDGR1*) was found to have the same p.R148X (c.564C→T) mutation in 60 patients indicating a founder effect (Kalaydjieva *et al.*, 2000).

The disease causing gene, *NDRG1*, consists of 16 exons including an untranslated first exon (Kalaydjieva *et al.*, 2000). A study done with mice showed that mouse homolog *Ndrg1* is essential for the maintenance of the myelin sheaths in peripheral nerves (Okuda *et al.*, 2004). In another expression study by Berger *et al.* it was shown that the gene was expressed in the peripheral nervous system only in myelinating Schwann cells but not in the sensory or motor neuron and neither in their axons (2004). As Schwann cell dysfunction and early axonal involvement occurs at the same time in the disease, it was suggested that the disease pathogenesis depends on the defects in the axon-glia interactions. However, it is still not known whether the primary defect is in the nerve or the Schwann cell (Kalaydjieva *et al.*, 2000).

1.1.1.5. CMT4E. CMT4E is also known as congenital hypomyelinating neuropathy (CHN). The disease starts at early ages with hypotonia, slow nerve conduction velocities, areflexia and distal muscle weakness. Hypomyelination is observed in all or most of the fibers. *Krox20*, a member of multigene family of zinc finger proteins, is expressed in the nervous system and speculated to be an immediate early protein. The expression pattern and knockout model of *Krox20* indicated that *EGR2*, the human homolog, could be a good candidate for CMT4E and a homozygous I218N missense mutation which segregated perfectly within an affected family was identified in the EGR2 gene (Warner *et al.*, 1998). Depending on this information, Warner *et al.* hypothesized *Krox20* to be a transcription factor affecting late myelin genes (*PMP22*, *Cx32*, *MPZ*) and *EGR2* is accepted to be responsible from human myelinopathies of the PNS (1998).

1.1.1.6. CMT4F. CMT4F locus, located on 19q13.1-13.3, spans a region of more than 8.5 cM interval. CMT4F is an early childhood disease in which patients suffer from distal muscle weakness and severe sensory loss (Delague *et al.,* 2000).

The periaxin gene (*PRX*) in human was mapped to 19q13 locus and known to encode for L- and S-periaxin proteins expressed in myelinating Schwann cells making it a good candidate gene for CMT4F. A nonsense mutation in *PRX* was identified in the affected individuals of a Lebanese family and a similar phenotype was observed in periaxin-null mice providing evidence for *PRX* to be the causative gene for CMT4F phenotype in human (Guilbot *et al.*, 2001).

1.1.1.7. CMT4G (HMSNR). CMT4G was named as hereditary motor and sensory neuropathy – Russe (HMSNR) since most of the affected individuals live in the city Russe in Bulgaria. It is a severe form of autosomal recessive Charcot-Marie-Tooth disease characterized by decreased MNCV, high threshold for electrical nerve stimulation and noticeable sensory loss in all modalities (Rogers *et al.*, 2000).

The disease was found to be linked to the 10q22-q23 region and the *EGR2* gene located in this region was excluded for mutations in CMT4G patients. All the patients had the same seven-marker haplotype for the region suggesting the probability of a founder mutation (Rogers *et al.*, 2000).

1.1.1.8. CMT4H. CMT4H was described in 2005 in two families form Lebanon and Algeria. The clinical findings of two families were similar; the age of onset was at 2 years and progression was slow. Other features observed in the patients were severe scoliosis, pes cavus, muscle weakness and atrophy of distal extremities, absent tendon reflexes, ataxia and waddling gait. A severe loss of myelinated fibers occurred in the patients indicating a severe demyelinating motor and sensory neuropathy (De Sandre-Giovannoli *et al.*, 2005).

CMT4H has linkage to the locus on chromosome 12p11.21-q13.11 that spans approximately 15.8 Mb and has more than 90 genes. Although *PRPH* (encoding a type III intermediate filament protein, peripherin) and *CNTN1* (encoding a neuronal cell adhesion molecule, contactin) located in this region were screened for mutations because of their functional properties, no association could be identified. Since, two families showing linkage to CMT4H locus have different haplotypes the possibility of having a founder mutation was excluded (De Sandre-Giovannoli *et al.*, 2005).

1.1.2. Autosomal Recessive Charcot-Marie-Tooth Disease Type 2 (ARCMT2)

Autosomal recessive Charcot-Marie-Tooth disease type 2 is an early onset severe neuropathy with a low prevalence. The common clinical features observed in 90 per cent of the patients include symmetrical muscle weakness and wasting of the distal lower limbs, walking difficulties and foot deformities. In ARCMT2, the NCV values of the median motor nerve are higher than 38m/s and despite the loss of myelinated fibers, regeneration is not observed (De Sandra-Giovannoli *et al.*, 2002). Until now three loci have been identified to be responsible for ARCMT2 (Berghoff *et al.*, 2004).

Table 1.2. ARCMT2 genes and loci

Affected Gene	Loci	Feature	Nomenclature
GDAP1	8q13-q21	Demyelinating & Axonal	CMT4A, ARCMT2
LMNA	1q21.2-q21.3	Axonal	ARCMT2A
Unknown	19q13.3	Axonal	ARCMT2B

1.1.2.1. ARCMT2A (CMT2B1). ARCMT2A was linked to 1q21.2-q21.3 region by Bouhouche *et al.* in a Moroccan family (1999). De Sandra-Giovannoli *et al.* (2001) also found linkage to this locus in three Algerian families and identified a disease causing mutation (c.892C→T) in *LMNA* gene with a homozygous p.R298C amino acid substitution.

LMNA is an approximately 24kb gene with 12 exons. An alternative splicing occurs in exon 10 (Figure 1.5) that gives rise to two isoforms of the protein, lamin A and lamin C. Head domain, central rod domain, carboxyl-terminal tail and nuclear localization signal are present in both isoforms of the protein (Lin and Worman, 1993).

The p.R298C mutation affects a highly conserved residue of the evolutionarily conserved rogd domain of LMNA present in both isoforms. As this domain is required for the protein-protein interactions, it was suggested that the mutation might be disrupting the

interactions of LMNA with other proteins. A similar phenotype was observed in the *lmna* null mice indicating *LMNA* as the disease causing gene in ARCMT2A (De Sandra-Giovannoli *et al.*, 2002).

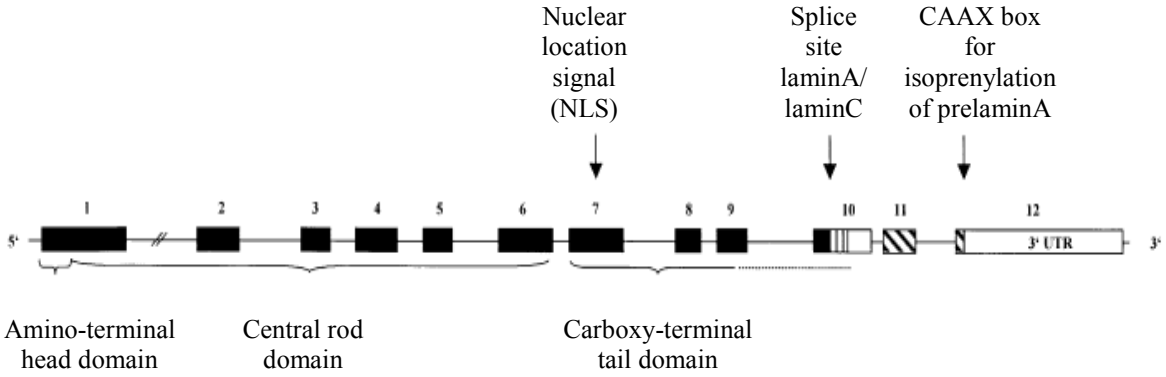

Figure 1.5. Scheme of the LMNA gene domains and alternative splicing (Genschel and Schmidt, 2000)

LMNA is a ubiquitously expressed gene which causes several human diseases (laminopathies) when mutated. However, discovery of its involvement in axonopathies indicates further functions of the gene required for the integrity and maintenance of different cell lineages. Moreover, as a nuclear lamin, LMNA belongs to the intermediate filament multigene family, like NEFL protein involved in CMT2E indicating that other intermediate filaments can also be the cause of such axonal neuropathies (De Sandra-Giovannoli *et al.* 2002).

Furthermore, c.99G→T (p.E33D) mutation identified in *LMNA* caused mixed phenotypes of autosomal dominant axonal neuropathy as well as muscular dystrophy, cardiac disease and leuconychia. This suggests the role of *LMNA* in autosomal dominant neuropathies as well as ARCMT2 (Goizet *et al.*, 2005; Vital *et al.*, 2005). The same glutamine residue, at position 33, was found to be mutated (p.E33G) in ARCMT2 and Emery-Dreifuss muscular neuropathy (EDMD) indicating the difficulty of genotype-phenotype correlation (Goizet *et al.*, 2005).

1.1.2.2. ARCMT2B. ARCMT2B was linked to chromosomal locus 19q13.3 spanning a 5.5 cM region in a Costa Rican family. Epithelial membrane protein 3 (*EMP3*) located in

this locus was a good candidate gene since it is a member of four-transmembrane-domain gene family to which PMP22 belongs. However, no disease causing mutations could be identified in this gene (Leal *et al.*, 2001) or in the others linked to that locus until now (Berghoff *et al.*, 2004).

The disease symptoms appear between ages of 26-42 years. Mostly the lower limbs are severely affected and distal atrophy, motor involvement, muscle weakness, reduced or absent tendon reflexes are the other features. In the later stages of the disease skeletal deformities in foot can be observed. Furthermore, different features can also be observed in different members of the family carrying the same disease causing mutation (Berghoff *et al.*, 2004).

1.1.2.3. ARCMT+Hoarseness. The phenotype was linked to 8q21.3 (Barhoumi *et al.*, 2001) that harbors the GDAP1 gene. Identification of mutations in *GDAP1* in these patients showed that the gene was responsible for both autosomal recessive axonal (Cuesta *et al.*, 2002) and demyelinating CMT (Baxter *et al.*, 2002). GDAP1 gene function and mutations were discussed in detail in section 1.1.1.1.

1.2. Distal Hereditary Motor Neuropathy (dHMN)

Clinical and electrophysiological evaluation of several CMT patients revealed that some had only motor abnormalities but not sensory abnormalities (Harding and Thomas, 1980). This entirely motor variant of CMT was named as spinal CMT or hereditary spinal muscular atrophy and classified as the distal hereditary motor neuropathy (dHMN) group (Irobi *et al*., 2004b). However, whether the pure motor neuropathy definition is suitable for dHMN is questionable since weak sensory involvements can be observed in some patients (De Jonghe *et al.*, 1997; Irobi *et al.*, 2004).

Progressive weakness and wasting of the extensor muscles of the toes and feet represents the overall clinical picture of the disease. In its later stages, weakness and wasting of the distal upper limb muscles can also be observed in the patients. Foot deformity is another common feature of the disease. In the rare “complicated” form of distal HMN, predominance in the hands, vocal cord and diaphragm paralysis and

pyramidal tract signs are also observed. It is hard to differentiate dHMN from CMT because the only difference, plain sensory signs, is not clinically observable. Thus, electrophysiological examinations are necessary for the certain diagnosis of the disease (Harding and Thomas, 1980).

Table1.3. The loci and the genes associated with dHMN subtypes (AD: Autosomal Dominant; AR: Autosomal Recessive) (Stock *et al.*, 2003; Irobi *et al*., 2004b; Tang *et al*., 2005)

Gene	Locus	Disease	Inheritance and Phenotype
Unknown	Unknown	dHMN-I	AD juvenile-onset with distal wasting and weakness
HSPB8	12q24.3	dHMN-II CMT2L	AD adult-onset with distal muscle wasting and weakness
HSPB1	7q11.23	dHMN-II CMT2F	AD adult-onset with distal muscle wasting and weakness
Unknown	11q13	dHMN-III	AR early adult-onset, slow progressive muscle wasting and weakness and no diaphragmatic paralysis
		dHMN-IV	AR juvenile-onset, severe muscle wasting and weakness, and diaphragmatic paralysis
GARS	7p15	dHMN-V, CMT2D	AD upper limb predominance; occasionally pyramidal features
BSCL2	11q12-q14	dHMN-V, Silver Syndrome	AD prominent hand muscle weakness and wasting, and mild to severe spasticity of the lower limbs
IGHMBP2	11q13.2-13.4	dHMN-VI, SMARD1	AR severe infantile form with respiratory distress
Unknown	2q14	dHMN-VII	AD adult-onset with vocal cord paralysis
DCTN1	2p13	dHMN-VII	AD adult-onset with vocal cold paralysis and facial weakness
SETX	9q34	dHMN, ALS4	AD early-onset with pyramidal tract sign
Unknown	9p21.1-p12	dHMN-J	AR juvenile-onset with pyramidal features
Unknown	12q23-q24	Congenital distal SMA	AD congenital non-progressive distal HMN with contractures

Distal HMN is a clinically and genetically heterogeneous disease and classified according to the age at onset, mode of inheritance, and presence of additional features. Twelve chromosomal loci and seven disease-causing genes (Table 1.3) have been found for the autosomal dominant and recessive forms of the disease. On the other hand, there is no X-linked inheritance reported up to now (Irobi *et al*., 2004) and still some dHMN families could not be classified according to the conventional system (van der Vleuten *et al.*, 1998; Chistodoulou *et al.*, 2000; De Jonghe *et al.*, 2002). The causative genes usually have house keeping functions in glycosylation, axonal trafficking, RNA processing, editing, stress response and apoptosis. Functional characterization of the mutations is required to determine the cellular processes leading to motor neuropathies (Irobi *et al*., 2004b).

1.2.1. Small Heat Shock Protein 22 (*HSP22*; *HSPB8; H11*; *E2IG1*)

HSPB8 is a member of mammalian small heat shock protein (stress protein) superfamily. Small heat shock proteins (sHSPs) work as molecular chaperones in the cell but their roles also include providing the correct folding of the denatured proteins by assisting them in a variety of stress conditions such as high temperatures, in the presence of heavy metals, oxidation, and preventing their aggregation. Furthermore, they interact with cytoskeleton and programmed cell death components, intervening with the apoptotic pathways (Dierick *et al.*, 2005).

In all organisms, there are genes coding for sHSPs. The human genome has 10 sHSP which are named as HSPB1-HSPB10 (Kappé *et al.*, 2003). A conserved C-terminal α-crystallin domain, a more variable N-terminal sequence and a short variable C-terminal tail are present in all members of the sHSP superfamily (Dierick *et al.*, 2005). The other conserved sequence of the gene, the WDPF motif, is located in the N-terminal region (Irobi *et al.,* 2004a).

Although HSPB8 was first announced to be a protein kinase, phylogenetic analysis indicated that it belongs to the mammalian sHSP superfamily and it is closely related to HSPB1 among other proteins in the family (Sun *et al.,* 2004).

sHSPs form homo- and heterooligomers which are thought to be necessary for the sHSPs to function because these complexes have important roles in the cell survival under stress conditions. The complexes in which HSPB8 is involved were found by using different techniques including gel filtration HPLC, yeast two-hybrid method, cross-linking and fluorescence resonance energy transfer microscopy. The results showed that HSPB8 homodimers which can also form tetramers involve interactions between N-terminals of the proteins as well as the N-terminal of one and the C-terminal of the other. HSPB8 forms heterodimers with HSPB1, HSPB2 and HSPB7. The interacting parts of the proteins were identified by using certain constructs of the gene coding for only C-terminal, N-terminal or full length protein. Heterodimers of HSPB7 and HSPB8 are formed through interactions between the C-terminals of the protein. However, heterodimers involving HSPB2 formed through C-terminal half of HSPB8 and full length HSPB2 whereas the ones involving HSPB1 are formed through full length HSPB8 and C-terminal half of HSPB1. The other sHSPs have not been tested as interaction partners of HSPB8, yet (Sun *et al.,* 2004).

The first mutation identified in *HSPB8* was a heterozygous transversion (c.423G→C) in Belgian and Czech dHMN-II families resulting in amino acid substitution p.K141N. The affected glutamine residue is located in the central part of the α-crystallin domain (Irobi *et al.,* 2004a). The same amino acid of *HSPB8* was found to be mutated in CMT2L patients with a c.423G→T missense substitution (Tang *et al.*, 2005). Another heterozygous transition (c.421A→G) was observed in two families from Bulgaria and England involving the same amino acid and resulting in the p.K141E substitution (Irobi *et al.,* 2004a). This critical residue which is known to be necessary for the functional and structural integrity of the αA-crystallin domain (Bera *et al.*, 2002) corresponds to Arg120 in HSPB5 (*αB-crystallin*, *CRYAB*) and causes a desmin-related myopathy (DRM) when mutated (Vicart *et al.*, 1998). The same residue corresponds to Arg116 and causes autosomal dominant congenital cataract when mutated in *HSPB4* (*αA-crystallin*, *CRYAA*) (Litt *et al.*, 1998).

HSPB8, with a high expression level in skeletal and smooth muscles, heart and brain, was found to be an interaction partner of HSPB1 by yeast two-hybrid screen of a human heart cDNA library. A mimic of phosphorylated HSPB1 (^{3D}HSP27) was used as bait construct. A 21.6 kDa protein was obtained which has a α-crystallin domain and named as HSPB8 (Benndorf *et al.*, 2001). In a coimmunoprecipitation study it was found that the

expression of the mutant proteins (p.K141N and p.K141E) strengthened the interaction of HSPB8 and HSPB1 forming aggregates in cytoplasm and perinuclei. Wild type and mutant HSPB8 tagged with enhanced green fluorescent protein (EGFP) were transiently expressed in simian fibroblasts (COS) and human embryonic kidney cells (HEK293T). The western blot analysis that was used to check the presence of HSPB1 in the immunoprecipitates indicated that more HSPB1 were pulled down by both mutants of HSPB8 than by wild type protein. Immunofluorescence studies identified perinuclear and cytoplasmic aggregates in the COS cells transfected by mutant forms of HSPB8. It was also found that, the cell viability in N2a neuronal cells transfected with p.K141E and p.K141N mutants decreased in comparison with the cells transfected with the wild type in a measurement done 48 hours after the transfection (Irobi *et al.,* 2004a). However, as these results are from in vitro studies, experiments on model animals are necessary to see whether these changes also occur during the slow progress of the motor neuron disease dHMN (Irobi *et al.,* 2004a).

The mutations affecting Lys141 residue of HSPB8 probably acts via a gain-of-function effect and may interfere with axonal transport, regulation of cytoskeleton and finally cause motor neuron death in dHMN. Although the mechanism leading to the pathogenesis can be completely different it was shown that HSPB8 has an important key role in biology of motor axons (Irobi *et al.,* 2004a).

1.2.2. Small Heat Shock Protein 27 (*HSP27*; *HSPB1*)

HSPB1 is another member of the sHSP superfamily with a proposed role in the contraction of smooth muscle cells in its phosphorylated form. Phosphorylation of human HSPB1 occurs at three positions which are Ser^{15}, Ser^{78} and Ser^{82} by MAPKAPK-2. This process causes the disassembly of large complexes usually giving rise to tetramers. The two interaction sites of HSPB1 are present in C-terminal α-crystallin domain and N-terminal end. The C-terminal interaction site is thought to be involved in the homodimer formations whereas N-terminal parts are used for the further multimerization to form tetramer structures. It is also possible that HSPB1 may have other interaction sites (Sun *et al.*, 2004).

After the detection of mutations in the HSPB8 gene, *HSPB1* was also reported to cause both CMT2 and dHMN. Firstly, *HSPB1* was found to be mutated in a Russian family suffering from CMT2F with an age of onset at 15-25. The family members with the disease had absent or depressed tendon reflexes together with distal sensory abnormalities ranging from mild to moderate. The atrophy and progressive symmetrical weakness were present in the distal limb muscles especially affecting the peroneal muscles in the legs. Following this findings, four families of different origins (England, Belgium, Croatia and Austria) were also found to carry *HSPB1* mutations causing either CMT2 or dHMN (Evgrafov *et al.*, 2004). A total of six mutations were identified in *HSPB1* until so far (Evgrafov *et al.*, 2004; Kijima *et al.,* 2005).

One of the mutations, c.404C→T (p.S135F), caused both CMT2F and dHMN-II phenotypes (Evgrafov *et al.*, 2004). P182L and P182S mutations are located in the C-terminal region of the protein and cause dHMN phenotype (Evgrafov *et al.*, 2004; Kijima *et al.,* 2005). P182 is close to the location of dominant mutations observed in αB-crystallin affecting the chaperone function as well as solubility of the protein (Evgrafov *et al.*, 2004).

Four of the mutations (p.R127W, p.S135F, p.R136W and p.T151I) occurred in the α-crystallin domain of *HSPB1*, close to the conserved residue Arg140 (Evgrafov *et al.*, 2004). Arg140 is an important amino acid as it is necessary for the functional and structural integrity of αA-crystallin (Bera, *et al.*, 2002). It corresponds to Arg116, Arg120 and Arg141 in HSPB4, HSPB5 and HSPB8, respectively and cause several human diseases when mutated. All six mutations occurred at conserved residues among HSPB1 homologs (Evgrafov *et al.*, 2004).

Different expression studies were carried on to find out the function of HSPB1 in the cell. For this purpose, mouse neuroblastoma cells (N2a) were transiently transfected with wild type and p.S135F *HSPB1* mutant constructs for a cell viability and proliferation assay. The results indicated a reduced cell number in the cells transfected with the mutant *HSPB1* in comparison with the wild type gene. This was not an unexpected result as the primary cause of CMT and dHMN is the premature axonal degeneration. The p.S135F mutant was also coexpressed with *NEFL*, the causative gene for CMT2E, in SW13.cl.2Vim$^-$ cells, an adrenal carcinoma cell line that does not contain an endogeneous intermediate filament

network. Aggregates of neurofilament light protein as well as a decrease in the amount of filamentous NEFL were observed at the end of the experiment (Evgrafov *et al.*, 2004).

Another expression study involving the p.P182L mutant located in the variable C-terminal of the protein also demonstrated the role of mutant *HSPB1* in cellular transport processes. Cortical cells were transfected with wild type and p.P182L mutant constructs in this study. A high amount of HA-tagged mutant HSPB1 was observed in aggresomes mostly in the cell body as well as a small amount in the neurites in comparison with the cells transfected with the wild type construct. The distance of transport for the wild type and mutant proteins labelled by GFP indicated that p.P182L mutant could only moved until the proximal portions of the neuritis while the wild type protein was transported through the whole neurites. Amorphous and non-filamentous structures were observed in the cell bodies, instead of fine filamentous network. Furthermore, a selective disruption of certain cargoes was present in the cortical cells transfected with mutant *HSPB1*. The transport of mitochondria was not affected while synaptotagmin I, the vesicle-associated protein, was not transported through the axons (Ackerley, *et al.*, 2005).

HSPB1 was shown to be expressed in ventral horn and sensory ganglia of mouse embryos. This expression pattern is compatible with the pure motor neuropathy, dHMN, and a mixed neuropathy involving both motor and sensory neurons, CMT, caused by *HSPB1* mutations (Evgrafov *et al.*, 2004). Mutations in *GARS* were also reported by Antonellis *et al.* to cause both CMT2D and dHMN-V (2003) similar to the situation of *HSPB8* and *HSPB1*.

Small heat shock proteins as molecular chaperons were already implicated to cope with the misfolding and abnormal aggregation of the proteins in neurodegenerative diseases (Muchowski and Wacker, 2005). The disease causing mutations in HSPB1 (Evgrafov *et al.*, 2004) and its molecular partner HSPB8 suggests a disease mechanism possibly involving the functions of both proteins. When mutated, *HSPB8* and *HSPB1* cause dysfunction of the axonal transport and axon cytoskeleton that are the major pathways leading to distal HMN. However, the way of functioning of these molecular chaperons with other proteins involved in the motor neuron function is not known yet (Irobi *et al.,* 2004a).

1.3. Hereditary Spastic Paraplegias (HSP, Strümpell-Lorrain Syndrome)

Hereditary spastic paraplegia (HSP) patients have the bilateral, symmetric, progressive lower limb spastic weakness as the characteristic symptoms. However, this feature of the disease is shared by many other neurodegenerative diseases and spastic gait is the distinctive feature for HSP. There are also other features of the disease like urinary urgency and wheelchair dependence. The age of onset and degree of disability differs among the patients as well as between the members of the same family. HSP is classified as pure (uncomplicated) and complicated depending on whether the paraplegia occurs in isolation or with the other features of the disease, respectively. The disease is in the pure form if it is associated with lower extremity hyperreflexia, lower extremity spastic weakness, loss of vibratory sensation and extensor plantar responses. However, the complicated disease appears with presence of systemic or neurologic impairments such as cataracts, mental retardation, epilepsy, cerebellar signs, optic atrophy, muscle wasting and motor neuropathy in addition to the symptoms of the pure type. The disease is genetically heterogeneous and autosomal recessive, dominant and X-linked recessive inheritance can be observed for both the pure and complicated types of paraplegias. However, pure HSP is usually autosomal dominantly inherited, while the complicated ones present autosomal recessive inheritance (Reid, 1999; Fink, 2003).

Thirty-three loci are linked to the disease phenotype while eight genes for autosomal dominant (*Atlastin*, *Spastin*, *KIF5A*, *HSP60*, *NIPA1*, *BSCL2*, *REEP1* and *ZFYVE27*) and three genes for autosomal recessive (*Paraplegin*, *Spartin*, *Maspardin*) forms as well as two genes for X-linked form (*L1CAM*, *PLP*) have been identified so far (Patel *et al.*, 2001; Fink, 2003; Windpassinger *et al.*, 2004; Klebe *et al.*, 2006; Züchner *et al.*, 2006b; WUSTL). Among these genes, spastin and paraplegin were suggested to have chaperon activities (Hansen *et al.*, 2002).

1.3.1. Heat Shock Protein 60 (*HSP60*, *Cpn60*, *HSPD1*)

There are type 1 and type 2 chaperonins which are classified according to the number of monomers forming the ring structures of the subunits. Type 1 and type 2 chaperonins have 7-mer and 8-mer ring structures, respectively. *HSP60* together with its co-chaperonin,

HSP10, as well as their *E. coli* homologs *GroEL* and *GroES* (Bukau and Horwich, 1998), respectively belong to the group of type 1 chaperonins.

HSP60 is located head to head with *HSP10* (heat shock protein 10, *Cpn10*, *HSPE1*) sharing the same bidirectional promoter and together they span a 17kb region on human genome (Figure 1.6). The start codons of two genes are seperated with a 1588 bp sequence. The first exon of *HSP60* is non-coding while the last codon of the first exon of *HSP10* is the start codon for the protein. The alternative splicing occurs within the first exon of *HSP60* giving rise to transcripts of different sizes. It is suggested that the alternatively spliced 5'-UTR region might be controlling the stability of transcripts, starting region of translation or introducing different mechanisms of translational initiation (Hansen *et al.*, 2003).

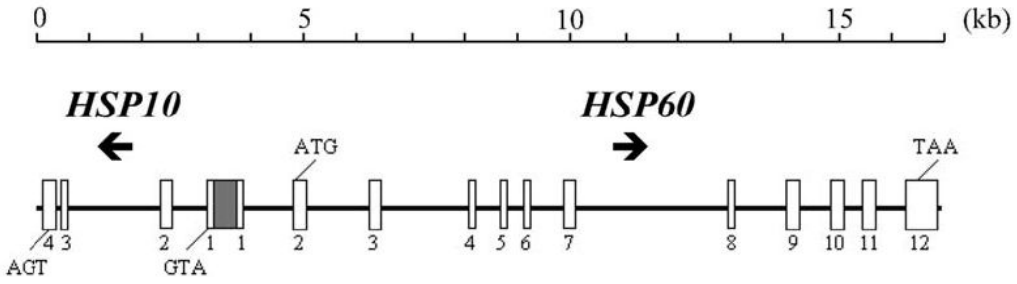

Figure 1.6. Schematic view of *HSP10* and *HSP60* genes in human genome (Hansen *et al.*, 2002)

The bidirectional promoter region between the genes has different activities for the two genes and the promoter works twice as efficient as *HSP10* for *HSP60* gene transcription. In heat shock conditions, although this ratio does not change, the transcription level of the genes increases 12 times (Hansen *et al.*, 2003).

HSP60 (heat shock protein 60, *Cpn60*, *HSPD1*), a mitochondrial chaperonin, is one of the genes causing autosomal dominant pure form of HSP. This gene is located on the 2q33.1 region, which was previously linked to SPG13 (Spastic Paraplegia 13) locus in a French HSP family (Fontaine *et al.*, 2000; Hansen *et al.*, 2002). The gene was found to be mutated in this family and it was the first *HSP60* mutation causing a human disease. Sequencing of the 12 exons revealed a heterozygous G→A substitution at position 292.

The variation substituted the valine at position 72 with an isoleucine residue (p.V72I). A second mutation c.551A→G replaced the N158 residue with a serine residue (p.N158S). The Val72 residue corresponds to Val74 in the *E. coli* HSP60 homolog GroEL and found in conserved helix C of the equatorial domain whereas N158 corresponds to L160 which is located in the side chain of the intermediate domain protruding from the barrel structure of the protein. Although the wild type human *HSP60-HSP10* and p.N158S mutant constructs could compensate the deletion of the wild type *E. coli* groESgroEL operon, p.V72I mutant *HSP60-HSP10* construct failed to provide viable *E. coli* strains. This indicates the importance of the Val72 residue for the functioning of the protein. No mutation could be identified in the four exons of the HSP10 gene (Hansen *et al.*, 2002; 2003). As *HSP60* mutation shows its effect in an autosomal dominant fashion, involvement of mutant subunits along with the wild type monomers in the formation of chaperonin ring might be decreasing the activity of HSP60 which cannot be compensated by the wild type allele, especially under stress conditions (Hansen *et al.*, 2002).

Another mitochondrial protein that was recently reported to cause HSP is Receptor Expression-Enhancer Protein 1 (*REEP1*) (Saito et al., 2004). The gene is located on chromosome 2p12 that was designated as the SPG31 locus by Züchner *et al.* (2006a). Among the nine candidate genes in the region, *REEP1* was found to have mutations in a Caucasian family suffering from uncomplicated autosomal dominant HSP. Depending on the domain similarities the protein was suggested to have chaperone-like activities and immunohistochemistry studies indicated that, REEP1 is localized in mitochondria (Züchner *et al.*, 2006b).

Four of the proteins (Paraplegin, Spastin, HSP60 and REEP1) reported to be involved in hereditary spastic paraplegia have chaperon-like activities. Thus, the importance of chaperones in neurodegenerative diseases is increasing and it was suggested that a high proportion of hereditary spastic paraplegias are mainly chaperonopathies (Hansen *et al.*, 2003). As it has been known that misfolding of the proteins is responsible for many diseases, it is not unexpected to find out many proteins with chaperon activities, like HSPB8, HSPB1, HSP60, Paraplegin, Spastin and REEP1, are involved in several human neurodegenerative diseases like CMT, dHMN and HSP.

Defects in mitochondrial proteins were linked with several diseases (Figure 1.7). Mitochondria's important roles in neurodegenerative diseases were also underlined by the discovery of many mitochondrial proteins like GDAP1, paraplegin, BCL2 (antiapoptotic β-cell lymphoma protein), REEP1 and HSP60 are involved in the disease mechanisms of CMT, HMN and HSP in the last decade. Mitochondria are abundant at the synapses which are important neuronal communication sites (Ly and Verstreken, 2006). It was also shown that mutations in the neurofilament gene, NEFL, prevent the transport of mitochondria to nerve terminals and ends up with CMT. This indicates the importance of mitochondria in nerve terminals and they are necessary for the processes like aerobic energy mobilization and biosynthesis of metabolites in this region (Brownless *et al.*, 2002). This also suggests an explanation for why longer axons, especially the distal parts of the neurons are mostly affected in neuropathies caused by mitochondrial proteins (Pedrola *et al.*, 2005).

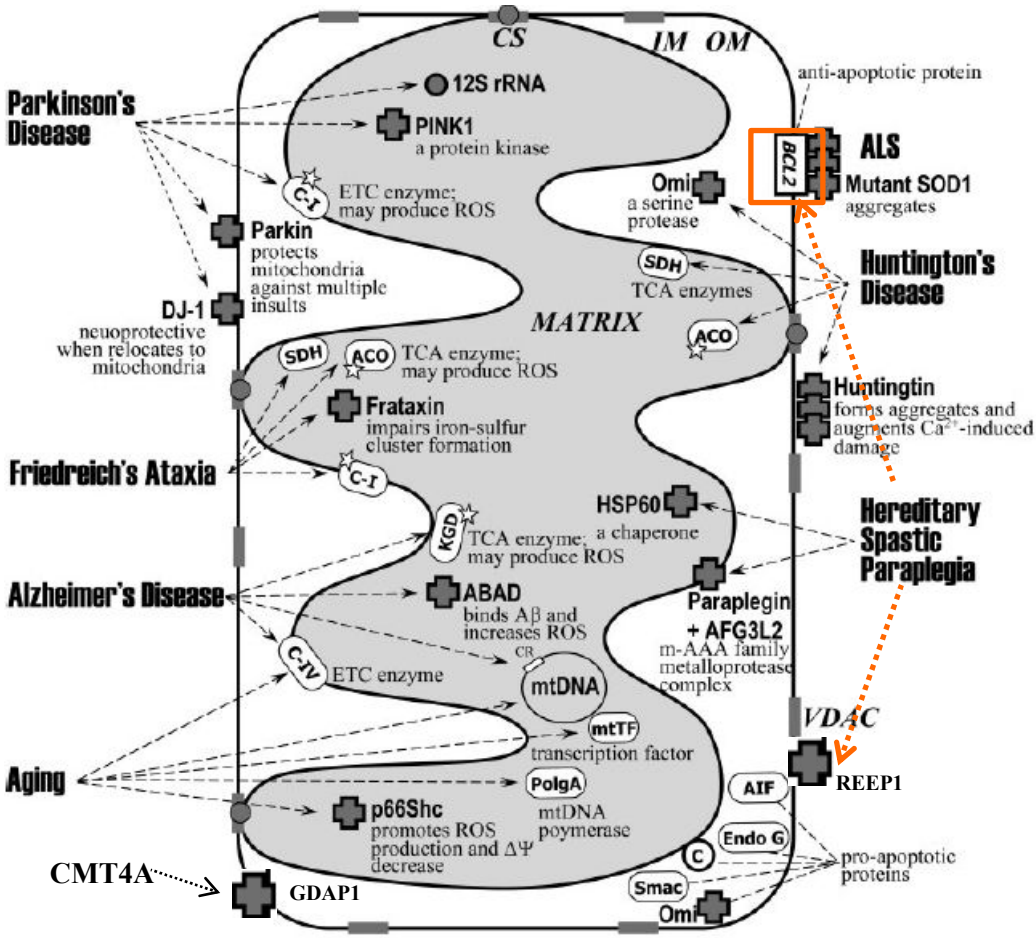

Figure 1.7. Role of mitochondrial proteins in human diseases and aging (Modified from Beal, 2005)

2. AIM OF THE STUDY

In the preceding studies of our group, we have assessed a high frequency of autosomal recessive CMT cases in the Turkish population. In the light of this information, we aimed to identify the involvement of the known autosomal recessive CMT2 loci in our cohort of patients. For this purpose, the recently identified ARCMT2 genes, namely, *GDAP1* and *LMNA* were screened for mutations and the third locus, ARCMT2B, was analyzed for homozygosity since the responsible gene in this region has not been identified, yet.

The role of small heat shock proteins, *HSPB1* and *HSPB8*, in distal hereditary motor neuropathy and *HSP60* in hereditary spastic paraplegia has also been reported recently. Thus, we aimed to identify the contribution of these genes to Turkish dHMN and HSP genetic backgrounds. Since mutations in *HSPB8* and *HSPB1* were reported in several autosomal dominant CMT2 patients, our cohort of CMT2 patients was also included in the study.

3. MATERIALS

3.1. Human Peripheral Blood Samples

The peripheral blood samples of the CMT, HMN and HSP patients and their family members were provided by Istanbul University Medical School, Department of Neurology with an informed consent.

3.2. Chemicals

All solid and liquid chemicals used in this study (Table 3.1) were purchased from Sigma (USA), Merck (Germany), Riedel de-Häen (Germany), and Carlo Erba (Germany), unless stated otherwise in the text.

3.3. Fine Chemicals

3.3.1. Enzymes

Taq DNA Polymerase and the restriction enzyme *Hpa*II were purchased from Promega (USA).

3.3.2. Oligonucleotide Primers

The sequences of the primers used to amplify the exons and the flanking intronic regions of the *LMNA, GDAP1*, *HSPB8*, *HSP60* and *HSPB1* genes are given in Table 3.1, Table 3.2, Table 3.3, Table 3.4, and Table 3.5, respectively. The primers were purchased from Integrated DNA Technologies, Inc. (USA). The sets of primers used for homozygosity mapping of CMT4A locus and ARCMT2B locus are listed in Table 3.6 and Table 3.7, respectively. The primers used in the Amplification Refractory Mutation System (ARMS) are given in Table 3.8. The primers used in the homozygosity analysis and ARMS method were purchased from GenSet Oligos.

Table 3.1. Sequences of the primers used for exon amplification of the LMNA gene (F: Forward primer, R: Reverse primer)

Exon	Primer Name	Primer Sequence	PCR Product Length (bp)	PCR Annealing Temp (^{0}C)
Exon1	LMNA 1F	CCGAGCAGTCTCTGTCCTTC	294	60
	LMNA 1aR	GACCACCTCTTCAGACTCGG		
	LMNA 1b.F	CTCGCTGGAAACGGAGAAC	299	63.3
	LMNA 1R	CCCTCTCACTCCCTTCCTG		
Exon2	LMNA 2F	GCACTGTCTAGGCACACAGACT	290	62
	LMNA 2R	GGGAGGGCCTAGGTAGAAGA		
Exon3	LMNA 3F	TGTGACCCCTTTTCCTCATC	281	56
	LMNA 3R	CACTAGGGCAAGGGACTCAG		
Exon4	LMNA 4F	GGTTTCTGTGTCCTTCCTCC	289	63.3
	LMNA 4R	CTGATCCCCAGAAGGCATAG		
Exon5	LMNA 5F	CTCCCAGTCACCACAGTCCT	306	62
	LMNA 5R	GTGGTTGTGGGGACACTTTT		
Exon6	LMNA 6F	TCCTTCCCCATACTTAGGGC	348	63.3
	LMNA 6R	GGGGTCTAGTCAAGGCCAG		
Exon7	LMNA 7F	GGCAACTGGCCTTGACTAGA	330	65
	LMNA 7R	CTGTCTTGCCACTCTCTCCC		
Exon8	LMNA 8F	GCAAGATACACCCAAGAGCC	246	65
	LMNA 8R	GAAAAGGACACTTACCCCAGC		
Exon9	LMNA 9F	GCTGGGGTAAGTGTCCTTTTC	243	65
	LMNA 9R	GAATTGGCAAACTTGGGTTG		
Exon10	LMNA 10F	GTAGACATGCTGTACAACCC	287	62
	LMNA 10R	GGCCAGCGAGTAAAGTTCCA		
Exon11	LMNA 11F	TTGGGCCTGAGTGGTCAGTC	373	62
	LMNA 11R	GACCCGCCTGCAGGATTTGG		
Exon12	LMNA 12F	ATCGAGGGGTAGGACGAGGT	314	63.3
	LMNA 12aR	TGGCAGGTCCCAGATTACAT		
	LMNA 12b.F	TTTCTCTCTTAGAGCCCCCA	329	63.3
	LMNA 12R	TAAGGCAGATGTGGAGTTTCC		

Table 3.2. Sequences of the primers used for exon amplification of the GDAP1 gene (F: Forward primer, R: Reverse primer)

Exon	Primer Name	Primer Sequence	PCR Product Length (bp)	PCR Annealing Temp (^{0}C)
Exon1	G1F	GCCCTTCATAACCAGGGTCT	456	68
	G1R	GCCCGATCCGCGCTACCCTCCG		
Exon2	G2F	GGCTGCTTAGCGGTGTCCAGGG	330	60.9
	G2R	GGGAACACATAGTTGTGTTG		
Exon3	G3F	GCTTTTGAGTGTAACAACTCATG	317	65
	G3R	GACCATGAGACATGCTAGGTC		
Exon4	G4F	CAGGGTAAGCCCAAGGCAGAG	288	66
	G4R	GTAGAACATTTACTCCGTGCAG		
Exon5	G5F	GGCTGAACTCTGTAAGAGTTTG	281	51
	G5R	GACCTAAGAATGTTCCCATG		
Exon6	G6F	CCACTGATACCAGCTGG	530	66
	G6R	CAGAGAGCCACGGGCAATCAC		

Table 3.3. Sequences of the primers used for exon amplification of the HSPB8 gene (F: Forward primer, R: Reverse primer)

Exon	Primer Name	Primer Sequences	PCR Product Length (bp)	PCR Annealing Temp (^{0}C)
Exon1	HSP22.1a.F	GAGAGGCCGGCTGAACTT	257	64
	HSP22.1a.R	CCAGAACCGCTGAGGTCTA		
	HSP22.1b.F	CGTGCCCTGGGTTTATTAAG	260	64
	HSP22.1b.R	CTTCAGCTTCCGAAAATGCT		
	HSP22.1c.F	GTTGGTTCTGCTTCTCCCTG	289	62.5
	HSP22.1c.R	CCAAGAGGCTGTCAAGTCGT		
	HSP22.1d.F	GCTTTGGCATGGACCCCTTC	327	64
	HSP22.1d.R	CAGGGCTGAGGGCTACATC		
Exon2	HSP22.2aF	GGATGCCCAAGGAACATAGA	197	64
	HSP22.2R	AGGGAGAGACCCCAGATCAT		
Exon3	HSP22.3aF	ACAACAATAAATGAATAAAATCGTGTG	240	64
	HSP22.3aR	CCTAGGGTTGGGGACAAAAC		

Table 3.4. Sequences of the primers used for exon amplification of the HSP60 gene (F: Forward primer, R: Reverse primer)

Exon	Primer Name	Primer Sequence	PCR Product Length (bp)	PCR Annealing Temp (^{0}C)
Exon1	H60.1F	ATCCCCGTACGCCTCAGAC	481	58
	H60.1aR	GCGCTCAGCCCTCTC		
	H60.1b.F	GGCCGGAGAGGGCTG	521	59
	H60.1R	AGCGGGCCTAAGTGGTTACAA		
Exon2	H60.2F	ACAGGTGGGCATGTTTGTTC	331	52
	H60.2R	TGTTGAATAGTTCAGTGCGAC		
Exon3	H60.3F	TTAGGGTATGTCTGATCCTGT	376	52
	H60.3R	TTAACACTTTCCTTAGGTCCAA		
Exon4	H60.4F	TAGAAGCCATGAGAGAAATAAA	237	52
	H60.4R	TGGGTAGTATTGTTATTCTGAC		
Exon5	H60.5F	CTGGATGGAAGTATCAATTTGG	389	52
	H60.5R	AATTCACATAAAACACAGTAAGTA		
Exon6	H60.6F	CCTGGGCTGTTTCATACTCT	333	55
	H60.6R	GAGCAACGCGCCACCACAT		
Exon7	H60.7F	CCTTGGTTTCGCTTTTCATTTA	329	55
	H60.7R	CACATGATGGAAACTGCAAACA		
Exon8	H60.8F	AGCTTGAGGGGAATTAAACAG	283	55
	H60.8R	AGAGCCAAAAGAAACAGATAGT		
Exon9	H60.9F	TGATGATTCTCTTGCATGGTGT	443	52
	H60.9R	TCCTCAAGTATTCGTTTAGTTC		
Exon10	H60.10F	ACCTCAGGATTGCTTTTTAAGT	354	52
	H60.10R	CCATTTAGGGGACTGCAACAT		
Exon11	H60.11F	GATCTGTAGTAGGATTGGGATT	389	52
	H60.11R	TTAGACTATTTTTCTGGTGACAA		
Exon12	H60.12F	AGCCACCATGCCCAGACAGA	578	56
	H60.12R	TGGCAAGCACTAAAATCCTGA		

Table 3.5. Sequences of the primers used for exon amplification of the HSPB1 gene (F: Forward primer, R: Reverse primer)

Exon	Primer Name	Primer Sequences	PCR Product Length (bp)	PCR Annealing Temperature (^{0}C)
Exon1	HSP27.1a.F	CCGACTGGAGGAGCATAAAA	220bp	64
	HSP27.1a.R	TAACCACTGCGACCACTCCT		
	HSP27.1b.F	ATAGCCGCCTCTTCGACC	293bp	62.5
	HSP27.1b.R	ACCGGTGATCTCCACCAC		
	HSP27.1c.F	CGTGTCCCTGGATGTCAAC	228 bp	63
	HSP27.1c.R	CTGAGCAAGGGAATCAGGAG		
Exon2	HSP27.2F	CCAACCCCCTCTGTTAATCC	300bp	64
	HSP27.2R	GAGGAAAGGCAAGCGTTACA		
Exon3	HSP27.3F	CTTGCCTTTCCTCTCTGCAC	288bp	64
	HSP27.3R	CAAAAGAACACACAGGTGGC		

Table 3.6. Sequences of the primers used for homozygosity mapping of the CMT4A locus (F: Forward primer, R: Reverse primer)

GenBank Accession Number	Primer Name	Primer Sequence	PCR Product Length (bp)	PCR Annealing Temp (^{0}C)
Z17195	D8S286F	GCTGTTTATTTGCCCATGT	220-238	57
	D8S286R	GCATGAAACTGTCACTGAGA		
L18601	D8S318F	GCACAGGGGTTGACAGTGAATAGT	275-303	58
	D8S318R	CTGAAGAATGAAGACACTGTCCTTT		
Z23429	D8S501F	TGAGGTCATCCTGGAGCAGA	197-217	58
	D8S501R	AAAGGTAATTGAGTCCACGCTTCT		
Z24047	D8S541F	CTGCCTGTATTACTCAGGGT	194-228	58
	D8S541R	CCTCAGCCTGTAGGTGG		
Z24217	D8S548F	CTACCTCATGCAAGGCCA	228-248	58
	D8S548R	CATTGAGCACACCCTCAGT		

Table 3.7. Sequences of the primers used for homozygosity mapping of the ARCMT2B locus (F: Forward primer, R: Reverse primer)

GenBank Accession Number	Primer Name	Primer Sequence	PCR Product Length (bp)	PCR Annealing Temp (^{0}C)
Z52767	D19S879 - F	CTGAGTGTGAATGAGGCAAC	217-265	57
	D19S879 - R	AGGCCAGAGGACTGATTG		
Z53165	D19S902 - F	CCATCCTAATGAGGGCAA	199-217	60
	D19S902 - R	GCACCAGTGACTGCCTGT		
Z53244	D19S907 - F	GTGTCCAATCAACAGACCA	213-223	60
	D19S907 - R	CTGCACTCCAGCAGAAAT		

Table 3.8. Sequences of the primers used for ARMS (F: Forward primer, R: Reverse primer)

Amplified Region	Primer Name	Sequence	PCR Product Length (bp)	PCR Annealing Temp (^{0}C)
Wild Type Sequence	G2 WT F	GCGAGGAACATGATGTAAGTCTGCC	218	62
	G2 R	GGGAACACATAGTTGTGTTG		
Mutant Sequence	G2 M F	GCGAGGAACATGATGTAAGTCTTGTG	218	62
	G2 R	GGGAACACATAGTTGTGTTG		
Exon 2	G2 F	GGCTGCTTAGCGGTGTCCAGGG	330	60.9
	G2 R	GGGAACACATAGTTGTGTTG		

3.3.3. DNA Size Marker

The size marker used in this study was 100-bp DNA ladder with a range of 100-1000 bp (Fermentas, Lithuiania).

3.3.4. Other Fine Chemicals

Deoxyribonucleoside triphosphates (dNTPs) were purchased from Promega (USA). PCR products were purified by using QIAquick PCR Purification Kit (Qiagen, Germany).

3.4. Buffers and Solutions

The buffers, solutions and their ingredients used in this study are listed in Table 3.9.

Table 3.9. Buffers and Solutions

Experimental Procedure	Buffers and Solutions	Constituents
DNA Extraction from Peripheral Blood	Cell Lysis Buffer	155 mM NH_4Cl, 10 mM $KHCO_3$, 1 mM Na_2EDTA (pH 7.4)
	Nuclei Lysis Buffer	10 mM Tris-HCl, 400 mM NaCl, 2 mM Na_2EDTA (pH 7.4)
	Sodiumdodecylsulphate (SDS)	10 per cent SDS (w/v) (pH 7.2)
	Proteinase K	20 mg/ml
	TE Buffer	20 mM Tris-HCl (pH 8.0), 0.1 mM Na_2EDTA (pH 8.0)
	5 M NaCl solution	292.2g NaCl in 1 L dH_2O
Polymerase Chain Reaction (PCR)	10X PCR Buffer with $(NH_4)_2SO_4$	750 mM Tris-HCl (pH 8.8 at 25 ^{0}C), 200 mM $(NH_4)_2SO_4$, 0.1 per cent Tween20 (Fermentas, Lithuania)
	$MgCl_2$	25 mM $MgCl_2$ (Fermentas, Lithuania and Promega, USA)
Agarose Gel Electrophoresis	10X TBE (Tris-Boric Acid-EDTA) Buffer	0.89 M Tris-Base, 0.89 M Boric Acid, 20 mM Na_2EDTA (pH 8.3)
	1, 2 or 3 per cent Agarose Gel	1, 2 or 3 per cent (w/v) Agarose in 0.5X TBE Buffer
	Ethidium Bromide (EtBr)	10 mg/ml
	10X Loading Buffer	2.5 mg/ml Bromophenol Blue, 1 per cent SDS in 2 ml Glycerol

Table 3.9. Buffers and Solutions (Continued)

Polyacrylamide Gel Electrophoresis	10X TBE Buffer	0.89 M Tris-Base 0.89 M Boric Acid 20 mM Na_2EDTA (pH 8.3)
	30 per cent Acrylamide Stock (29:1)	29 per cent Acrylamide, 1 per cent N, N`-methylenebisacrylamide
	Ammonium Peroxodisulfate (APS)	10 per cent APS (w/v)
	10 X Denaturing Loading Dye	95 per cent formamide 20 mM EDTA 0.05 per cent Xylene Cyanol 0.05 per cent Bromophenol Blue
Denaturing PAGE	10X TBE Buffer	0.89 M Tris-Base, 0.89 M Boric Acid, 20 mM Na_2EDTA (pH 8.3)
	40 per cent Acrylamide Stock (39:1)	39 per cent Acrylamide, 1 per cent N, N`-methylenebisacrylamide
	8 per cent Insta gel	63gr Urea 15 ml 10X TBE 40 per cent Acrylamide Stock (39:1) in 150 ml dH_2O
	Ammonium Peroxodisulfate (APS)	10 per cent APS (w/v)
	10 X Denaturing Loading Dye	95 per cent formamide 20 mM EDTA 0.05 per cent Xylene Cyanol 0.05 per cent Bromophenol Blue
Silver Staining	Buffer A	10 per cent Ethanol, 0.5 per cent Glacial Acetic Acid
	Buffer B	0.1 per cent $AgNO_3$ in dH_2O
	Buffer C	1.5 per cent NaOH, 0.01 per cent $NaBH_4$, 0.015 per cent Formaldehyde
	Buffer D	0.75 per cent Na_2CO_3

3.5. Equipment

Equipments used in the framework of this thesis were available in the Department of Molecular Biology and Genetics laboratory, Boğaziçi University (Istanbul, Turkey) and are listed in Table 3.10.

Table 3.10. Equipments

Autoclave	Model MAC-601 (Eyela, Japan)
Balances	Electronic Balance Model VA124 (Gec Avery, UK) Electronic Balance Model CC081 (Gec Avery, UK)
Centrifuges	Centrifuge 5415C (Eppendorf, Germany) Universal 16R (Hettich, Germany)
Deep Freezers	-20 °C (Bosch, Germany) -20 °C 2021D (Arçelik, Turkey) -70 °C (GFL, Germany)
Documentation System	BioDoc Video Documentation System (Biometra, Germany)
Electrophoretic Equipments	Sequi-Gen Sequencing Cell (Bio-Rad, USA) Horizon 58, Model 200 (BRL, USA)
Heat Blocks	Hotplate SH1D (Cytocell, UK)
Incubators	Oven EN400 (Nuve, Turkey)
Magnetic Stirrer	MK418 (Nüve, Turkey)
Ovens	Microwave Oven (Vestel, Turkey) 65 ^{o}C EN400 (Nuve, Turkey) 56 ^{o}C (LEEC, UK)
Power Supplies	Power Pac Model 3000 (Bio-Rad, USA) Apelex Biolab PS304
Refrigerators	4 °C Medicool (Sanyo, Japan) 2082C (Arçelik, Turkey)
Shaker	SL350 (Nüve, Turkey)
Spectrophotometer	CE 5502 Scanning Double Beam 5000 Series (CECIL Elegant Technology, UK)
Thermocyclers	iCycler (Bio-Rad, USA) MyCycler (Bio-Rad, USA) Techne (Progene, UK)
UV Transilluminator	Chromato-Vue Transilluminator, Model 1 TM-20UVP (USA)
Vortex	Nuvemix, NM110 (Nuve, Turkey)
Water Purification System	Millipore Elix 3 (Millipore, France)

4. METHODS

4.1. DNA Extraction from Peripheral Blood

A modified version of salting-out method (Miller *et al.*, 1988) was used for the extraction of genomic DNA from peripheral blood samples. Five-ten ml of blood was collected from individuals into sterile vacutainer tubes containing K_2EDTA as anticoagulant and was kept at 4 ^{0}C until the extraction. For the extraction, 30 ml ice-cold red blood cell (RBC) lysis buffer was added to 10 ml blood sample and mixed thoroughly. The samples were kept at 4 ^{0}C for half an hour for the lysis of erythrocyte membranes. After the centrifugation at 5000 revolution per minute (rpm), at 4 ^{0}C for 10 minutes, leukocyte nuclei were collected by discarding the supernatant. The nuclei in the pellet were resuspended in 10ml RBC lysis buffer by vortexing. The suspension was centrifuged again at 5000 rpm, at 4 ^{0}C for 10 minutes. The supernatant was discarded and the pellet was washed with 1 ml RBC lysis buffer. The nuclei in the pellet were resuspended in three ml nuclei lysis buffer by vortexing. Storage of nuclei at -20 ^{0}C or -70^{0}C was possible at this stage. The mixture was incubated in the presence of 30 µl of proteinase K and 40 µl of 10 per cent SDS at 37 ^{0}C overnight or at 56 ^{0}C for three hours. Afterwards five ml of distilled H_2O and five M NaCl were added to mixture. The tube was shaken vigorously and centrifuged at 5000 rpm at room temperature for 20 minutes. The supernatant was transferred to a sterile 10 ml Falcon tube and two volumes of absolute ethanol were added. DNA was precipitated and became visible with the gentle inversion of the tube for several times. The DNA samples were fished-out by a micropipette tip and transferred into a 1,5 ml Eppendorf tube containing 200-500 µl of Tris-EDTA (TE) buffer. The solution was left overnight at room temperature to dissolve DNA completely.

4.2. Quantitative and Qualitative Analysis of the Extracted DNA

The methods used for the quantitative and qualitative determination of isolated DNA are spectrophotometric analysis and agarose gel electrophoresis, respectively.

4.2.1. Spectrophotometric Method

The DNA extracts were diluted in a ratio of 1/100 with dH_2O. After the measurement of optical density of the sample at 260 nm, the concentration of isolated DNA was calculated according to the formula given below. These calculations are based on the fact that 50 µg of double-stranded DNA has an absorbance of 1.0 at 260 nm.

$$50\ \mu g/ml \times OD_{260} \times \text{dilution factor} = \text{concentration in } \mu g/ml$$

4.2.2. Agarose Gel Electrophoresis

One per cent agarose gel was prepared by boiling 0.4 g agarose in 40 ml of 0.5X TBE buffer. Three µl of EtBr was added to make DNA visible under the UV light and poured onto an electrophoresis plate with two combs and left at room temperature until it solidifies. Later, the plate was placed into the electrophoresis tank containing 0.5X TBE buffer and the combs were removed. 1-2 µl from each DNA dilution was mixed with 3 µl 1X loading buffer and loaded into slots. The gel was run at appropriate voltage and was visualized under UV light. The amount of DNA was estimated by comparing the density of the sample with a known amount of genomic DNA.

4.3. Homozygosity Mapping

4.3.1. PCR for Homozygosity Mapping

Eighty six patients were screened for homozygosity in CMT4A (8q13-q21) locus using the primers listed in Table 3.3. Homozygosity mapping was also carried out to test linkage to ARCMT2B (19q13.3) locus in nine CMT families.

Markers D8S286, D8S318, D8S501, D8S541 and D8S548 spanning a five Mb region were used to identify patients carrying homozygous alleles in CMT4A (8q13-q21) locus. In order to test linkage to ARCMT2B locus in 11 CMT2 families with autosomal recessive inheritance, markers D19S879, D19S902 and D19S907 spanning a 5.5 cM region were used (Leal *et al.*, 2001).

PCR reactions were performed in a 25 µl volume containing approximately 200 ng genomic DNA, 1X PCR Buffer with $(NH_4)_2SO_4$ buffer, 1.5 mM of $MgCl_2$, 0.4 µM of each primer, 0.25 mM of each dNTP and 1 U of Taq DNA polymerase.

The PCR program used for the amplification of markers for CMT4A locus was as follows: an initial denaturation step at 94°C for three minutes followed by 30 cycles of 30 second (sec) at 94°C, 30 sec at the appropriate annealing temperature (Table 3.6), 45 sec at 72°C, and a final elongation at 72°C for five minutes.

The PCR program used for the amplification of markers for ARCMT2B locus was as follows: an initial denaturation step at 94°C for five minutes followed by 35 cycles of 30 sec at 94°C, 30 sec at appropriate the annealing temperature (Table3.7), 30 sec at 72°C, and a final elongation at 72°C for seven minutes.

Five µl of each sample was mixed with three µl loading buffer and electrophoresed on one per cent agarose gel to check the quality and quantity of amplification.

4.3.2. Denaturing Polyacrylamide Gel Electrophoresis (PAGE) for Homozygosity Mapping

Glass surface of the sequencing apparatus and its glass plate were cleaned with alcohol to prevent any oily fingerprints and dust between the surfaces. Then, 0.3 mm thick spacers to the edges and a piece of Whatman paper to the bottom of the apparatus were placed. The glass plate was covered over them and tightened with clamps. Twenty ml dH_2O was poured into the space between glass and plastic surfaces of the sequencing apparatus to prevent solidification of gel in this part which can interfere with the electrophoresis if it covers the electrode in this part.

Thirty-five ml freshly prepared 8 per cent insta gel was mixed with 350 µl APS and 35 µl TEMED and poured between the glass surfaces from one corner. The comb was placed in the opposite position. After covering the open side with a piece of stretch film, the gel was left overnight for solidification.

The next day, the gel placed into the electrophoresis tank and filled with 1L 1X preheated TBE. The comb was removed and placed in the correct position to form the wells. The power supply was connected and it was let to work at 35 W to heat the gel until 50 ^{0}C before the electrophoresis of samples start. Three µl of each sample was mixed with three µl denaturing loading buffer and kept at 94 ^{0}C heat block for five minutes for denaturation. They were kept on ice for an additional five minutes before loading to the gel. The electrophoresis was started at 35 W for 10 minutes and they were run 2-3 hours at 30 W.

4.3.3. Silver Staining

The gel was removed carefully with the help of a Whatman paper, top of the gel was marked and incubated with Buffer A for five minutes to fix the DNA fragments. Buffer A was removed and the gel was kept in Buffer B for 10-15 minutes. After washing the gel with dH_2O freshly prepared Buffer C was poured on to the gel and incubated for approximately 10 minutes until the bands appear. If the bands were not clear enough, washing steps with Buffer B and C were repeated after rinsing the gel in dH_2O and ddH_2O several times. The color reaction was terminated in Buffer D and after five minutes the gel was placed in a transparent folder for preservation and sealed.

4.3.4. Evaluation of the Results

The genotypes of the family members were determined and the haplotypes were constructed. MLINK program of the LINKAGE computer package, version 5.1 was used in the data processing.

4.4. Single Strand Conformation Polymorphism (SSCP) Analysis

4.4.1. PCR for SSCP Analysis

The ingredients of the PCR reactions were given in section 4.3.1.

The PCR program used for the amplification of the exons of the GDAP1 (Table 3.2) (except exon 2, Table 4.1) and exons 10 and 11 of the LMNA (Table 3.1) genes and flanking intronic regions was as follows: an initial denaturation step at 94°C for 5 minutes followed by 35 cycles of 45 sec at 94°C, 30 sec at the appropriate annealing temperature, 60 sec at 72°C, and a final elongation at 72°C for 10 minutes.

The PCR program used for the amplification of the exons 2, 3, 8 and 9 of the LMNA gene and flanking intronic regions was as follows: an initial denaturation step at 94°C for five minutes followed by 30 cycles of 30 sec at 94°C, 30 sec at the appropriate annealing temperature (Table 3.1), 30 sec at 72°C, and a final elongation at 72°C for seven minutes.

The PCR program used for the amplification of the exons of the HSPB8 and HSPB1 genes, exons 1, 4, 6, 7 and 12 of the LMNA gene and HSP60 gene (except exons 1, 11 and 12, Table 4.1) and flanking intronic regions was as follows: an initial denaturation step at 94 °C for five minutes followed by 35 cycles of 45 sec at 94°C, 45 sec at the appropriate annealing temperature given in corresponding tables for each gene, 50 sec at 72°C, and a final elongation at 72 °C for 10 minutes.

Amplification of the PCR fragments was checked on one per cent agarose gel.

Table 4.1. Exceptional PCR programs for the amplifications of the exons of the GDAP1, LMNA and HSP60 genes (‘: minutes)

	GDAP1 exon2		LMNA exon5		HSP60 exon1		HSP60 exon11		HSP60 exon12	
94°C	4’		10’		5’		5’		5’	
94°C annealing°C 72°C	45” 45” 30”	40 cycles	30” 30” 25”	30 cycles	45” 30” 60”	35 cycles	45” 45” 60”	35 cycles	30” 30” 45”	35 cycles
72°C	7’		5’		5’		5’		5’	

4.4.2. PAGE for SSCP Analysis

Surfaces of glass plates of 20cm x 20cm were cleaned with alcohol to prevent any oily finger prints and dust between the surfaces. Then, one mm thick spacers were placed to the edges of the glass plates and tightened with clamps.

Fourty ml of 8 per cent SSCP gel was prepared by mixing 31 ml dH_2O, six ml 5X TBE, 13 ml 30 per cent acrylamide solution (29:1), 500 µl APS and 50 µl TEMED. It was poured between the glasses. The comb was placed and the gel was left at room temperature for one hour for solidification.

The solidified gel was placed into the electrophoresis tank containing 0.6X TBE buffer after the removal of the comb. Three µl of each PCR sample was mixed with three µl denaturing loading buffer and kept at 94^0C heat block for five minutes for denaturation. They were kept on ice for an additional five minutes before loading to the gel. After loading four µl from each sample the electrophoresis was started at 200V and kept on overnight.

4.4.3. Silver Staining for SSCP Analysis

Silver staining of the SSCP gels were performed by the procedure explained in section 4.3.3.

4. 5. DNA Sequence Analysis

PCR samples which had different banding patterns in the SSCP analysis were purified by using QIAquick purification kit and sequencing of the sense and antisense strands were performed by the Iontek Company.

4.6. Restriction Endonuclease Analysis

Sequence variations were tested with restriction endonuclease analysis if they create or abolish a restriction enzyme recognition site. Ten µl of the PCR product was mixed with

three units of the suitable enzyme and two µl of its 10X buffer in a 20 µl reaction volume. The mixture was incubated overnight at 37 ^{o}C. The digested products were mixed with five µl 1X loading buffer and visualized on 2 per cent agarose gel under UV light.

4.7. Screening for Novel Mutation in the GDAP1 Gene with Amplification Refractory Mutation System (ARMS)

The novel base substitution identified in the GDAP1 gene of the patient F17.3 was planned to be verified using ARMS method. Two new allele specific forward primers (Table 3.8) were designed in such a way that at the 3'-end the last four nucleotides of the mutant forward primer (G2MF) could allow the amplification of the mutant sequence whereas wild type forward primer (G2WTF) could amplify the wild type sequence. Wild type G2R primer was used as the reverse primer in each reaction. G2F primer was used as an internal control.

Using G2MF, G2WTF, G2F and G2R primers, two multiplex PCR reactions were performed. In the first reaction, forward primers G2WTF and G2F were used together with G2R primer to check the amplification of the wild type sequence. In the second reaction, forward primers G2MF and G2F were used together with G2R primer to check the amplification of the mutant sequence. Each reaction was performed by using the genomic DNA of both the patient and control individuals. The preparation of the mixtures was as described in section 4.4.1 and PCR program used was as for exon 2 of *GDAP1*.

Amplifications of the PCR fragments were checked on 1.5 per cent agarose gel.

5. RESULTS

The molecular basis of CMT, dHMN and HSP diseases were investigated in our cohort of hereditary neuropathy patients. Eighty six patients were analyzed for CMT4A locus. 37 isolated cases and nine ARCMT2 families were investigated for ARCMT2 linkage. 29 patients were tested for mutations in HSPB1 and HSPB8 genes. 12 HSP patients were also analyzed for mutations in the HSP60 gene.

5.1. Homozygosity Mapping

5.1.1. Homozygosity Mapping for CMT4A locus

CMT4A locus was screened for homozygosity using five markers (D8S286, D8S318, D8S501, D8S541 and D8S548) in 86 CMT patients that were suspected to have autosomal recessive inheritance according to the clinical data and pedigree analysis. Twenty nine patients were found to be homozygous for at least two of the markers and were further screened for mutations in the GDAP1 gene. Gel views of some of the markers were given in Figure 5.1, Figure 5.2 and Figure 5.3.

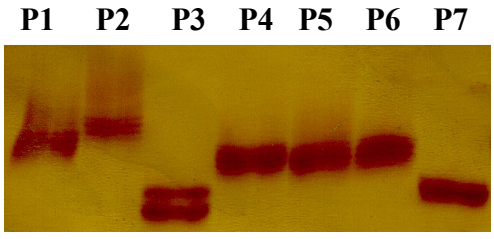

Figure 5.1. Alleles of CMT patients tested for homozygosity with marker D8S286 (P: Patient)

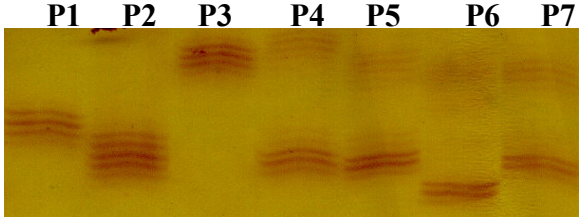

Figure 5.2. Alleles of CMT patients tested for homozygosity with marker D8S541 (P: Patient)

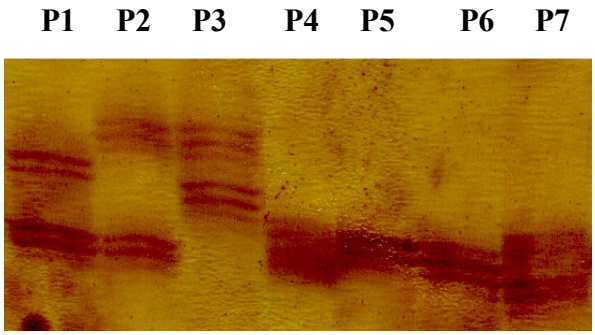

Figure 5.3. Alleles of CMT patients tested for homozygosity with marker D8S548 (P: Patient)

5.1.2. Homozygosity Mapping for ARCMT2B locus

Nine families with a clinical diagnosis of ARCMT2 were tested for homozygosity in locus 19q13.3 using markers D19S879, D19S902 and D19S907 (Figure 5.4). Marker D19S879 was not informative for families P118 and P192. Haplotypes in all families demonstrated heterozygosity in affected individuals, excluding linkage to ARCMT2B locus in these families. The pedigrees showing the haplotype analysis of the three largest families, P118, P192 and P435, analyzed in this study were given in Figures 5.5, 5.6 and 5.7, respectively.

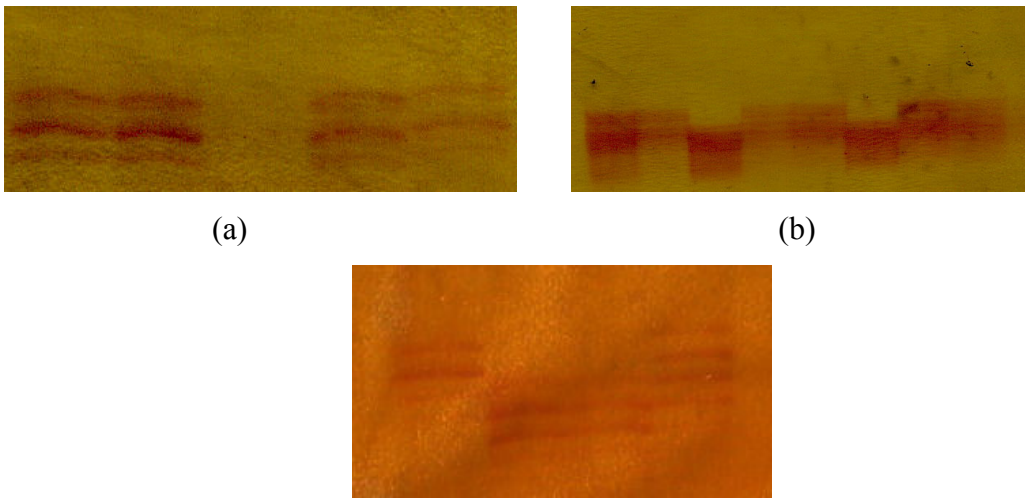

Figure 5.4. The alleles of the members of three families analysed with markers D19S879 (a), D19S902 (b) and D19S907 (c)

Lod score analysis was performed for the statistical evaluation of the genotype data. The assumptions used in the calculation of two-point lod score analysis were equal marker-allele frequencies, a disease allele frequency of 0.00001 and equal recombination frequencies for males and females.

The result of the two-point lod-score analysis was given in Table 5.1. Since the lod score values at $\theta = 0.00$ were smaller than -2 in all families, this locus can be excluded as the cause of ARCMT2B in patients P118, P192 and P435.

The family of P210 was noninformative for two of the markers (D19S879 and D19S907) and lod-score analysis was not performed for the family. In the rest of the families (P226, P234, P412, P472 and SD family) the haplotype analysis was not informative since the blood samples were available only from one affected child and either from one parent or an unaffected sibling.

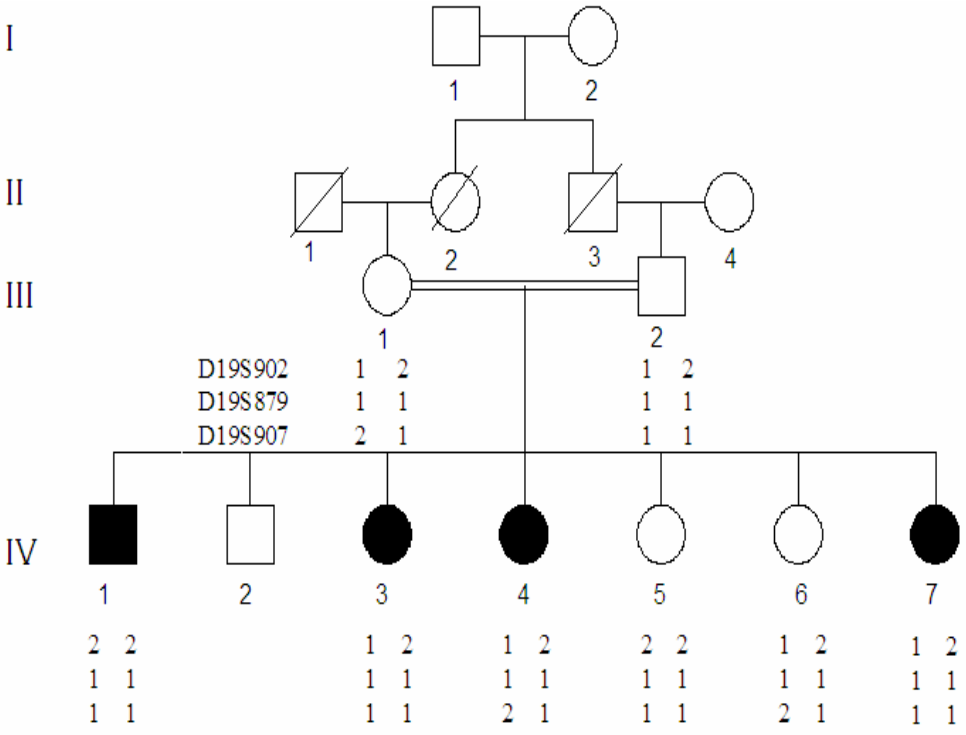

Figure 5.5. Haplotypes of the members of family of P118 for ARCMT2B markers D19S902, D19S879 and D19S907

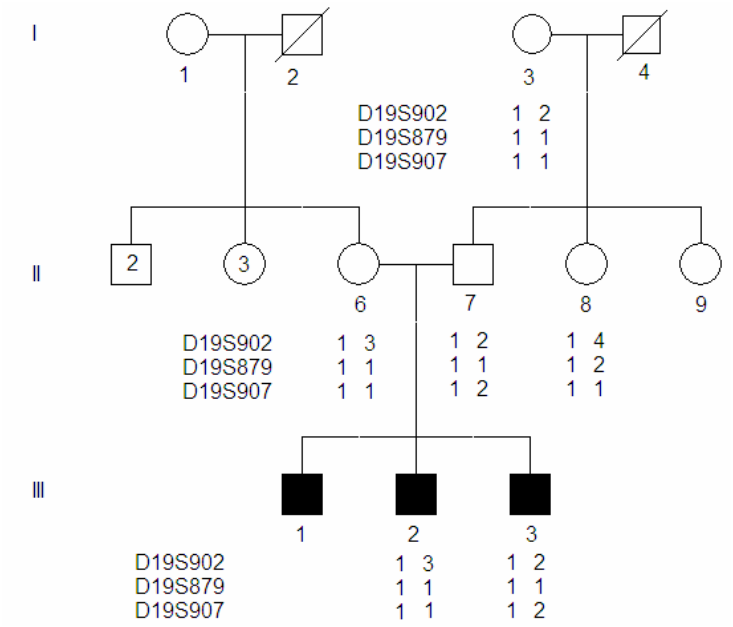

Figure 5.6. Haplotypes of the members of family of P192 for ARCMT2B markers D19S902, D19S879 and D19S907

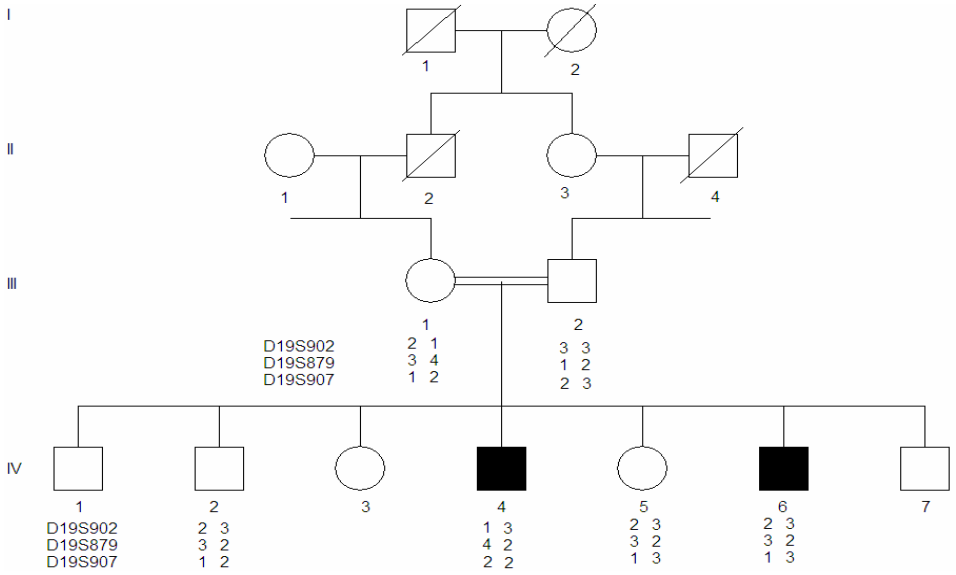

Figure 5.7. Haplotypes of the members of family of P435 for ARCMT2B markers D19S902, D19S879 and D19S907

A recombination was observed in the individuals IV-2 and IV-4 in the pedigree of patient P435 between markers D19S879 and D19S907 (Figure 5.7). However, this situation did not affect the results since the patients were heterozygous.

Table 5.1. Two-point lod scores for three markers in families P118, P192 and P435

Family	Locus	Lod score at θ=								
		0.00	0.05	0.10	0.20	0.30	0.40	0.45	Z_{max}	θ_{max}
P118	D19S902	-∞	-0.28	-0.11	-0.05	-0.03	-0.01	0.00	0.00	0.45
	D19S879	-	-	-	-	-	-	-	-	-
	D19S907	-∞	-0.50	-0.26	-0.08	-0.02	0.00	0.00	0.00	0.40
P192	D19S902	-∞	-1.44	-0.89	-0.39	-0.15	-0.04	-0.01	-0.01	0.45
	D19S879	-	-	-	-	-	-	-	-	-
	D19S907	-∞	-0.72	-0.44	-0.19	-0.08	-0.02	0.00	0.00	0.45
P435	D19S902	-∞	-0.68	-0.41	-0.27	-0.11	-0.04	0.00	0.00	0.45
	D19S879	-∞	-0.55	-0.34	-0.17	-0.07	-0.02	0.00	0.00	0.45
	D19S907	-∞	-1.48	-0.91	-0.39	-0.15	-0.04	-0.01	-0.01	0.45

5.2. SSCP Analysis

5.2.1. Variations in the GDAP1 Gene

SSCP analysis revealed a different banding pattern in the second exon of the GDAP1 gene in patient F17.3 among 29 patients (Figure 5.8).

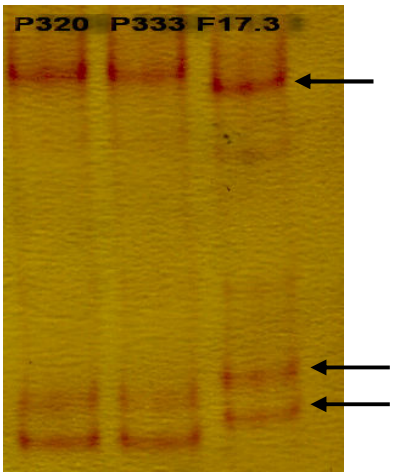

Figure 5.8. Eight per cent SSCP gel indicating an altered banding pattern in the second exon of the GDAP1 gene for patient F17.3

A deletion-insertion mutation, c.174_176delinsTGTG (p.P59delinsVLEfsX62), in homozygous condition was identified in the patient (Figure 5.9). The sequence variation did not create or abolish a restriction site. Thus, ARMS method was selected for the verification of the mutation. However, the mutant forward primer (G2MF) together with wild type reverse primer (G2R) amplified the 218 bp region in patient F17.3 and in healthy controls as well. A very faint amplification was also observed upon use of wild type forward (G2WTF) and wild type reverse primers (G2R) in the healthy controls and in patient F17.3. Use of G2F primer together with G2R primer as an internal control in the experiment amplified the 330bp region in almost all samples. Because of this problem, SSCP method was used to prove that the novel c.174_176delinsTGTG change is not a polymorphism.

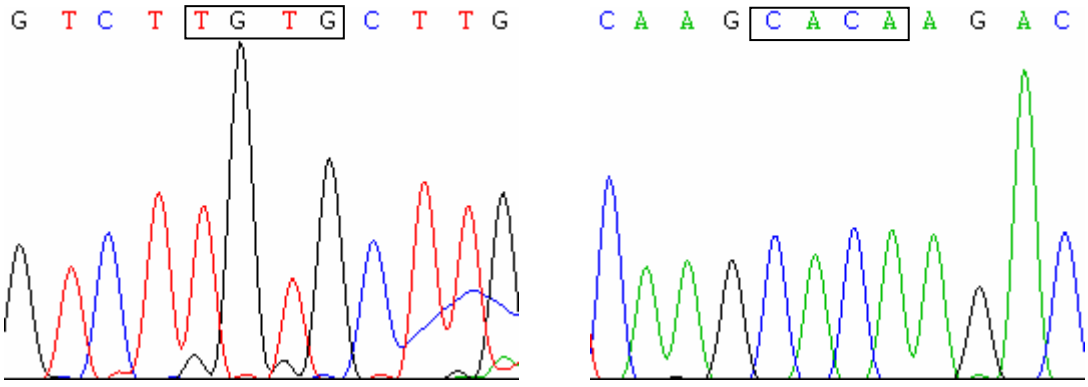

(a) (b)

Figure5.9. Chromatograms showing c.174_176delinsTGTG change in patient F17.3 in the second exon of *GDAP1* in the sense (a) and antisense (b) strands.

Fifty healthy individuals were screened by SSCP method and the altered migration pattern observed in the patient F17.3 was not observed in the control individuals. The segregation of the mutation among the family members could not be investigated since the DNA samples were not available.

P429 was a good candidate to have a *GDAP1* mutation as the clinical findings including hoarseness was suitable for a CMT4A phenotype. However, as the DNA sample

of this patient arrived after the SSCP analysis of the GDAP1 gene was completed, direct sequencing analysis of was applied for the six exons of the GDAP1 gene. This analysis revealed a heterozygous c.507T>G (p.S169S) (Figure 5.10) previously reported by Senderek *et al.* as a polymorphism (2003).

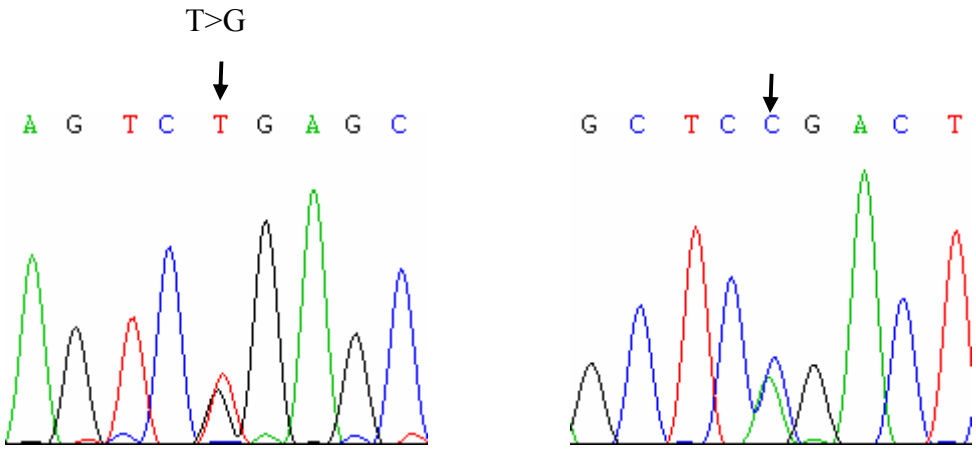

(a) (b)

Figure 5.10. Chromatograms showing the c.507T>G substitution in the fourth exon of *GDAP1* in patient P429 in the sense (a) and antisense (b) strands

5.2.2. Variations in the LMNA Gene

Altered migration patterns for the third exon of the LMNA gene were observed in two patients, P226 and P375 (Figure 5.11.a and 5.11.b respectively).

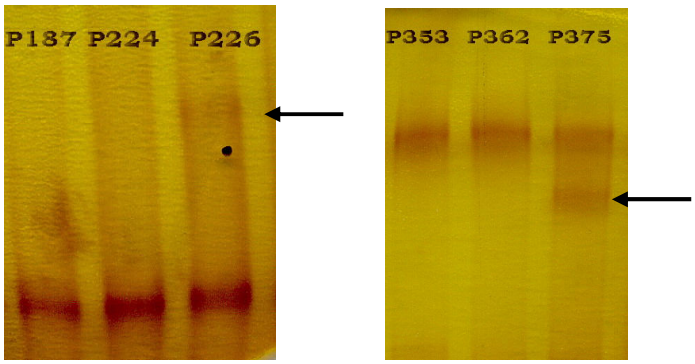

(a) (b)

Figure 5.11. Eight per cent SSCP gel indicating the abnormal migration patterns for patients P226 (a) and P375 (b) in the third exon of *LMNA*

Sequencing analysis of the DNA sample of patient P226 revealed a G to A transition at position 612 (c.612G>A) (Figure 5.12) without changing the leucine residue at position 204. This variation was reported in NCBI as a polymorphism by the reference number 12117552.

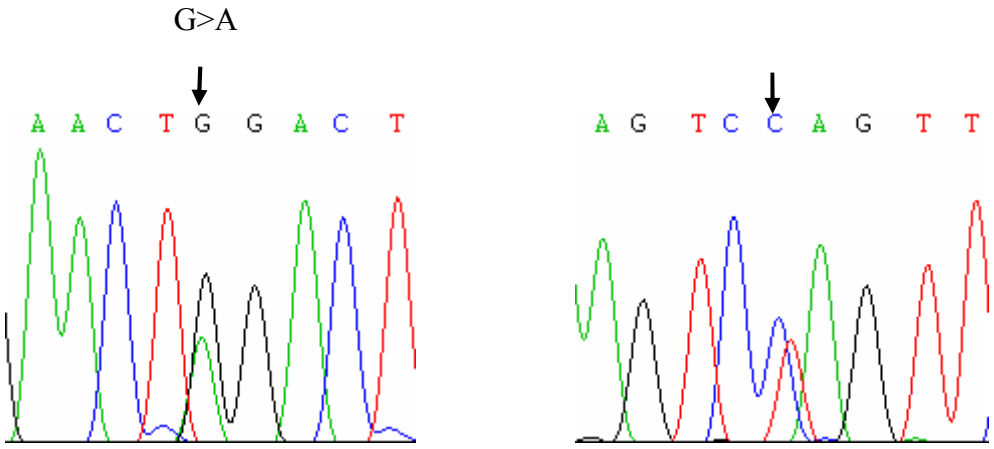

(a) (b)

Figure 5.12. Chromatograms indicating the c.612G>A substitution in patient P226 in the third exon of the LMNA gene in the sense (a) and antisense (b) strands

The sequence analysis of the PCR samples for exon 3 of *LMNA* also revealed heterozygous IVS3+56G>T and IVS3+73C>T substitutions in patient P375 (Figure 5.13). The substitutions were previously reported in the in NCBI as polymorphisms by the reference numbers 11264443 and 11264442, respectively.

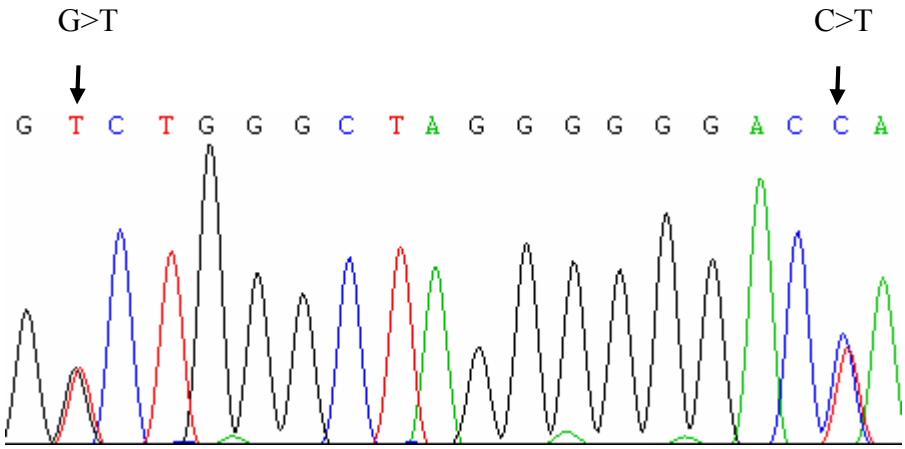

Figure 5.13. Chromatogram showing IVS3+56G>T and IVS3+73C>T substitutions in patient P375 in the third intron of *LMNA* in the sense strand

An altered migration pattern was observed in the SSCP analysis of the fourth exon of the LMNA gene for patient P298 (Figure 5.14).

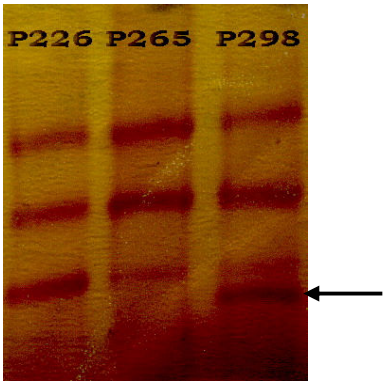

Figure 5.14. Eight per cent SSCP gel indicating an abnormal banding pattern for the fourth exon of the LMNA gene

The chromatograms indicated two base substitutions in the fourth intronic region of the LMNA gene for patient P298 which are IVS4+13G>T (Figure 5.15.a) and IVS4+61C>T (Figure 5.15.b) reported in the NCBI database as polymorphisms with the reference numbers 11264445 and 11264444, respectively.

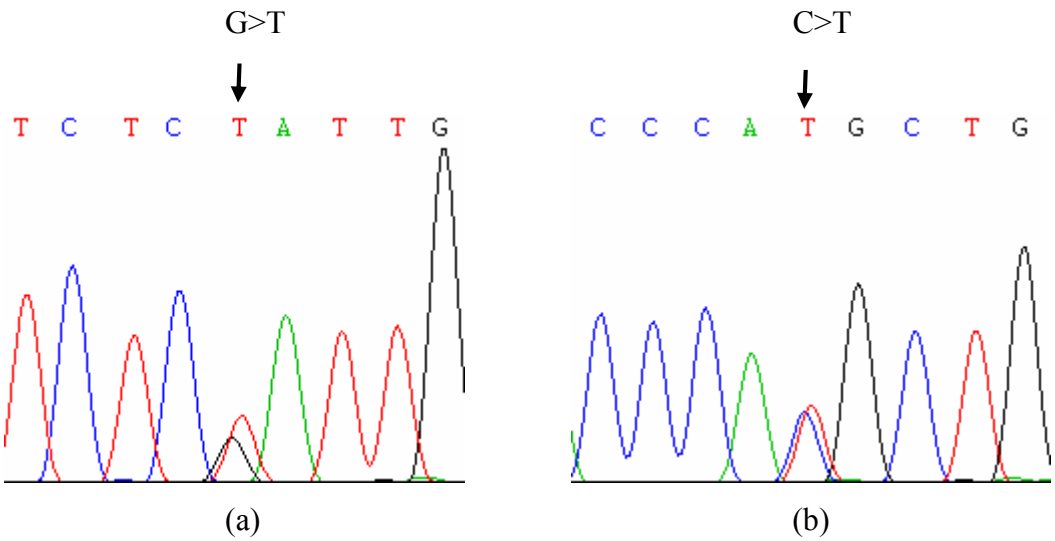

Figure 5.15. Chromatograms showing IVS4+13G>T (a) and IVS4+61C>T (b) substitutions in patient P298 in the intron 4 of the LMNA gene in the sense strand

SSCP analysis of exon 5 of the LMNA gene indicated an SSC polymorphism present in almost half of the analyzed patients (Figure 5.16).

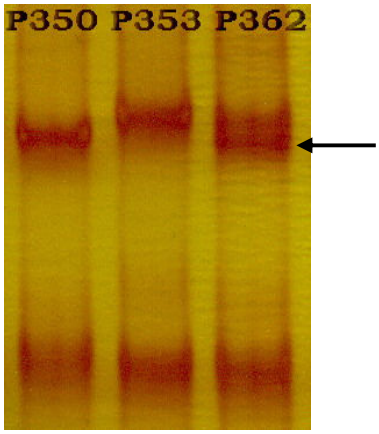

Figure 5.16. Eight per cent SSCP gel showing an SSC polymorphism for exon 5 of the LMNA gene

The sequence analysis of the samples of exon 5 in LMNA revealed a homozygous c.861C>T substitution in patient P350 (Figure 5.17). The substitution did not change the alanine residue at position 287 and the variation was reported in the in NCBI as a polymorphism by the reference number 538089.

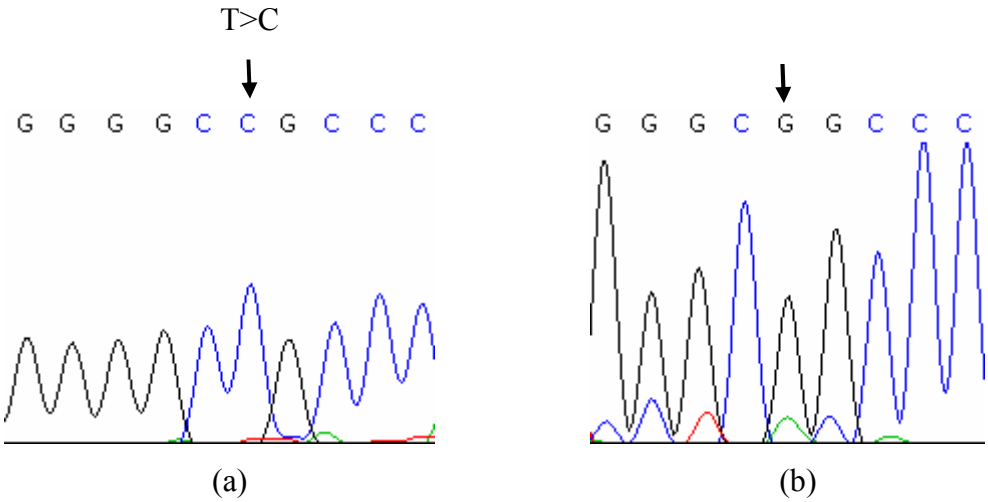

Figure 5.17. Chromatograms showing the homozygous c.861C>T substitution in patient P350 in the fifth exon of LMNA in sense (a) and antisense (b) strands

The SSCP analysis of the exon 8 of the LMNA gene exhibited an abnormal migration profile in almost half of the patients (Figure 5.18).

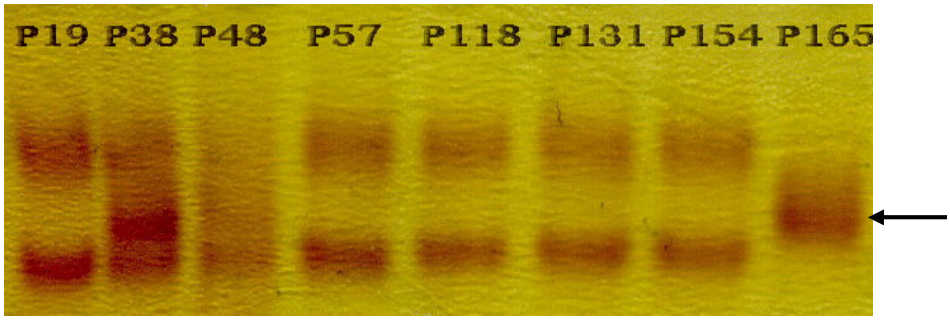

Figure 5.18. Eight per cent SSCP gel exhibiting the abnormal banding profile in the eighth exon of the LMNA gene

The subsequent sequence analysis of the sample from patient P48 revealed a IVS8+44C>T variation (Figure 5.19) published in NCBI as an SNP with the reference number 553016.

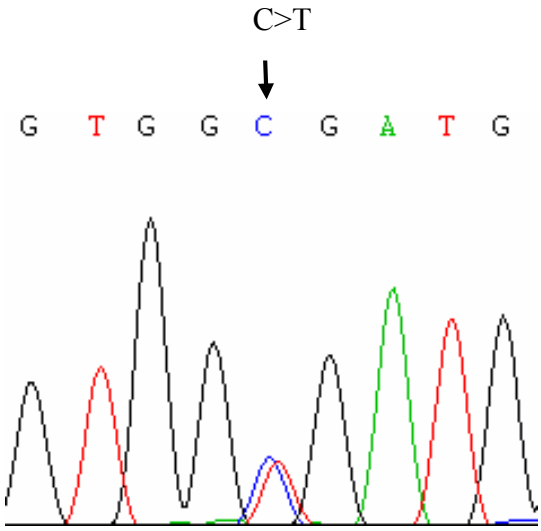

Figure 5.19. Chromatogram showing the IVS8+44C>T variation in the eighth exon of the LMNA gene in patient P48 in the sense strand

Some of the samples showed an abnormal migration profile exon 10 in the SSCP analysis (Figure 5.20).

Figure 5.20. Eight per cent SSCP gel showing the abnormal banding pattern in the exon 10 of the LMNA gene

Sequencing of the PCR sample of patient P265 revealed a heterozygous substitution c.1698C>T (Figure 5.21). The histidine residue at position 566 does not change and the variation was reported in NCBI as an SNP with the reference number 4641.

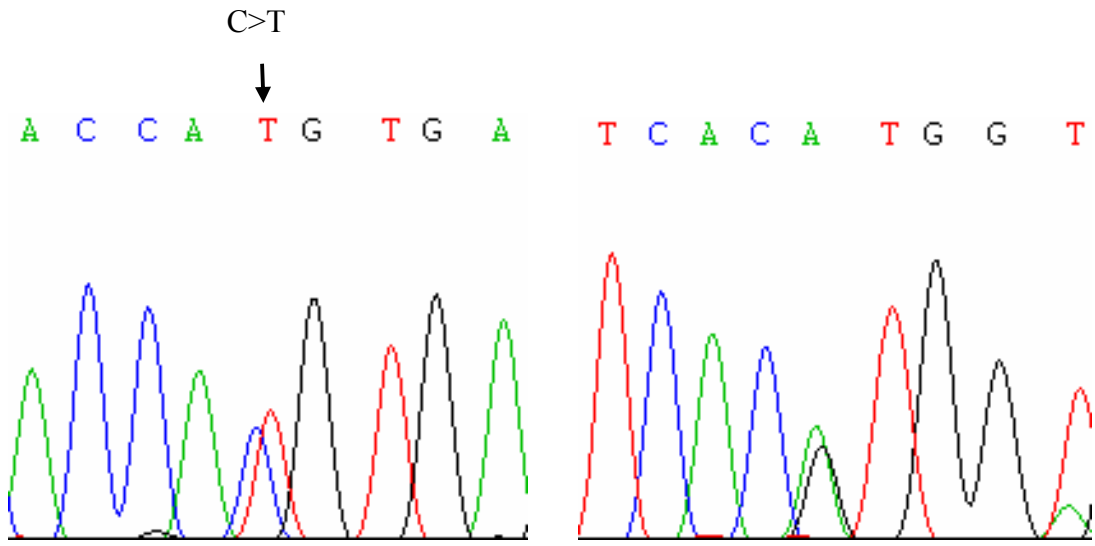

Figure 5.21. Chromatograms showing the C>T variation in the exon 10 of the LMNA gene in patient P265 in the sense (a) and antisense (b) strands

An altered migration pattern was observed in the SSCP analysis of exon 12 of the LMNA gene (Figure 5.22).

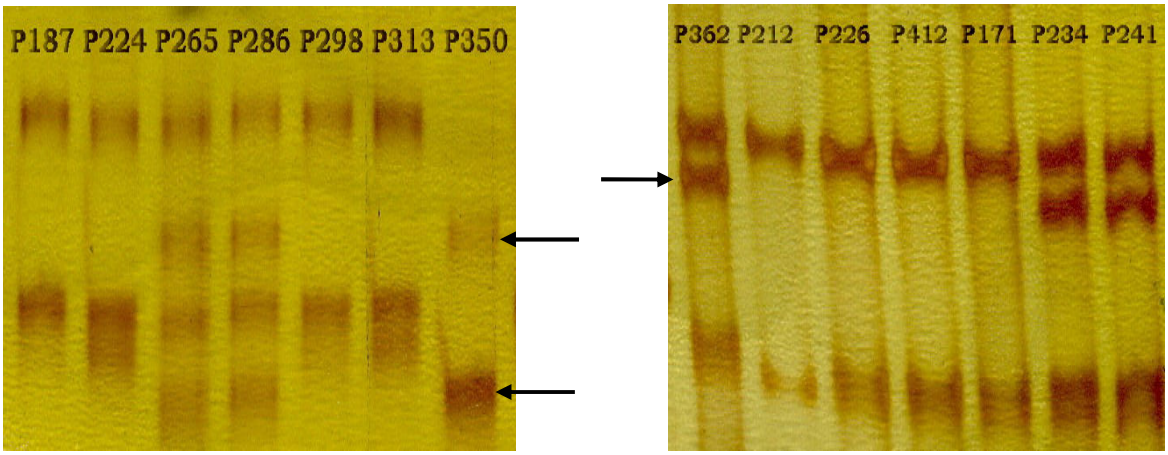

Figure 5.22. Eight per cent SSCP gels showing the abolished migration profile in the exon 12 of the LMNA gene

The subsequent sequence analysis revealed two polymorphisms reported in the NCBI previously. The first polymorphism in the exon 12 is a c.2074G>C substitution (Figure 5.23) and 7339 is the reference number of the SNP in NCBI databases.

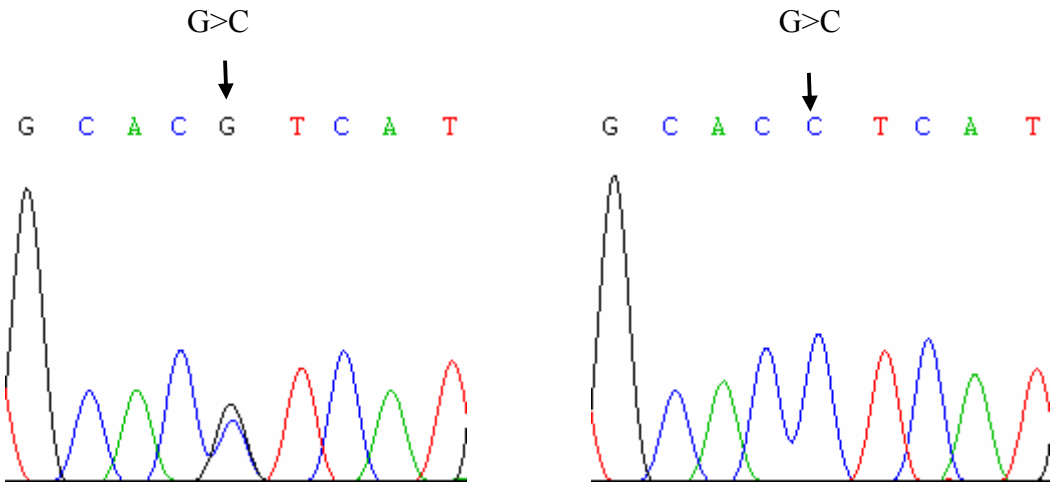

Figure 5.23. Chromatograms indicating the heterozygous (a) and homozygous (b) states of the c.2074G>C substitution in patient P362 and P350 respectively in sense strands

The second polymorphism in exon 12 (Figure 5.24), c.2206_2207insA, has a reference number of 35750865 in NCBI databases.

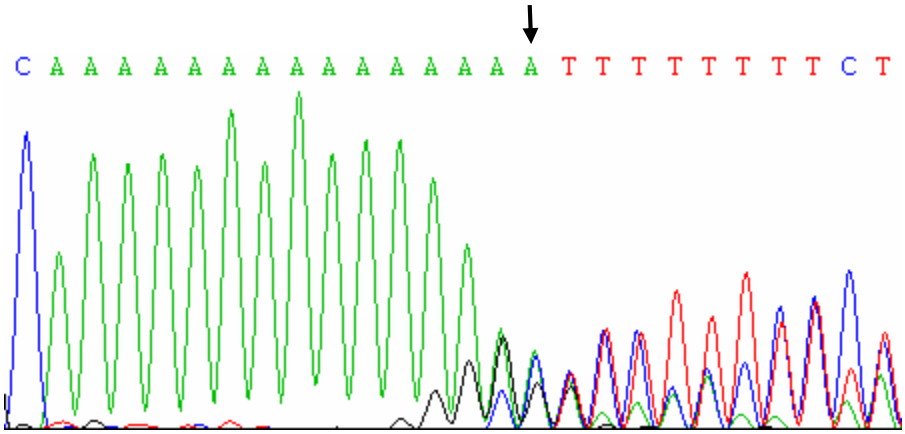

Figure 5.24. Chromatogram showing the c. 2206_2207insA insertion shared by the patients P350 and P362 in the sense strand

5.2.3. Variations in the HSPB8 Gene

Sequence variations could not be identified in the HSPB8 gene in our cohort of patients.

5.2.4. Variations in the HSPB1 Gene

An abnormal migration pattern was observed in the SSCP analysis of patients P164 and P241 in the samples of the first exon of the HSPB1 gene (Figure 5.25).

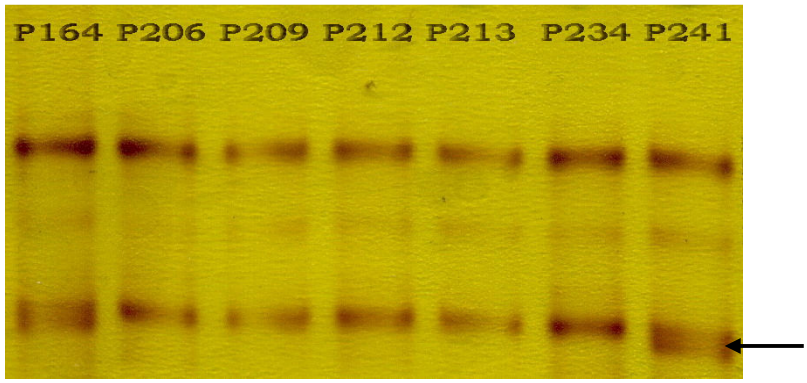

Figure 5.25. Eight per cent SSCP gel indicating the abnormal banding pattern in patients P164 and P241 in the PCR samples of the first exon of HSPB1

The following sequencing results indicated a heterozygous g.52C>T substitution in the noncoding region before the first exon of *HSPB1* in both patients (Figure 5.26). The variation was previously reported in the NCBI with the reference number 53759978.

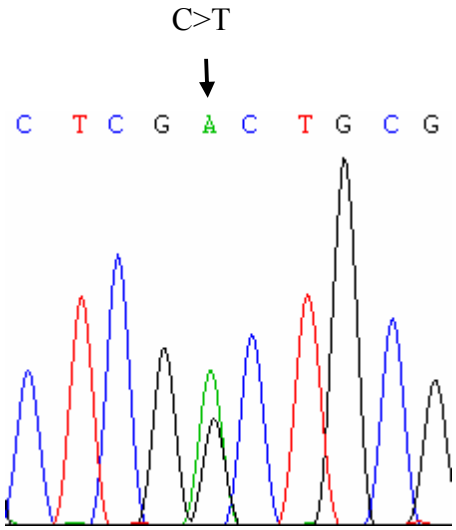

Figure 5.26. Chromatogram showing the g.52C>T substitution in patient P164 in the region before the first exon of *HSPB1* in the antisense strand

A second SSC polymorphism in exon 1 was identified in patient P77 (Figure 5.27).

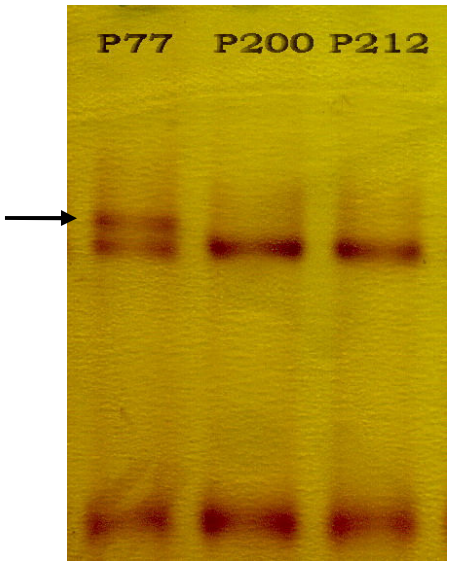

Figure 5.27. Eight per cent SSCP gel exhibiting the abnormal banding pattern in the PCR samples of the first exon of the HSPB1 gene for patient P77

Subsequent sequencing analysis revealed a heterozygous IVS1+100C>A substitution in the sense and antisense strands of the HSPB1 gene for patient P77 (Figure 5.28). This variation was also reported in NCBI databases with the reference numbers 28708645 and 34976596.

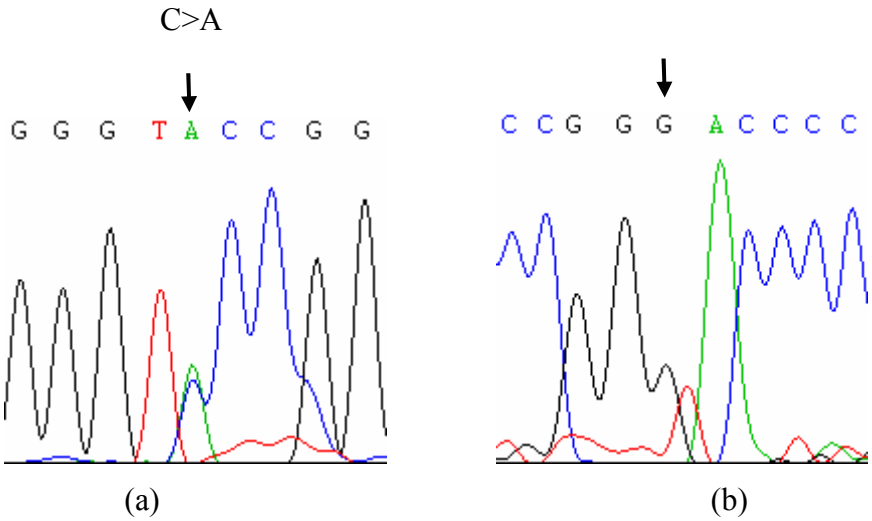

Figure 5.28. Chromatograms showing the IVS1+100C>A in the first intron of the HSPB1 gene for patient P77 in the sense (a) and antisense (b) strands

The SSCP analysis of the same patient revealed another SSC shift in the second exon PCR product (Figure 5.29).

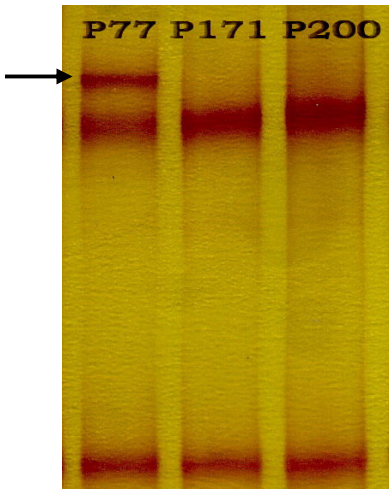

Figure 5.29. Ten per cent SSCP gel showing the abnormal migration profile of the PCR samples of the exon 2 of the HSPB1 gene for patient P77

The sequencing analysis of exon 2 in patient P77 revealed a IVS2+60G>A substitution (Figure 5.30) which was previously reported in the databases of NCBI with the reference numbers 7804492 and 34174779.

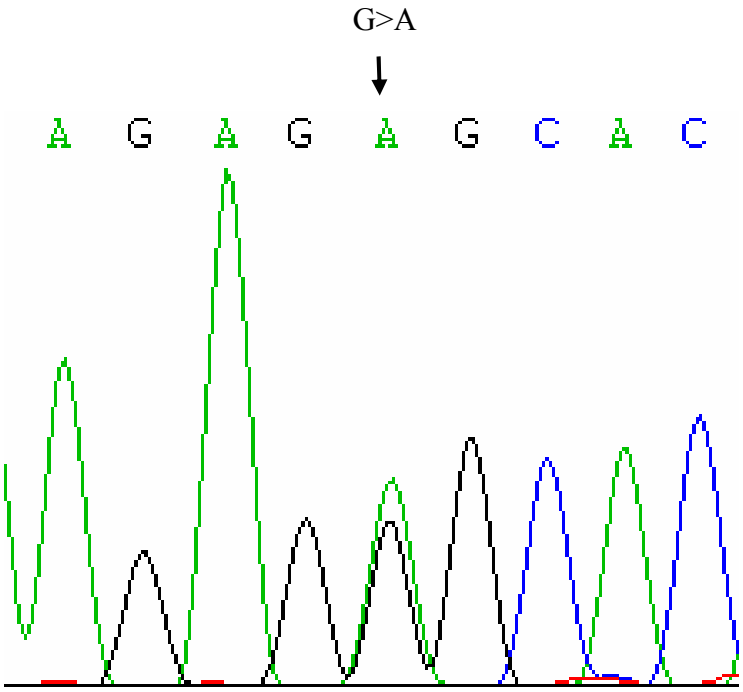

Figure 5.30. The chromatogram showing the IVS2+60G>A substitution for patient P77 in the sense strand

A difference in the migration pattern of the third exon of *HSPB1* was also observed in patient P286. Sequencing analysis of this region revealed a heterozygous insertion mutation, c.439_440insC, leading to a stop codon at position 160 (p.G147fsX160) (Figure 5.31). This sequence variation did not create or abolish a restriction site and the site of insertion was not appropriate to apply the ARMS method. Denaturing gels were not informative for the verification of the insertion since another insertion in the same exon had already been reported previously as an SNP with a database number 35408134 in OMIM. As a result, SSCP analysis was repeated with 50 healthy individuals. The results indicated that the different migration pattern observed for patient P286 was absent in the 50 healthy individuals (Figure 5.32.a). Furthermore, the same migration pattern was also observed for the mother of patient P286 (Figure 5.32.b).

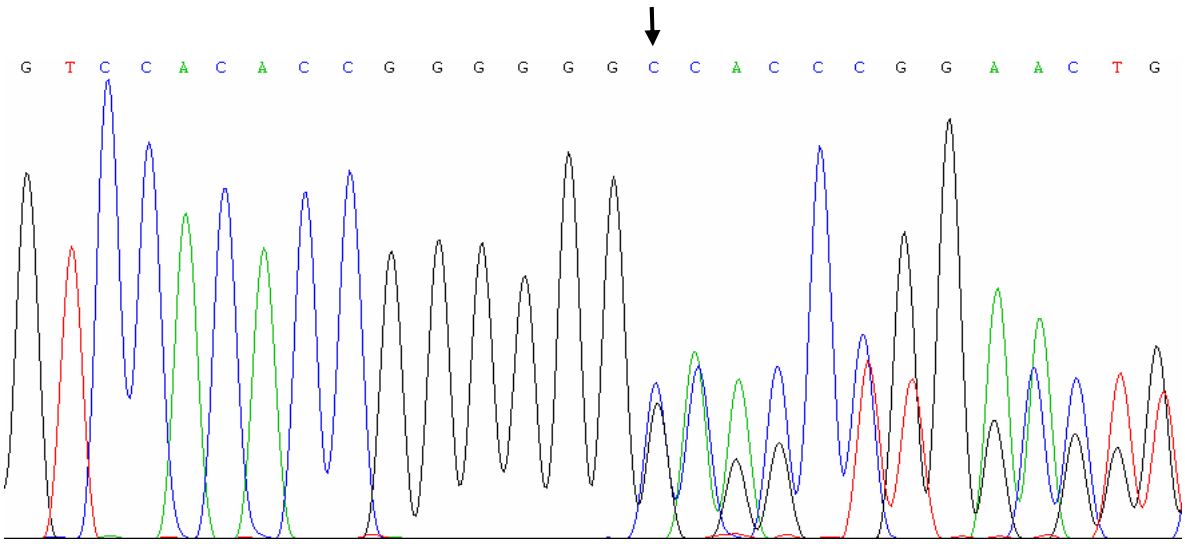

Figure 5.31. Chromatogram showing c.439_440insC change in the third exon of *HSPB1* for patient P286 in the antisense strand

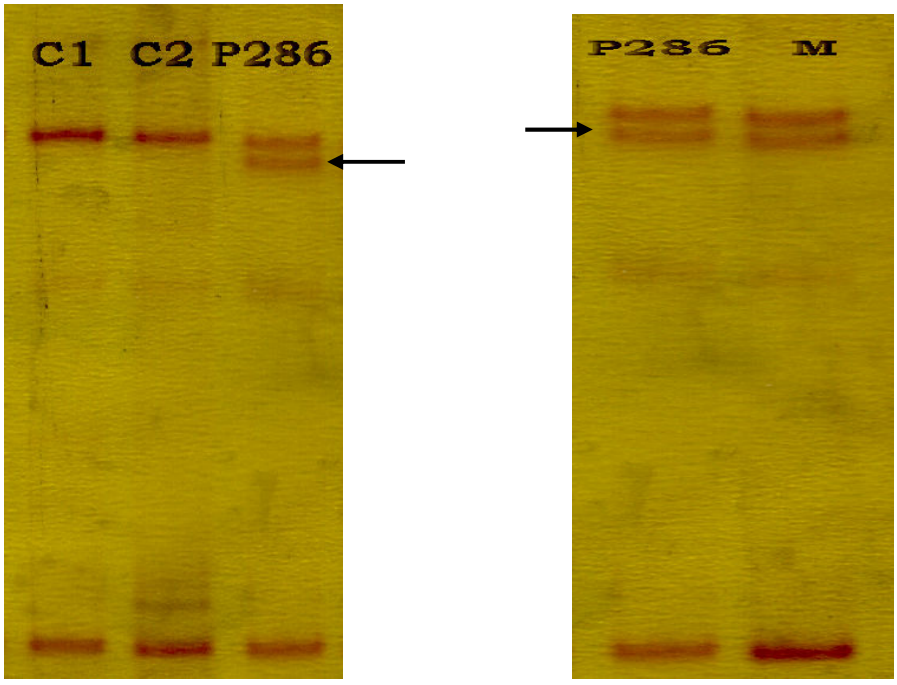

(a) (b)

Figure 5.32. Eight per cent SSCP gels indicating an altered banding pattern in the third exon of *HSPB1* for patient P286 in comparison with the healthy controls (a) and the shared migration pattern with her mother (C: Control; M: Mother)

5.2.5. Variations in the HSP60 Gene

Differences in the banding patterns of the second and fifth exons of the HSP60 gene were observed in patient P461 (Figure 5.33 and Figure 5.34).

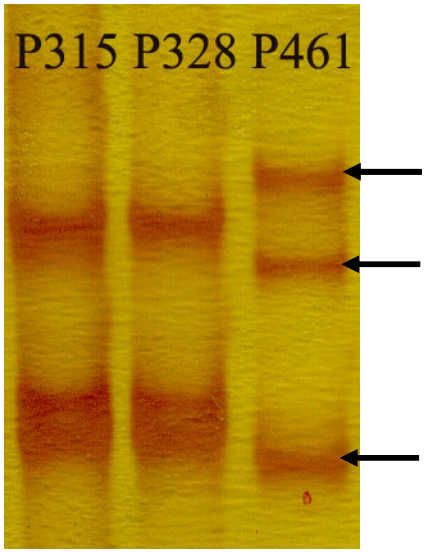

Figure 5.33. The SSCP gels indicating the different migration profile of the exon 2 of the HSP60 gene for patient P461

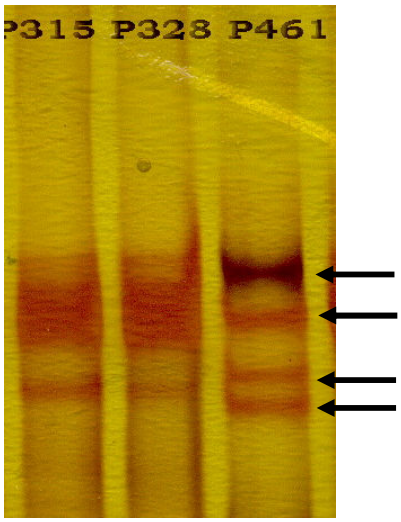

Figure 5.34. The SSCP gels indicating the different migration profile of the exon 5 of the HSP60 gene for patient P461

Sequencing analysis of this region revealed two base substitutions in the second exon of *HSP60* for patient P461 (Figure 5.35). The c.40G>T substitution gives rise to the amino acid change p.V14L while the c.69T>C substitution does not affect the threonine residue at position 23.

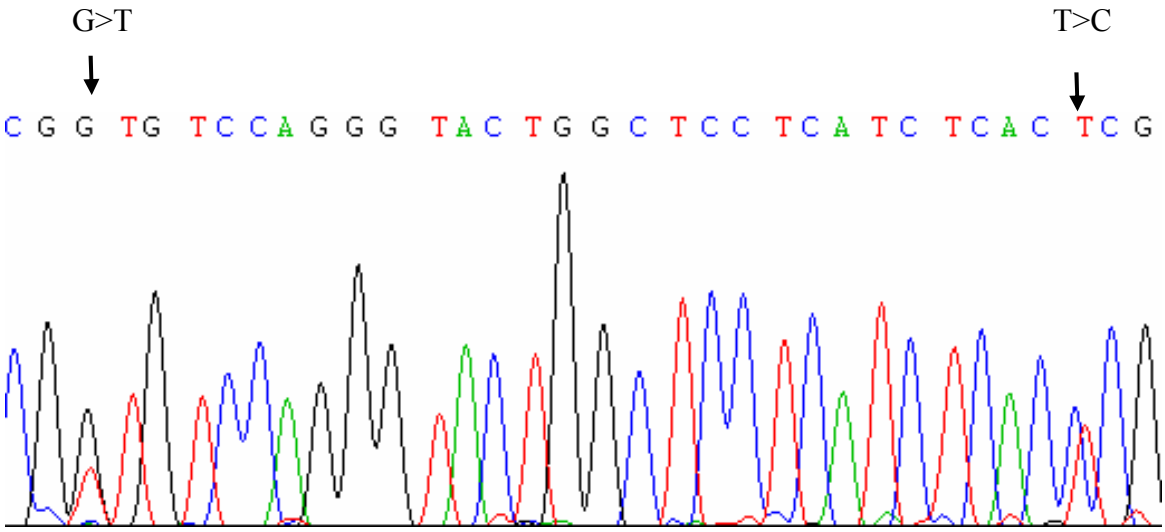

(a)

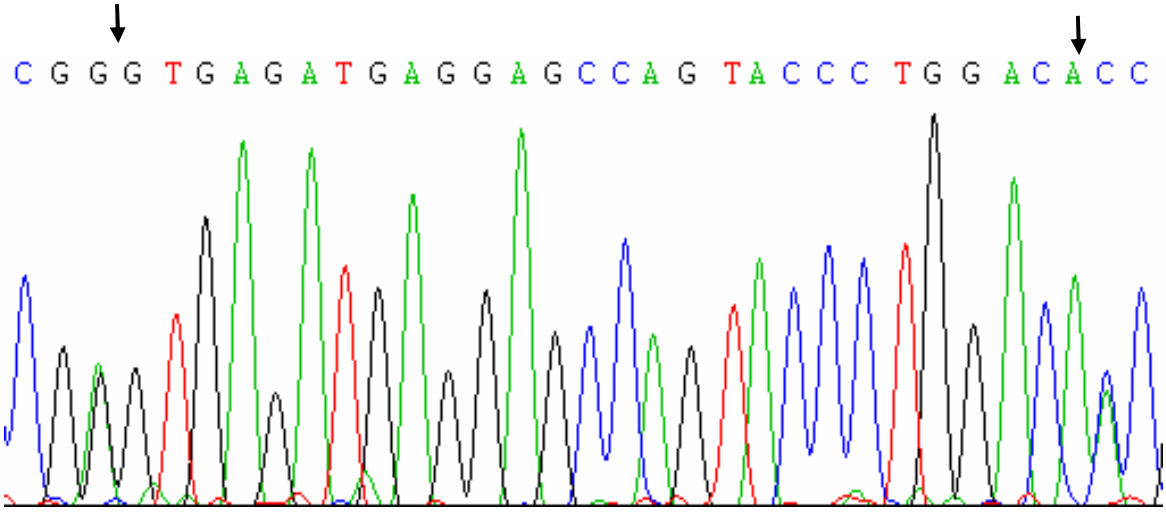

(b)

Figure 5.35. Chromatograms showing c.40G>T and c.69T>C change in the second exon of *HSP60* gene for patient P461 in the sense (a) and antisense (b) strands

The c.40G>T sequence variation abolishes an *Hpa*II restriction site and it was verified by restriction fragment length polymorphism (RFLP) method (Figure 5.36).

Digestion of the wild type samples gave rise to two fragments of 219 and 111 bp in length while the samples with the variation resulted in an undigested 330bp fragment. The c.69T>C sequence variation created an *Hpa*II restriction site and it was verified by restriction fragment length polymorphism (RFLP) method. Digestion of the wild type samples gave rise to two fragments of 219 and 111 bp in length while the samples with the variation resulted in a digestion pattern with three fragments of 187, 111 and 32 bp in size. On the other hand the samples with both c.40G>T and c.69T>C variations created two fragments with the sizes 143 and 187 bp.

The results of the restriction analysis revealed that P461 had both of the mutations separately in two alleles giving rise to a restriction pattern with an undigested 330bp fragment as well as a digested pattern of 187 and 111 bp and a not observable 32 bp fragment. The variations observed in the DNA sequence of patient P461 was also shared by healthy individuals. The second c.69T>C variation was not detected in the sister of patient P461 (Figure 5.36). The first mutant allele was present in 8 chromosomes and the frequency of the second allele in the control population was 9 in 70 chromosomes.

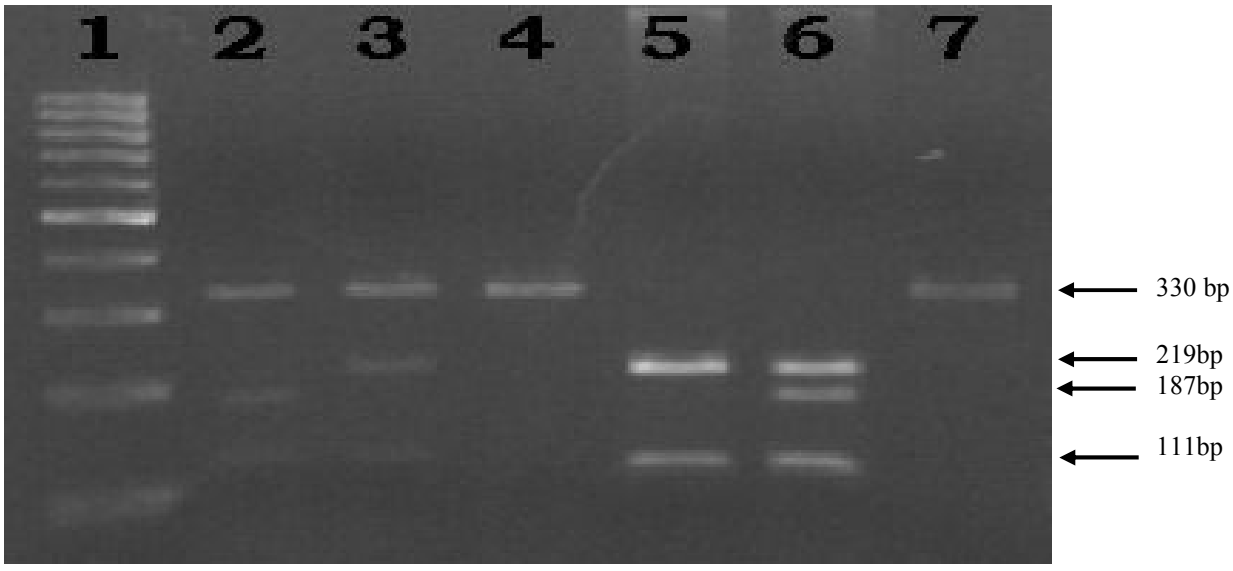

Figure 5.36. Agarose gel image showing the result of *Hpa*II restriction digestion of the second exon of *HSP60* gene for patient P461 (1: Marker; 2: P461; 3: sister of P461; 4: homozygous c.40G>T; 5: Wild Type; 6: heterozygous c.69T>C; 7: Uncut)

The SSCP analysis also revealed an abnormal migration profile in three of the patients in exon 3 of the HSP60 gene (Figure 5.37).

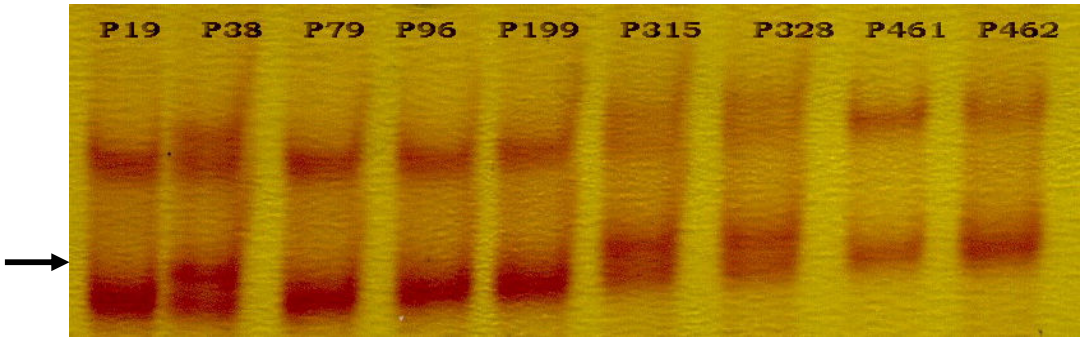

Figure 5.37. The SSCP gel indicating an abnormal migration pattern in exon 3 of *HSP60*

The sequencing analysis of exon 3 of the HSP60 gene for patient P38 revealed a heterozygous c.273A>G substitution which does not change the lysine residue at position 91 (Figure 5.38).

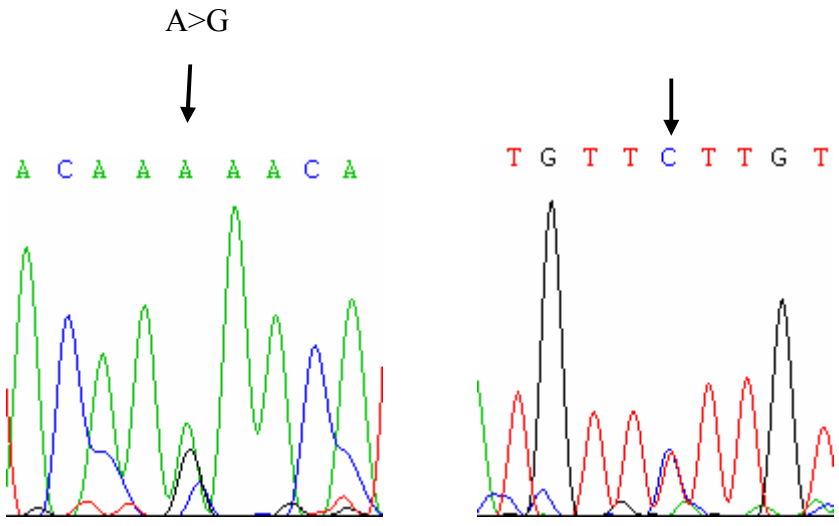

Figure 5.38. Chromatograms showing c.273A>G change in exon 3 of *HSP60* gene in heterozygous state for patient P38 in the sense (a) and antisense (b) strands.

An abnormal migration pattern was observed in the SSCP analysis of exon 5 of the HSP60 gene for the screened patients (Figure 5.39).

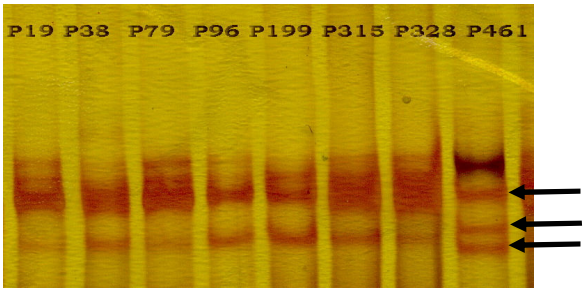

Figure 5.39. The SSCP gel showing the abnormal migration pattern in exon 5 of the HSP60 gene

Sequencing analysis of exon 5 of *HSP60* for patients P19, P38 and P461 revealed an insertion variation (IVS5+113_114insAG) in intron 5 (Figure 5.40).

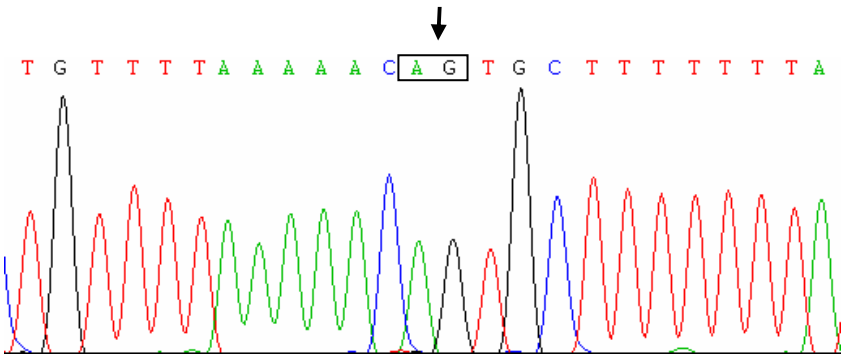

Figure 5.40. Chromatograms showing the IVS5+113_114insAG variation in homozygous state for patient P19

This sequence variation was tested by a splice site prediction program, Neural Network (Reese *et al.*, 1997), and it is found that a cryptic splice site is not created by the insertion.

The sequence alterations identified in this study are summarized in Table 5.2.

Table 5.2. The sequence variations identified in this project (ND: not determined)

Index Patient	Clinical Diagnosis	Gene	Nucleotide Change	Variations	Amino acid Change
F17.3	CMT	GDAP1	c.174_176delinsTGTG	Delins (Novel)	p.P59delinsVLEfsX62
P429	CMT	GDAP1	c.507T>G	Polymorphism	p.S169S
P226	CMT	LMNA	c.612G>A	Polymorphism	L204L
P375	CMT	LMNA	IVS3+56G>T	Polymorphism	-
P375	CMT	LMNA	IVS3+73C>T	Polymorphism	-
P298	CMT	LMNA	IVS4+13G>T	Polymorphism	-
P298	CMT	LMNA	IVS4+61C>T	Polymorphism	-
P350	CMT	LMNA	c.861C>T	Polymorphism	A287A
P48	CMT	LMNA	IVS8+44C>T	Polymorphism	-
P265	CMT	LMNA	c.1698C>T	Polymorphism	H566H
P350	CMT	LMNA	g.24479G>C	Polymorphism	-
P350	CMT	LMNA	g.24610_24611insA	Polymorphism	-
P164	CMT	HSPB1	g.52C>T	Polymorphism	-
P77	CMT	HSPB1	IVS1+100C>A	Polymorphism	-
P77	CMT	HSPB1	IVS2+60G>A	Polymorphism	-
P286	CMT2	HSPB1	c.439_440insC	Insertion (Novel)	p.G147fsX160
P641	HSP	HSP60	c.40G>T	Polymorphism (Novel)	p.V14L
P641	HSP	HSP60	c.69T>C	Polymorphism (Novel)	p.T23T
P38	HSP	HSP60	c.273A>G	ND	p.L91L
P38	HSP	HSP60	IVS5+113_114insAG	ND	-

6. DISCUSSION

In the scope of this thesis, the genetic background of autosomal recessive CMT2 disease was investigated in a cohort of Turkish families and isolated cases. Since GDAP1 gene mutations can cause both autosomal recessive CMT4 and ARCMT2, homozygosity mapping was also performed to test linkage to the locus in CMT4 patients. The study was extended to screening of the small heat shock protein genes, HSPB1, and HSPB8, that have been recently shown to be responsible for autosomal dominant CMT2 and distal HMN. The involvement of another heat shock protein gene, HSP60, was tested in a small group of Hereditary Spastic Paraplegia patients.

Linkage was excluded to 19q13.3 locus in the three ARCMT2 families (P118, P192, and P435) by haplotype and lod-score analysis. In the other families tested for linkage to the locus the results were inconclusive either because the families were noninformative for the markers used or they were too small to get a significant lod-score data. The study can be repeated in family of P210 by testing new marker loci for which the family can be informative.

Patient P118 was clinically diagnosed as ARCMT2 and appropriate loci and genes were screened in this patient and his family. Homozygosity mapping also excluded linkage to the CMT4A locus harboring *GDAP1* for P118, thus, he was not screened further for *GDAP1* mutations. Moreover, he was negative for mutations in the LMNA gene. These results suggest that there is at least one more locus responsible for ARCMT2 phenotype. Although linkage to 19q13.3 was excluded and LMNA mutations were absent in patients P192 and P435, GDAP1 gene should also be excluded as the disease causing gene to complete the study in these two families.

A total of eighty-six CMT patients were tested for homozygosity in the CMT4A locus. Twenty-five of these patients were clinically diagnosed as ARCMT2 and 10 of them were found to be homozygous with at least two markers tested. However, disease causing mutations could not be identified with the SSCP method in any of these patients. These ARCMT2 patients were also screened for mutations in the LMNA gene but again no

mutations were detected in the 12 exons and their flanking intronic regions of the gene. For these patients homozygousity can be tested in 19q13.1 locus in further studies.

Twenty of the 86 patients were clinically diagnosed as CMT4 and homozygosity mapping showed that eight of these patients were homozygous for the CMT4A locus. Among these only the patient F17.3 was found be homozygous for a novel mutation (c.174_176delinsTGTG; p.P59delinsVLEfsX62) in the second exon of the GDAP1 gene.

Patient F17.3 was a 5-year-old female, born to consanguineous parents and the only affected sibling in the family. Hypothetically, the mutation creates a premature translational stop codon upstream of the GST-N domain (p.P59delinsVLEfsX62). The age of onset was quite early (1,5 years) and compatible with the finding that truncated protein is produced by both alleles in the patient. She had MNCV value of 32 m/s at the time of examination (1989) indicating a demyelinating type of CMT. Identification of the GDAP1 mutation in homozygous condition confirms the clinical findings and diagnoses the patient as CMT4A.

Another truncation mutation, W31X, causing premature termination of GDAP1 translation was previously reported by Baxter *et al.* and diagnosis for the patient was CMT4A with a motor NCV around 31 m/s (2002). However, truncation mutations in the gene were also detected in ARCMT2. Thus, phenotype/genotype correlations are still insufficient to unravel the disease mechanisms of CMT4A/ARCMT2 and new patients have to be screened for mutations in the GDAP1 gene.

A group of 27 patients, that were clinically diagnosed as demyelinating CMT and were the only affected individuals in the families without reported consanguinity among parents, were analyzed for homozygosity in the GDAP1 locus. Seven of these patients were found to be homozygous for the locus but without detectable mutations in the gene. This finding indicates that the patients' haplotypes were identical by state rather than being identical by descent.

The status of inheritance could not be determined for fourteen CMT2 patients since pedigrees were not available or they represent the only affected sibling of consanguineous

parents. These patients were also tested in the homozygosity mapping of the CMT4A locus. Although four of them were homozygous for at least two of the markers no causative mutations could be detected in *GDAP1*. Observation of homozygosity for CMT4A locus in the patients who do not have *GDAP1* mutations may again indicate that the homozygous alleles were identical by state.

Patient P429 with vocal cord paralysis was a good candidate for *GDAP1* screening since mutations in exons four and five have been reported to be associated with vocal cord paralysis in CMT4 patients (Boerkoel *et al.*, 2003; Cuesta *et al.*, 2002). However, direct sequencing of the patient's DNA for *GDAP1* revealed no mutations except a previously reported polymorphism (c.507T>G; p.S169S). If the patient has no mutations in the intronic or regulatory sites of *GDAP1*, this finding indicates that the gene can be excluded to have a causative role in vocal cord paralysis in at least some of the CMT4A cases.

Although vocal cord paralysis is frequently associated with CMT4A phenotype (Boerkoel *et al.*, 2003; Cuesta *et al.*, 2002), it is also observed in CMT1 patients with *PMP22* duplication or *EGR2* mutations (Azzedine *et al*.2003) and CMT2 patients (Sevilla *et al.*, 2003). Patient P429 has been referred to our laboratory with a possible Dejerine-Sottas Syndrome (DSS). However, *PMP22* duplication or deletion could not be detected in this patient. Furthermore, the age at onset for the patient was 10-20 years that is not compatible with an *EGR2* mutation, thus, the patient should be further screened for other CMT genes.

Although *GDAP1* mutations were reported previously to be a frequent cause of CMT4 cases (Nelis *et al.*, 2002), only one individual with suspected autosomal recessive inheritance was identified to carry a mutation in *GDAP1* among 86 patients in our cohort. This finding shows that *GDAP1* mutations might constitute a low per cent of the whole autosomal recessive cases in the Turkish population. On the other hand, individuals that were not homozygous for the GDAP1 gene locus with the markers used could have been homozygous for a smaller interval around the gene but were not screened for mutations. In addition, efficiency of the SSCP technique might not be enough to detect some of the mutations.

The SSCP analysis of the LMNA gene revealed ten previously reported polymorphisms in a patient population of 24 ARCMT2 patients as well as 12 patients that could not be defined to have either an autosomal dominant or autosomal recessive inheritance. However, all patients tested negative for causative mutations in the gene, excluding the LMNA locus involvement. This finding suggests a very low contribution of this gene to Turkish ARCMT2 population.

In the second part of the study, the involvement of the small heat shock protein genes in CMT disease were tested by SSCP and subsequent DNA sequencing of SSC polymorphisms identified in HMN, CMT2, and HSP patients.

HSPB1 gene was screened in eight HMN, 10 CMT2, and 11 patients that could not be classified as an autosomal dominant or recessive inheritance. A novel insertion mutation (c.439_440insC) was identified in the exon 3 in patient P286. The patient was found to be heterozygous for the mutation indicating a dominant inheritance. This mutation created an early termination codon at the end of Hsp20-alpha-crystallin domain (p.G147fsX160) that is known to be critical for the functioning of the protein. The parents were consanguineous and P286 was the only affected child among the four siblings. The proband's mother, for whom unfortunately there was no clinical data, had the same migration profile in the SSCP analysis. Thus, the variation identified could be a polymorphism rather than a causative mutation. However, by personal communication the mother reported paresthesia at the finger tips of the feet that could be an indication of a mild affect of the variation in the *HSPB1* sequence. It is possible that the same mutation causes variable phenotypes in affected individuals because of modifier effects. *HSPB1* is located in the UPD7 (UniParental Disomy on chromosome 7) region that is suspected to be imprinted. As the differential expression of HSPB1 was reported during development, the presence of genomic imprinting in the region is of great possibility (Stock *et al.*, 2003). The genetic redundancy can also be one of the mechanisms leading to variable phenotypes. *HSPB1* has two pseudogenes located on chromosomes 9q21 and Xp11.2 and they might be compensating the mutant copy of the HSPB1 if they are transcribed. In addition, the other nine sHSPs in the human genome having the functional α-crystallin domain might also replace the activity of the mutant HSPB1.

The patient P286 with the HSPB1 mutation was a 24-year-old female at the time of examination with an age of onset between two to ten years. She had abnormal mobility and distal weakness in the upper limbs. Hand wrists and pes cavus were also observed in the patient. Nerve median and ulnar NCV values were reported as 44,8 and 45,7 m/s., respectively, however her sensory nerves were inexcitable. The patient was referred to our laboratory with a CMT2 diagnosis rather than an HMN phenotype. Since *HSPB1* mutations have been reported to cause CMT2F phenotype, we have compared their clinical findings with that of our patient. P286 had weakness in the feet that was a common feature, however, the age of onset was 4 years in P286 while it was reported to be 15-25 years for CMT2F patients. It was also reported that the disability is at the highest levels after 15-20 years in CMT2F patients but interestingly, patient P286 reported by personal communication that she had a less severe phenotype after physiotherapy. These findings showed that the progression of the disease varies between patients with HSPB1 mutation. The disease causing mutation identified in the patient will be the seventh mutation reported for HSPB1 and is a truncation while previously reported cases are all missense mutations. The patient and her mother should be further evaluated clinically in the light of genetic diagnosis.

On the other hand, no other HSP gene mutations could be identified in this cohort of patients. Thus, these cases should be further analyzed for mutations in other genes and loci responsible for HMN and CMT2 (Table 1.2). Further clinical classification of the patients according to the subtypes of the disease would ease the identification of the responsible genes.

Three reported polymorphisms of *HSPB1* were also identified in our cohort. Two of these polymorphisms (IVS1+100C>A and IVS2+60G>A) were found in patient P77 in the first and second introns.

Four variations were defined in the HSP patients. The restriction endonuclease analysis of two of the variations in *HSP60* (c.40G>T and c.69T>C) were identified as novel polymorphisms in the second exon. The other two variations (c.273A>G and IVS5+113_114insAG) were not present in the databases of NBCI, thus the healthy population should be screened to unravel whether they are novel polymorphisms or

causative mutations. Further screening of other genes involved in HSP may reveal the disease causing mutations in HSP patients.

We have encountered several technical problems during confirmation of the identified DNA variations. None of the variations except the ones in the HSP60 gene were suitable for the restriction endonuclease digestion. ARMS method could not be used either for the verification of the variation in the HSPB1 gene (c.439_440insC) because a cytosine residue was inserted after six cytosines interfering with the primer design. Since the length of the PCR product increases one base pair, it was thought that denaturing gel could be a suitable method to test the presence of this variation in the control population. However, it was not successful either since variable lengths of DNA were observed in a high number of healthy controls. Since the variation leads to a premature stop codon, identification of the variation in a large number of healthy individuals was unexpected. When the single nucleotide polymorphism (SNP) database of NCBI was searched for the region, another insertion was found to be reported previously. The last method used to screen the healthy controls was SSCP analysis that finally proved that it was a polymorphism rather than a causative mutation.

Another problem was encountered in the ARMS method used to test the presence of the c.174_176delinsTGTG variation in *GDAP1* in healthy controls and non-specific amplifications were observed. However, subsequent use of SSCP analysis in the screening of control population led to the confirmation that this variation was a novel disease causing mutation.

The SSCP method used to screen the genes for mutations is a convenient system. However, it is not sufficient enough to detect all the sequence variations. Because of this reason, there can be further mutations in the genes tested that could not be identified. Furthermore, the regulatory regions and whole intronic parts of the genes were not screened for mutations and any variation in these regions causing disease phenotype might have been missed.

The most widely used methods for the verification of DNA variations did not work in this study indicating that development of new techniques is required that are more

convenient and less time consuming. On the other hand, the SNP database of NCBI was a quite useful tool for the identification of the reported polymorphisms and searching the DNA sequences for possible SNPs.

The functional studies of the identified mutations in *GDAP1* and *HSPB1* were not performed. Although both mutations cause truncated proteins, it is necessary to test the functional properties of the mutant proteins and demonstrate the disease causing effects of them. The contribution of the polymorphisms to the disease phenotypes was also not investigated in this study.

To sum up, all ARCMT2 loci were excluded in an ARCMT2 family demonstrating the presence of further locus or loci responsible from this disease. Two novel mutations were also identified in the GDAP1 and HSPB1 genes in CMT4 and CMT2 patients, respectively. The mutations hypothetically cause truncated proteins, functions of which should be investigated. Although variations were identified in *LMNA* and *HSP60* genes, no disease causing mutation could be detected that indicates the requirement for further gene screening. *HSPB8* was also free from variations.

The molecular genetic diagnosis of diseases helps accurate genetic counseling, prevents unnecessary medical treatment and surgical applications required for the clinical diagnosis. The identification of novel genes and their mutations can shed light on genotype-phenotype correlations and may help to see the light at the end of the tunnel leading to the disease mechanisms.

7. CONCLUSION

This thesis is an important study revealing the missing parts of ARCMT2 disease in the Turkish population. Exclusion of all known loci for the ARCMT2 was an important outcome of this thesis emphasizing the necessity of identification of new locus/loci for ARCMT2. Two novel mutations hypothetically causing truncated proteins, identified in *GDAP1* and *HSPB1* in this study should be investigated functionally. The genotype-phenotype correlations was compatible for the patient carrying the *GDAP1* mutation whereas the patient with the HSPB1 gene mutation did not obey the criteria completely for either CMT2F or dHMN phenotypes that are both caused by *HSPB1* mutations. Moreover, the differences in the phenotypes of the patient and her mother carrying the same mutation demonstrate the demand for further research in this family. To conclude with, to be able to determine the genetic causes of the diseases of patients studied in this thesis project, screening of other genes responsible for the corresponding diseases should be completed and functional studies should be performed for constituting genotype-phenotype correlations which leads to the identification of roles of the proteins involved in disease pathogenesis.

REFERENCES

Ackerley, S., Paul A. James, Arran Kalli, Sarah French, Kay E. Davies and Kevin Talbot, "A Mutation in the Small Heat-Shock Protein HSPB1 Leading to Distal Hereditary Motor Neuronopathy Disrupts Neurofilament Assembly and the Axonal Transport of Specific Cellular Cargoes", *Human Molecular Genetics*, 2006, Vol. 15, No. 2 347–354.

Ammar, N., E Nelis, L. Merlini, N. Barišić, R. Amouri, C. Ceuterick, J. J. Martin, V. Timmerman, F. Hentati, and P. De Jonghe, 2003, "Identification of Novel *GDAP1* Mutations Causing Autosomal Recessive Charcot-Marie-Tooth Disease", *Neuromuscular Disorders*, Vol. 13, pp. 720–728.

Antonellis A, R. E. Ellsworth, N. Sambuughin, I. Puls, A. Abel, S. Q. Lee-Lin, A. Jordanova, I. Kremensky, K. Christodoulou, L. T. Middleton, K. Sivakumar, V. Ionasescu, B. Funalot, J. M. Vance, L. G. Goldfarb, K. H. Fischbeck and E. D. Green, 2003, "Glycyl tRNA Synthetase Mutations in Charcot-Marie-Tooth Disease Type 2D and Distal Spinal Muscular Atrophy Type V", *American Journal of Human Genetics,* Vol. 72, pp. 1293–1299.

Azzedine, H., M. Ruberga, D. Ente, C. Gilardeau, S. Pèriè, B. Wechsler, A. Brice, E. LeGuern, and O. Dubourg, 2003a, "Variability of Disease Progression in a Family with Autosomal Recessive CMT Associated with a S194X and New R310Q Mutation in the GDAP1 Gene", *Neuromuscular Disorders*, Vol. 13, pp. 341-346.

Azzedine, H., A. Bolino, T. Taieb, N. Birouk, M. Di Duca, A. Bouhouche, S. Benamou, A. Mrabet, T. Hammadouche, T. Chkili, R. Gouider, R. Ravazzolo, A. Brice, J. Laporte, and E. LeGuern, 2003b, "Mutations in MTMR13, a New Pseudophosphatase Homologue of MTMR2 and Sbf1, in Two Families with an Autosomal Recessive Demyelinating Form of Charcot-Marie-Tooth Disease Associated with Early-Onset Glaucoma" *American Journal of Human Genetics,* Vol. 72, pp. 1141–1153.

Barhoumi C., R. Amouri, C. Ben Hamida, M. Ben Hamida, S. Machghoul, M. Gueddiche and F. Hentati, 2001, "Linkage of a New Locus for Autosomal Recessive Axonal Form of Charcot-Marie-Tooth Disease to Chromosome 8q21.3" *Neuromuscular Disorders*, Vol. 11, pp. 27-34.

Baxter, R.V., K. B. Othmane, J. M. Rochelle, J. E. Stajich, C. Hulette, S. Dew-Knight, F. Hentati, M. Ben Hamida, S. Bel, J. E. Stenger, J. R. Gilbert, M. A. Pericak-Vance and J. M. Vance, 2002, "Ganglioside-Induced Differentiation associated Protein-1 is Mutant in Charcot-Marie-Tooth Disease Type 4A/8q21", *Nature Genetics,* Vol. 30, pp. 21-22.

Beal, M. F., 2005, "Mitochondria Take Center Stage in Aging and Neurodegeneration", *Annals of Neurology*, Vol. 58, pp. 495–505.

Ben Othmane, K., F. Hentati, F. Lennon, C. Ben Hamida, S. Blel, A. D. Roses, M. A. Pericak-Vance, M. Ben Hamida and J. M. Vance, 1993, "Linkage of a Locus (CMT4A) for Autosomal Recessive Charcot-Marie-Tooth Disease to Chromosome 8q", *Human Molecular Genetics*, Vol. 2, pp. 1625-1628.

Ben Othmane K., D. Loeb, R. Haywoth-Hodge, F. Hentati, N, Rao, A.D. Roses, M. Ben Hamida, M.A. Pericak-Vance and J.M.Vance, 1995, "Physical and Genetic Mapping of the CMT4A Locus and Exclusion of PMP-2 as the Defect in CMT4A", *Genomics*, Vol. 28, pp. 286-290.

Ben Othmane, K., Julie M. Rochelle, M. Ben Hamida, B. Slotterbeck, N. Rao, F. Hentati, M. A. Pericak-Vance and J. M. Vance, 1998, "Fine Localization of the CMT4A Locus Using a PAC Contig and Haplotype Analysis", *Neurogenetics*, Vol. 2, pp.18-23.

Ben Othmane, K., E. Johnson, M. Menold, F. L. Graham, M. Ben Hamida, O. Hasegawa, A. D. Rogala, A. Ohnishi, M. Pericak-Vance, F. Hentati, and J. M. Vance, 1999, "Identification of a New Locus for Autosomal Recessive Charcot–Marie–Tooth

Disease with Focally Folded Myelin on Chromosome 11p15", *Genomics*, Vol. 62, pp. 344–349.

Benndorf R., X. Sun, R. R. Gilmont, K. J. Biederman, M. P. Molloy, C. W. Goodmurphy, H. Cheng, P. C. Andrews, and M. J. Welsh, 2001, "HSP22, a New Member of the Small Heat Shock Protein Superfamily, Interacts with Mimic of Phosphorylated HSP27 (3DHSP27)", *Journal of Biological Chemistry*, Vol. 276, pp. 26753–26761.

Bera, S., P. Thampi, W. J. Cho, and E. C. Abraham, 2002, "A Positive Charge Preservation at Position 116 of Alpha A-Crystallin is Critical for its Structural and Functional Integrity", *Biochemistry*, Vol. 41, pp. 12421-12426.

Berger P., P. Young and U. Suter, 2002, "Molecular Cell Biology of Charcot-Marie-Tooth Disease", *Neurogenetics*, Vol. 4, pp. 1-15.

Berger, P., E. E. Sirkowski, S. S. Scherer, and U. Suter, 2004, "Expression Analysis of the N-Myc Downstream-Regulated Gene 1 Indicates that Myelinating Schwann Cells are the Primary Disease Target in Hereditary Motor and Sensory Neuropathy-Lom", *Neurobiology of Disease*, Vol. 17, pp. 290– 299.

Philipp Berger, Axel Niemann, and Ueli Suter, 2006, "Schwann Cells and the Pathogenesis of Inherited Motor and Sensory Neuropathies (Charcot-Marie-Tooth Disease)", *Glia* Vol. 54, pp. 243–257.

Berghoff, C., M Berghoff, A. Lealb, B. Morera, R. Barrantes, A. Reis, B. Neundörfer, B. Rautenstrauss, G. D. Valle and D. Heussa, 2004, "Clinical and Electrophysiological Characteristics of Autosomal Recessive Axonal Charcot-Marie-Tooth Disease (ARCMT2B) that Maps to Chromosome 19q13.3", *Neuromuscular Disorders*, Vol. 14, pp. 301–306.

Biancheri, R., F. Zara, P. Striano, M. Pedemonte, D. Cassandrini, S. Stringara, F., Manganelli, L. Santoro, A. Schenone, E. Bellone and C. Minetti, 2006, "GDAP1

Mutation in Autosomal Recessive Charcot-Marie-Tooth with Pyramidal Features", *Journal of Neurology*, Vol. 253, pp. 1234-1235.

Boerkoel, C. F., H. Takashima, M. Nakagawa, S. Izumo, D. Armstrong, I. Butler, P. Mancias, S. C. H. Papasozomenos, L. Z. Stern, and J. R. Lupski, 2003, "CMT4A: Identification of a Hispanic GDAP1 Founder Mutation", *Annals of Neurology*, Vol. 53, pp. 400-405.

Bolino, A., V. Brancolini, F. Bono, A. Bruni, A. Gambardella, G. Romeo, A. Quattrone and M. Devoto, 1996, "Localization of a Gene Responsible for Autosomal Recessive Demyelinating Neuropathy with focally folded myelin sheaths to chromosome 11q23 by homozygosity mapping and haplotype sharing", *Human Molecular Genetics*, Vol. 5, pp. 1051-1054.

Bolino A., M. Muglia, F. L. Conforti, E. LeGuern, M. A. M. Salih, D. M. Georgiou, K. Christodoulou, I. Hausmanowa-Petrusewicz, P. Mandich, A. Schenone, A. Gambardella, F. Bono, A. Quattrone, M. Devoto and A. P. Monaco, 2000, "Charcot-Marie-Tooth Type 4B is Caused by Mutations in the Gene Encoding Myotubularin-Related Protein-2", *Nature Genetics*, Vol. 25, pp. 17-19.

Bouhouche, A., A. Benomar, N. Birouk, A. Mularoni, F. Meggouh, J. Tassin, D. Grid, A. Vandenberghe, M. Yahyaoui, T. Chkili, A. Brice, and E. LeGuern, 1999, "A Locus for an Axonal Form of Autosomal Recessive Charcot-Marie-Tooth Disease Maps to Chromosome 1q21.2-q21.3", *American Journal of Human Genetics*, Vol. 65, pp. 722–727.

Brownlees, J., S. Ackerley, A. J.Grierson, N. J. O. Jacobsen, K. Shea, B. H. Anderto, P. N. Leigh, C. E. Shaw and C. C. J. Miller, 2002, "Charcot–Marie–Tooth Disease Neurofilament Mutations Disrupt Neurofilament Assembly and Axonal Transport", *Human Molecular Genetics*, Vol. 11, pp. 2837–2844.

Bruey, J. M., C. Ducasse, P. Bonniaud, L. Ravagnan, S. A. Susin, C. Diaz-Latoud, S. Gurbuxani, A. P. Arrigo, G. Kroemer, E. Solary and C. Garrido, 2000, "Hsp27

Negatively Regulates Cell Death by Interacting with Cytochrome C", *Nature Cell Biology,* Vol. 2, pp. 645–652.

Bukau, B. and A. L. Horwich, 1998, "The Hsp70 and Hsp60 Chaperone Machines", *Cell*, Vol. 92, pp. 351-366.

Charcot J. M. and P. Marie, 1886, "Sur Une Forme Particuliere Datrophie Musculaire Progressive Souvent Familiale Debutant par les Pieds et les Jambes et Atteignant Plus Tard les Mains", *Reviews in Médicine*, Vol.6, pp. 97-138.

Christodoulou, K., E. Zamba, M. Tsingis, A. Mubaidin, K. Horany, S. Abu-Sheikh, M. El-Khateeb, K. Kyriacou, T. Kyriakides and A. Al-Qudah, 2000, "A Novel Form of Distal Hereditary Motor Neuronopathy Maps to Chromosome 9p21.1–p12", *Annals of Neurology*, Vol. 48, pp. 877–884.

Claramunt, R., L. Pedrola, T. Sevilla, A. Lòpez de Munain, J. Berciano, A. Cuesta, B. Sánchez-Navarro, J. M. Millàn, G. M. Saifi, J. R. Lupski, J. J. Vílchez, C. Espinòs and F. Palau, 2005, "Genetics of Charcot–Marie–Tooth Disease Type 4A: Mutations, Inheritance, Phenotypic Variability, and Founder Effect", *Journal of Medical Genetics*, Vol. 42, pp. 358–365.

Cuesta, A. , L. Pedrola, T. Sevilla, J. García-Planells, M. J. Chumillas, F. Mayordomo, E. LeGuern, I. Marín, J. J. Vílchez and F. Palau, 2002, "The Gene Encoding Ganglioside-Induced Differentiation-Associated Protein 1 is Mutated in Axonal Charcot-Marie-Tooth Type 4A Disease", *Nature Genetics*, Vol. 30, pp. 22-25.

De Jonghe, P., Timmerman, V., Van Broeckhoven, C. and workshop participants, 1998, "2nd Workshop of the European CMT Consortium: 53rd ENMC International Workshop on Classification and Diagnostic Guidelines for Charcot–Marie–Tooth Type 2 (CMT2–HMSN II) and Distal Hereditary Motor Neuropathy (distal HMN–spinal CMT)", *Neuromuscular Disorders*, Vol. 8, pp. 426–431.

De Jonghe, P., V. Timmerman, C. Ceuterick, E. Nelis, E. De Vriendt, A. Löfgren, A. Vercruyssen, C. Verellen, L. Van Maldergem, J.-J. Martin and C. Van Broeckhoven, 1999, "The Thr124Met Mutation in the Peripheral Myelin Protein Zero (MPZ) Gene is Associated with a Clinically Distinct Charcot-Marie-Tooth Phenotype", *Brain*, Vol. 122, pp. 281-290.

De Jonghe, P., I. Mersivanova, E. Nelis, J. Del Favero, J. J. Martin, C. Van Broeckhoven, O. C. Evgrafov, and V. Timmerman, 2001, "Further Evidence that Neurofilament Light Chain Gene Mutations can Cause Charcot–Marie–Tooth Disease Type 2E", *Annals of Neurology*, Vol. 49, pp. 245–249.

De Jonghe, P., M. Auer-Grumbach, J. Irobi, K. Wagner, M. L. Kennerson, B. Plecko, G. A. Nicholson, H. P. Hartung and V. Timmerman, 2002, "Autosomal Dominant Juvenile ALS and Distal Hereditary Motor Neuronopathy with Pyramidal Tract Signs: Synonyms for the Same Disorder?", *Brain*, 125, 1320–1325.

De Sandre-Giovannoli, A., M. Chaouch, S. Kozlov, J.- M. Vallat, M. Tazir, N. Kassouri, P. Szepetowski, T. Hammadouche, A. Vandenberghe, C. L. Stewart, D. Grid, and N. Lévy1, 2002, "Homozygous Defects in *LMNA,* Encoding Lamin A/C Nuclear-Envelope Proteins, Cause Autosomal Recessive Axonal Neuropathy in Human (Charcot-Marie-Tooth Disorder Type 2) and Mouse", *American Journal of Human Genetics,* Vol. 70, pp. 726–736.

De Sandre-Giovannoli, A., M. Chaouch, I. Boccaccio, R. Bernard, V. Delague, D. Grid, J. M. Vallat, N. Lévy and A. Mégarbané, 2003, "Phenotypic and Genetic Exploration of Severe Demyelinating and Secondary Axonal Neuropathies Resulting from GDAP1 Nonsense and Splicing Mutations", *Journal of Medical Genetics*, Vol. 40, pp. e87.

De Sandre-Giovannoli, A., V. Delague, T. Hamadouche, M. Chaouch, M. Krahn, I. Boccaccio, T. Maisonobe, E. Chouery, R. Jabbour, S. Atweh, D. Grid, A. Mégarbané and N. Lévy, 2005, "Homozygosity Mapping of Autosomal Recessive Demyelinating Charcot-Marie-Tooth Neuropathy (CMT4H) to a Novel Locus on Chromosome 12p11.21-q13.11", *Journal of Medicinal Genetics*, Vol. 42, pp. 260–265.

Delague, V., C. Bareil, S. Tuffery, P. Bouvagnet, E. Chouery, S. Koussa, T. Maisonobe, J. Loiselet, A. Mégarbané, and M. Claustres, 2000, "Mapping of a New Locus for Autosomal Recessive Demyelinating Charcot-Marie-Tooth Disease to 19q13.1-13.3 in a Large Consanguineous Lebanese Family: Exclusion of *MAG* as a Candidate Gene", *American Journal of Human Genetics*, Vol. 67, pp. 236–243.

Dierick, I., Irobi, J., P. D. Jonghe and V. Timmerman, 2005, "Small Heat Shock Proteins in Inherited Peripheral Neuropathies", *Annals of Medicine* Vol. 37, pp. 413-422.

Dyck, P. J. and E. H. Lambert, 1968a, "Lower Motor and Primary Sensory Neuron Diseases with Peroneal Muscular Atrophy I. Neurologic, Genetic, and Electrophysiologic Findings in Hereditary Polyneuropathies", *Archives of Neurology*, Vol. 18: pp. 603-18.

Dyck, P. J. and E. H. Lambert, 1968b, "Lower Motor and Primary Sensory Neuron Diseases with Peroneal Muscular Atrophy II - Neurologic, Genetic, and Electrophysiologic Findings in Various Neuronal Degenerations", *Archives of Neurology*, Vol. 18: pp. 619-25.

Evgrafov, O. V., I. Mersiyanova, J. Irobi, L. Van Den Bosch, I. Dierick, C. L. Leung, O. Schagina, N. Verpoorten, K. Van Impe, V. Fedotov, E. Dadali, M. Auer-Grumbach, C. Windpassinger, K. Wagner, Z. Mitrovic, D. Hilton-Jones, K. Talbot, J.-J. Martin, N. Vasserman, S. Tverskaya, A. Polyakov, R. K. H. Liem, J. Gettemans, W. Robberecht, P. De Jonghe and V. Timmerman, 2004, "Mutant Small Heat-Shock Protein 27 Causes Axonal Charcot-Marie-Tooth Disease and Distal Hereditary Motor Neuropathy", *Nature Genetics*, Vol. 36, pp. 602-606.

Fink, J. K., 2003, "Advances in the Hereditary Spastic Paraplegias", *Experimental Neurology*, Vol. 184 pp. S106–S110.

Fontaine, B., C. S. Davoine, A. Durr, C. Paternotte, I. Feki, J. Weissenbach, J. Hazan, A. Brice, 2000, "A New Locus for Autosomal Dominant Pure Spastic Paraplegia, on

Chromosome 2q24-q34", *American Journal of Human Genetics*, Vol. 66, pp. 702-707.

Genschel J. and H. H.-J. Schmidt, 2000, "Mutations in the LMNA Gene Encoding Lamin A/C", *Human Mutation,* Vol. 16: pp. 451-459.

Goizet, C., R. B. Yaou, L. Demay, P. Richard, S. Bouillot, M. Rouanet, E. Hermosilla, G. Le Masson, A. Lagueny, G. Bonne and X .Ferrer, 2004, "A New Mutation of the Lamin A/C Gene Leading to Autosomal Dominant Axonal Neuropathy, Muscular Dystrophy, Cardiac Disease, and Leuconychia", *Journal of Medical Genetics*, 2004; Vol. 41, pp. e29-34.

Guilbot, A., A. Williams, N. Ravisé, C. Verny, A. Brice, D. L. Sherman, P. J. Brophy, E. Leguern, V. Delague, C. Bareil, A. Mégarbané and M. Claustres, 2001, "A Mutation in Periaxin is Responsible for CMT4F, an Autosomal Recessive Form of Charcot-Marie-Tooth Disease", *Human Molecular Genetics*, Vol. 10, pp. 415-421.

Hahn, A.F., W. F. Brown, W. J. Koopman, and T. E. Feasby, 1990, "X-Linked Dominant Hereditary Motor and Sensory Neuropathy", *Brain*, Vol. 113, pp. 1511-25.

Hanemann C. O. and A. C. Ludolph, 2002, "Hereditary Motor Neuropathies and Motor Neuron Diseases: Which is Which", *ALS and Other Motor Neuron Disorders*, Vol. 3, pp. 186-189.

Hansen, J. J., A. Dürr, I. Cournu-Rebeix, C. Georgopoulos, D. Ang, M. N. Nielsen, C-S. Davoine, A. Brice, B. Fontaine, N. Gregersen, and P. Bross, 2002, "Hereditary Spastic Paraplegia SPG13 is Associated with a Mutation in the Gene Encoding the Mitochondrial Chaperonin Hsp60", *American Journal of Human Genetics,* Vol. 70, pp. 1328–1332.

Hansen, J. J., P. Bross, M. Westergaard, M. N. Nielsen, H. Eiberg, A. D. Børglum, J. Mogensen, K. Kristiansen, L. Bolund and N. Gregersen, 2003, "Genomic Structure of the Human Mitochondrial Chaperonin Genes: HSP60 and HSP10 are Localised

Head to Head on Chromosome 2 Separated by a Bidirectional Promoter", *Human Genetics*, Vol. 112, pp. 71–77.

Harding, A. E. and P. K. Thomas, 1980, "The Clinical Features of Hereditary Motor and Sensory Neuropathy Types I and II", *Brain*, Vol. 103, pp. 259-80.

Irobi, J., F. Tissir, P. De Jonghe, E. De Vriendt, C. Van Broeckhoven, V. Timmerman and Beuten J., "A Clone Contig of 12q24.3 Encompassing the Distal Hereditary Motor Neuropathy Type II Gene", 2000, *Genomics*, Vol. 65, pp. 34-43.

Irobi, J., Van Impe K, P. Seeman, A. Jordanova, I. Dierick, N. Verpoorten, A. Michalik, E. De Vriendt, A. Jacobs, V. Van Gerwen, K. Vennekens, R. Mazanec, I. Tournev, D. Hilton-Jones, K. Talbot, I. Kremensky, L. Van Den Bosch, W. Robberecht, J. Van Vandekerckhove, C. Broeckhoven, J. Gettemans, P. De Jonghe and V. Timmerman, 2004a, "Hot Spot Residue in Small Heat Shock Protein 22 Causes Distal Motor Neuropathy", *Nature Genetics,* Vol. 36, pp. 597-601.

Irobi, J., P. D. Jonghe and V. Timmerman, 2004b, "Molecular Genetics of Distal Hereditary Motor Neuropathies", *Human Molecular Genetics*, Vol. 13, pp. r195-202.

Ismailov, S. M., V. P. Fedotov, E. L. Dadali, A. V. Polyakov, C. Van Broeckhoven, V. I. Ivanov, P. De Jonghe, V. Timmerman and O. V. Evgrafov, 2001, "A New Locus for Autosomal Dominant Charcot-Marie-Tooth Disease Type 2 (CMT2F) Maps to Chromosome 7q11-q21", *European Journal of Human Genetics,* Vol. 9, pp. 646–650.

Kalaydjieva, L., J. Hallmayer, D. Chandler, A. Savov, A. Nikolova, D. Angelicheva, R. H. H. King, B. Ishpekova, K. Honeyman, F. Calafell, A. Shmarov, J. Petrova, I. Turnev, A. Hristova, M. Moskov, S. Stancheva, I. Petkova, A. H. Bittles, V. Georgieva, L. Middleton and P. K. Thomas, 1996, "Gene mapping in Gypsies identifies a novel demyelinating neuropathy on chromosome 8q24", *Nature Genetics,* Vol. 14, pp. 214-217.

Kalaydjieva, L., D. Gresham, R. Gooding, L. Heather, F. Baas, R. de Jonge, K. Blechschmidt, D. Angelicheva, D. Chandler, P. Worsley, A. Rosenthal, R. H. M. King and P. K. Thomas, 2000, "*N-myc Downstream-Regulated Gene 1* is Mutated in Hereditary Motor and Sensory Neuropathy–Lom", *American Journal of Human Genetics,* Vol. 67, pp. 47–58.

Kappe, G., Erik Franck, P. Verschuure, W. C. Boelens, J. A. M. Leunissen and W. W. de Jong, 2003, "The Human Genome Encodes 10 α-Crystallin–Related Small Heat Shock Proteins: HspB1–10", *Cell Stress and Chaperones*, Vol. 8, pp. 53–61.

Kijima K., C. Numakura , T. Goto, T. Takahashi , T. Otagiri , K. Umetsu and K. Hayasaka, 2005, "Small Heat Shock Protein 27 Mutation in a Japanese Patient with Distal Hereditary Motor Neuropathy", *Journal of Human Genetics*, Vol. 50, pp. 473–476.

Klebe, S., H. Azzedine, A. Durr, P. Bastien, N. Bouslam, N. Elleuch, S. Forlani, C. Charon, M. Koenig, J. Melki, A. Brice and G. Stevanin, 2006, "Autosomal Recessive Spastic Paraplegia (SPG30) with Mild Ataxia and Sensory Neuropathy Maps to Chromosome 2q37.3", *Brain*, Vol. 129, pp. 1456–1462.

Leal, A., B. Morera, G. Del Valle, D. Heuss, C. Kayser, M. Berghoff, R. Villegas, E. Hernandez, M. Mendez, H. C. Hennies, B. Neundorfer, R. Barrantes, A. Reis and B. Rautenstrauss, 2001, "Second Locus for an Axonal Form of Autosomal Recessive Charcot-Marie-Tooth Disease Maps to Chromosome 19q13.3", *American Journal of Human Genetics*, Vol. 68, pp. 269-274.

LeGuern, E., A. Guilbot, M. Kessali, N. Ravisé, J. Tassin, T. Maisonobe, D. Grid and A. Brice, 1996, "Homozygosity Mapping of an Autosomal Recessive Form of Demyelinating Charcot–Marie–Tooth Disease to Chromosome 5q23–q33", *Human Molecular Genetics,* Vol. 5, pp. 1685-1688.

Lin F. and H. J. Worman, 1993, "Structural Organization of the Human Gene Encoding Nuclear Lamin A and Nuclear Lamin C", *The Journal of Biological Chemistry,* Vol. 268, pp. 16321-16326.

Liu, H., T. Nakagawa, T. Kanematsu, T. Uchida and S. Tsuji, 1999, "Isolation of 10 Differentially Expressed cDNAs in Differentiated Neuro2a Cells Induced Through Controlled Expression of the GD3 Synthase Gene", *Journal of Neurochemistry*, Vol. 72, pp. 1781 - 1790

Litt, M., P. Kramer, D. M. LaMorticella, W. Murphey, E. W. Lovrienand R. G. Weleber, 1998, "Autosomal Dominant Congenital Cataract Associated with a Missense Mutation in the Human Alpha Crystallin Gene CRYAA", 1998, *Human Molecular Genetics*, Vol. 7, pp. 471-474.

Ly, C. V. and P. Verstreken, 2006, "Mitochondria at the Synapse", *The Neuroscientist*, Vol. 12, pp. 291-299.

Marco, A., A. Cuesta, L. Pedrola, F. Palau and Ignacio Marin, 2004, "Evolutionary and Structural Analyses of GDAP1, Involved in Charcot-Marie-Tooth Disease, Characterize a Novel Class Of Glutathione Transferase-Related Genes", *Molecular Biology and Evolution*, Vol. 21, pp. 176-187.

Mattson, M. P., 2002, "Neurogenetics: White Matter Matters", *TRENDS in Genetics,* Vol.18, p. 71.

Mersiyanova I. V., A. V. Perepelov, A. V. Polyakov, V. F. Sitnikov, E. L. Dadali, R. B. Oparin, A. N. Petrin and O. V. Evgrafov, 2000, "A New Variant of Charcot- Marie-Tooth Disease Type 2 (CMT2E) is Probably the Result of a Mutation in the Neurofilament Light Gene", *American Journal of Human Genetics*, Vol. 67, pp. 37–46.

McKusick, V. A., *Mendelian Inheritance in Man*, 10th ed., Baltimore: Johns Hopkins University Press, 1992.

Miller, S. A., D. D. Dykes and H. F. Polesky, 1988, "A Simple Salting Out Procedure for Extracting DNA from Human Nucleated Cells", *Nucleic Acids Research*, Vol. 16, p. 1215.

Muchowski, P.J. and Wacker, J.L. (2005) "Modulation of Neurodegeneration by Molecular Chaperones", *Nature Reviews Neuroscience*, Vol. 6, pp. 11–22.

Nelis, E., S. Erdem, P. Y. K. Van den Bergh, M. C. Belpaire-Dethiou, C. Ceuterick, V. Van Gerwen, A. Cuesta, L. Pedrola, F. Paula, A. A. W. M. Gabreels-Festen, C. Verellen, E. Tan, M. Demirci, C. Van Broeckhoven, P. De Jonghe, H. Topalogle, and V. Timmerman, 2002, "Mutations in GDAP1 Autosomal Recessive CMT with Demyelination and Axonopathy", *Neurology*, Vol. 59, pp.1865-1872.

Nicholson G. and R. Ouvrier, 2002, "GDAP1 Mutations in CMT4: Axonal and Demyelinating Phenotypes? The Exception Proves the Rule", *Neurology*, Vol. 59, pp.1835-1836.

Niemann, A., M. Ruegg, V. L. Padula, A. Schenone and U. Suter, 2005, "Ganglioside-Induced Differentiation Associated Protein 1 is a Regulator of the Mitochondrial Network: New Implications For Charcot-Marie-Tooth Disease" *The Journal of Cell Biology*, Vol. 170, pp. 1067–1078.

Okuda, T., Y. Higashi, K. Kokame, C. Tanaka, H. Kondoh and T. Miyata, 2004, "Ndrg1-Deficient Mice Exhibit a Progressive Demyelinating Disorder of Peripheral Nerves", *Molecular and Cellular Biology,* Vol. 24, pp. 3949-3956.

Patel, H., P. E. Hart, T. T. Warner, R. S. Houlston, M. A. Patton, S. Jeffery and A. H. Crosby, 2001, "The Silver Syndrome Variant of Hereditary Spastic Paraplegia Maps to Chromosome 11q12-q14, with Evidence for Genetic Heterogeneity within This Subtype", *American Journal of Human Genetics*, Vol. 69, pp. 209–215.

Pedrola, L., A. Espert, X. Wu, R. Claramunt, M. E. Shy and F. Palau, 2005, "GDAP1, The Protein Causing Charcot–Marie–Tooth Disease Type 4A, is Expressed in Neurons

and is Associated with Mitochondria", *Human Molecular Genetics*, Vol. 14, 1087–1094.

Reese, M. G., F. H. Eeckman, D. Kulp and D. Haussler, 1997, "Improved Splice Site Detection in Genie", *Journal of Computational Biology*, Vol. 4, pp. 311–323.

Reid, E., 1999, "The Hereditary Spastic Paraplegias", *Journal of Neurology*, Vol. 246, pp. 995–1003.

Rogers, T., D. Chandler, D. Angelicheva, P. K. Thomas, B. Youl, I. Tournev, V. Gergelcheva, and L. Kalaydjieva, 2000, "A Novel Locus for Autosomal Recessive Peripheral Neuropathy in the *EGR2* Region on 10q23", *American Journal of Human Genetics*, Vol. 67, pp. 664–671.

Rouger H., E. LeGuern, N. Birouk, R. Gouider, S. Tardieu, E. Plassart, M. Gugenheim, J. M. Vallat, J. P. Louboutin, P. Bouche, Y. Agid and A. Brice, 1997, "Charcot-Marie-Tooth Disease with Intermediate Motor Nerve Conduction Velocities: Characterization of 14 Cx32 Mutations in 35 Families", *Human Mutations*, Vol. 10, pp. 443-452.

Rozear, M. P., M. A. Pericak-Vance, K. Fischbeck, J. M. Stajich, P. C. Gaskell, D. A. Krendel, D. G. Graham, D. V. Dawson and A. D. Roses, 1987, "Hereditary Motor and Sensory Neuropathy, X-Linked: A Half Century Follow-Up", *Neurology*; Vol. 37, pp. 1460-5.

Saito H., M. Kubota, R. W. Roberts, Q. Chi and H. Matsunami, 2004, "RTP Family Members Induce Functional Expression of Mammalian Odorant Receptors", *Cell*, Vol. 119, pp. 679–691.

Salinas, A. E., and M. G. Wong, 1999, "Glutathione S-Transferases-a Review", *Current Medicinal Chemistry*, Vol. 6, pp. 279-309.

Selcen, D. and A. G. Engel, 2003, "Myofibrillar Myopathy Caused by Novel Dominant Negative Alpha B-Crystallin Mutations", *Annals of Neurology,* Vol. 54, 804–810.

Senderek, J., C. Bergmann, V. T. Ramaekers, E. Nelis, G. Bernert, A. Makowski, S. Züchner, P. De Jonghe, S. Rudnik-Schöneborn, K. Zerres and J. M. Schröder, 2003a, "Mutations In The Ganglioside-Induced Differentiation-Associated Protein-1 (GDAP1) Gene In Intermediate Type Autosomal Recessive Charcot-Marie-Tooth Neuropathy", *Brain*, Vol. 126, pp. 642-649.

Senderek, J., C. Bergmann, S. Weber, U. P. Ketelsen, H. Schorle, S. Rudnik-Schöneborn, R. Büttner, E. Buchheim and K. Zerres, 2003b, "Mutation of the SBF2 gene, encoding a novel member of the myotubularin family, in Charcot– Marie–Tooth neuropathy type 4B2/11p15", *Human Molecular Genetics*, Vol. 12, pp. 349-356.

Senderek, J., C. Bergmann, C. Stendel, J. Kirfel, N. Verpoorten, P. De Jonghe, V. Timmerman, R. Chrast, M. H. G. Verheijen, G. Lemke, E. Battaloglu, Y. Parman, S. Erdem, E. Tan, H. Topaloglu, A. Hahn, W. Müller-Felber, N. Rizzuto, G. M. Fabrizi, M. Stuhrmann, S. Rudnik-Schöneborn, S. Züchner, J. M. Schröder, E. Buchheim, V. Straub, J. Klepper, K. Huehne, B. Rautenstrauss, R. Büttner, E. Nelis and K. Zerres, 2003c, "Mutations in a Gene Encoding a Novel SH3/TPR Domain Protein Cause Autosomal Recessive Charcot-Marie-Tooth Type 4C Neuropathy", *American Journal of Human Genetics*, Vol. 73, pp. 1106-1119.

Sevilla, T., A. Cuesta, M. J. Chumillas, F. Mayordomo, L. Pedrola, F. Palau and J. J. Vìlchez, 2003, "Clinical, Electrophysiological And Morphological Findings of Charcot-Marie-Tooth Neuropathy Withvocal Cord Palsy and Mutations in the GDAP1 Gene" *Brain*, Vol. 126, pp. 2023-2033.

Shy, M. E., J. Y. Garbern and J. Kamholz, 2002, "Hereditary Motor and Sensory Neuropathies: A Biological Perspective", *The Lancet Neurology*, Vol. 1, pp. 110-118.

Skre, H., 1974, "Genetic and Clinical Aspects of Charcot-Marie-Tooth's Disease", *Proceedings of the Third International Congress on Clinical Genetics and Muscle Diseases,* Vol. 6, pp. 98-118.

Stock A. D., P. A. Spallone, T. R. Dennis, D. Netski, C. A. Morris, C. B. Mervis, and H. H. Hobart, 2003, "Heat Shock Protein 27 Gene: Chromosomal and Molecular Location and Relationship to Williams Syndrome" *American Journal of Medical Genetics* Vol., 120, pp. 320–325.

Stojkovic, T., P. Latour, G Viet, J. de Seze, J. F. Hurtevent, A. Vandenberghe and P. Vermersch, 2004, "Vocal Cord and Diaphragm Paralysis, as Clinical Features of a French Family with Autosomal Recessive Charot-Marie-Tooth Disease, Associated with a New Mutation in the GDAP1 Gene", *Neuromuscular Disorders,* Vol. 14, pp. 261–264.

Stojkovic, T., 2006, "Peripheral Neuropathies: The Rational Diagnostic Process", *La Revue de Médecine Interne*, Vol. 27, pp. 302-312.

Sun, X., J-M. Fontaine, J. S. Rest, E. A. Shelden, M. J. Welsh and R. Benndorf, 2004, "Interaction of Human HSP22 (HSPB8) with Other Small Heat Shock Proteins", *The Journal of Biological Chemistry*, Vol. 279, pp. 2394–2402.

Suter, U. and P. I. Patel, 1994, "Genetic Basis of Inherited Peripheral Neuropathies", *Human Mutation*, Vol. 3, pp. 95-102.

Tang, B., G. Zhao, W. Luo, K. Xia, F. Cai, Q. Pan, R. Zhang, F. Zhang, X. Liu, B. Chen, C. Zhang, L. Shen, H. Jiang, Z. Long and H. Dai, 2005, "Small Heat-Shock Protein 22 Mutated in Autosomal Dominant Charcot-Marie-Tooth Disease Type 2L", *Human Genetics*, Vol. 116, pp. 222–224.

Timmerman V., P. Raeymaekers, E. Nelis, P. De Jonghe, L. Muylle, C. Ceuterick, J. J. Martin and C. Van Broeckhoven., 1992, "Linkage Analysis of Distal Hereditary

Motor Neuropathy Type II (distal HMN II) in a Single Pedigree", *Journal of the Neurological Sciences*, Vol. 109, pp. 41-48.

Timmermann V., P. De Jonge, P. Spoelders, S. Simokovic, A. Löfgren, E. Nelis, J. Vance, J-J. Martin and C. Van Broeckhoven, 1996a, "Linkage and Mutation Analysis of Charcot-Marie-Tooth Neuropathy Type 2 Families with Chromosome 1p35–p36 and Xq13", *Neurology*, Vol. 46, pp. 1311–1318.

Timmerman, V., P. De Jonghe, S. Simokovic, A. Löfgren, J. Beuten, E. Nelis, C. Ceuterick, J.-J. Martin and C. Van Broeckhoven, 1996b, "Distal Hereditary Motor Neuropahy Type II (distal HMN II): Mapping to a Locus to Chromosome 12q24", *Human Molecular Genetics*, Vol. 5, pp. 1065-1069.

Tooth, H. H. (Ed.), 1886, *The Peroneal Type of Progressive Muscular Atrophy*, Lewis, London.

Vance, J. M., 2000, "The Many Faces of Charcot-Marie-Tooth Disease", *Archives in Neurology,* Vol. 57, pp. 638–640.

Van der Vleuten, A.J., C. M. van Ravenswaaij-Arts, C. J. Frijns, A. P. Smits, G. Hageman, G. W. Padberg and H. Kremer, 1998, "Localisation of the gene for a dominant congenital spinal muscular atrophy predominantly affecting the lower limbs to chromosome 12q23–q24", *European Journal of Human Genetics*, Vol. 6, pp. 376–382.

Vicart P., A. Caron, P. Guicheney, Z. Li, M. C. Prevost, A. Faure, D. Chateau, F. Chapon, F. Tom, J. M. Dupret, D. Paulin and M. Fardeau. 1998, "A Missense Mutation in the AlphaB-Crystallin Chaperone Gene Causes a Desmin-Related Myopathy", *Nature Genetics*, Vol. 20, pp. 92-95.

Vitala, A., X. Ferrerb, C. Goizetb, M. Rouanet-Larriviéreb, S. Eimera, G. Bonned and C. Vitala, 2005, "Peripheral Nerve Lesions Associated with a Dominant Missense

Mutation, E33D, of the Lamin A/C Gene", *Neuromuscular Disorders*, Vol. 15, pp. 618–621.

Warner L. E., P. Mancias, I. J. Butler, C. M. McDonald, L. Keppen, K. G. Koob and J. R. Lupski, 1998, "Mutations in the Early Growth Response 2 (EGR2) Gene are Associated with Hereditary Myelinopathies", *Nature Genetics,* Vol. 18, pp. 382-384.

Windpassinger C., M. Auer-Grumbach, J. Irobi, H. Patel, E. Petek, G. Horl, R. Malli, J. A. Reed, I. Dierick, N. Verpoorten, T. T. Warner, C. Proukakis, P. Van den Bergh, C. Verellen, L. Van Maldergem, L. Merlini, P. De Jonghe, V. Timmerman, A. H. Crosby and K. Wagner, 2004, "Heterozygous Missense Mutations in BSCL2 are Associated with Distal Hereditary Motor Neuropathy and Silver Syndrome", *Nature Genetics*, Vol. 36, pp. 271-276.

Züchner S., I. V. Mersiyanova, M. Muglia, N. Bissar-Tadmouri, J. Rochelle, E. L. Dadali, M Zappia, E. Nelis, A. Patitucci, J. Senderek, Y. Parman, O. Evgrafov, P. De Jonghe, Y. Takahashi, S. Tsuji, M. A. Pericak-Vance, A. Quattrone, E. Battologlu, A. V. Polyakov, V. Timmerman, J. M. Schröder and J. M. Vance, 2004, "Mutations in the Mitochondrial GTPase Mitofusin 2 Cause Charcot-Marie-Tooth Neuropathy Type 2A", *Nature Genetics*, Vol. 36, pp. 449-541.

Züchner S., M. E. Kail, M. A. Nance, P. C. Gaskell, I. K. Svenson, D. A. Marchuk, M. A. Pericak-Vance and A. E. Ashley-Koch, 2006a, "A New Locus for Dominant Hereditary Spastic Paraplegia Maps to Chromosome 2p12", *Neurogenetics*, Vol. 7, pp. 127–129.

Züchner S., G. Wang, K-N. Tran-Viet, M. A. Nance, P. C. Gaskell, J. M. Vance, A. E. Ashley-Koch and M. A. Pericak-Vance, 2006b, "Mutations in the Novel Mitochondrial Protein REEP1 Cause Hereditary Spastic Paraplegia Type 31" *The American Journal of Human Genetics*, Vol 79, pp. 365-369.